INVESTIGATION OF NEW THIAZOLE DERIVATIVES AND THEIR BIOLOGICAL EFFECTS

Master's Thesis

Abd Al Rahman ASFOUR

Eskişehir 2023

INVESTIGATION OF NEW THIAZOLE DERIVATIVES AND THEIR BIOLOGICAL EFFECTS

Abd Al Rahman ASFOUR

Master's Thesis

Department of Pharmaceutical Chemistry

Supervisor: Prof. Dr. Leyla YURTTAŞ

Eskişehir

Anadolu University

Graduate School of Health Sciences

May 2023

This thesis work was supported within the scope of the project numbered 2212S199 accepted by the BAP Commission.

FINAL APPROVAL FOR THESIS

This thesis titled “Investigation of New Thiazole Derivatives and Their Biological Effects” has been prepared and submitted by ABD AL RAHMAN MOHAMMD FAEZ ASFOUR in partial fulfillment of the requirements in “Anadolu University Directive on Graduate Education and Examination” for the Degree of Master of Science in Pharmaceutical Chemistry Department has been examined and approved on 29/05/2023.

Committee Members		**Signature**
Member (Supervisor)	: Prof. Dr. Leyla YURTTAŞ	……
Member	: Prof. Dr. Şeref DEMİRAYAK	……
Member	: Prof. Dr. Ahmet Çağrı KARABURUN	……

Prof. Dr. Gülşen AKALIN ÇİFTÇİ

Director

Graduate School of Health Sciences

ÖZET

YENİ TİYAZOL TÜREVLERİ VE BİYOLOJİK ETKİLERİNİN ARAŞTIRILMASI

Abd Al Rahman ASFOUR

Farmasötik Kimya Anabilim Dalı

Anadolu Üniversitesi, Sağlık Bilimleri Enstitüsü, Mayıs 2023

Danışman: Prof. Dr. Leyla YURTTAŞ

Bu tez kapsamında, Alzheimer ve Parkinson hastalıkları gibi nörodejeneratif bozuklukların tedavisinde kullanılabilecek potansiyel bir iskelet olan tiyazol halkasını içeren toplam oniki bileşiğin (**5a-5l**) tasarımı ve sentezi hedeflenmiştir. *N*-[4-(4-Asetamidofenil)tiyazol-2-il)-]2-((heteroaril)tiyo)propanamit (**5a-5l**) türevi bileşikler IR, NMR ve HRMS gibi çeşitli teknikler kullanılarak analiz edilmiş ve fiziksel özellikleri belirlenmiştir. Ardından sentezlenen bileşikler, asetilkolinesteraz (AChE), bütirilkolinesteraz (BChE) ve monoamin oksidaz (MAO-A ve MAO-B) enzimleri üzerindeki potansiyel inhibitör etkinlikleri için test edilmiştir. Bileşikler AChE inhibitörü olarak kayda değer etkinlik göstermiş, aralarından **5d, 5e** ve **5j** bileşikleri en yüksek AChE inhibitör aktivite sergilemiştir. Ancak bileşiklerin hem BChE enzimine karşı hem de MAO alt tiplerine karşı inhibitör etkinlikleri zayıf kalmıştır. En etkili bulunan üç bileşik, protein yörelerine bağlanma şekilleri, yaptıkları bağlar ve zaman-çevresel değişkenleri ile bu etkileşimler üzerindeki etkileri moleküler docking ve dinamik simülasyon analizleri ile incelenmiştir. Bu çalışma, ilaç geliştirme çalışmalarında tiyazol bileşiklerinin nörodejeneratif bozuklukların tedavisi için kullanılabilecek iyi bir iskelet olduğunu vurgulamaktadır.

Anahtar kelimeler: Tiyazol, AChE inhibitörleri, BChE inhibitörleri, MAO inhibitörleri, Moleküler docking analizi.

ABSTRACT

INVESTIGATION OF NEW THIAZOLE DERIVATIVES AND THEIR BIOLOGICAL EFFECTS

Abd Al Rahman ASFOUR

Department of Pharmaceutical Chemistry

Anadolu University, Graduate School of Health Sciences, May 2023

Supervisor: Prof. Dr. Leyla YURTTAŞ

In this thesis, it was aimed to design and synthesize a total of 12 compounds (**5a-5l**) containing the thiazole ring, which is a potential structure that can be used in the treatment of neurodegenerative disorders such as Alzheimer's and Parkinson's diseases. *N*-[4-(4-Acetamidophenyl)thiazol-2-yl)-]2-((heteroaryl)thio)propanamide (**5a-5l**) derivative compounds were analyzed using various techniques such as IR, NMR, and HRMS, and their physical properties were determined. The synthesized compounds were then tested for their potential inhibitory activity on acetylcholinesterase (AChE), butyrylcholinesterase (BChE) and monoamine oxidase (MAO-A and MAO-B) enzymes. The compounds showed remarkable activity as AChE inhibitors, of which compounds **5d, 5e** and **5j** exhibited the highest AChE inhibitory activity. However, the inhibitory activities of the compounds against both the BChE and the MAOs were weak. The three most effective compounds, the way they bind to protein sites, the bonds they make, and the effects of time-environmental variables on these interactions were investigated by molecular docking and dynamic simulation docking analyses. This study highlights that thiazole compounds are a good framework for the treatment of neurodegenerative disorders in drug development studies.

Keywords: Thiazole ring, AChE inhibitors, BChE inhibitors, MAO inhibitors, Molecular docking analysis.

ACKNOWLEDGMENTS

First and foremost, I would like to begin by expressing my deep appreciation to Allah for granting me the ability and opportunity to complete this thesis.

I am grateful to my family members for their unwavering support, my parents' Constant encouragement and support from all sides, my sisters' love and emotional support, and my brothers' advice and financial assistance have been instrumental in shaping my academic pursuits. I am forever indebted to them for their constant guidance and motivation.

I am also immensely grateful to my supervisor Prof. Dr. Leyla YURTTAŞ, for her exceptional guidance, support, and encouragement throughout the two years of my master's degree. Her valuable insights, constructive feedback, and tireless efforts have been instrumental in shaping the direction and quality of this research.

I would like to extend my thanks to Prof. Dr. Ahmet Çağrı KARABURUN for his valuable guidance and contributions to my research work.

Furthermore, I would like to thank Dr. Asaf Evrim EVREN for his invaluable assistance in all the time in the laboratory and out the laboratory, and for providing me with the necessary information and resources to carry out this research successfully.

And expresses my gratitude to Assoc. Prof. Dr. Begüm Nurpelin SAĞLIK for conducting the biological evaluation studies, Dr. Serkan LEVENT and Betül AYDIN for carrying out the chemical analysis measurements. Additionally, I am thankful to the Mer-Lab laboratory and AÜ-BİBAM laboratory, where the chemical analysis was conducted.

I'm deeply grateful to Anadolu University for supporting my research with materials and instruments, which were instrumental in achieving my project objectives.

Last but not least, I am thankful to Dr. Demokrat NUHA for his generous help, encouragement, and positive attitude, which were a constant source of motivation and inspiration. I also express my sincere gratitude to my colleagues Ahmed RADMAN and Amal AL-SHARABI for their exceptional support and invaluable guidance throughout my research project. Additionally, I thank Dr. Sam DAWBAA, Shroq NAJİ, and Sana SAFFOUR for their laboratory assistance and for answering my research inquiries.

29/05/2023

STATEMENT OF COMPLIANCE WITH ETHICAL PRINCIPLES AND RULES

I hereby truthfully declare that this thesis is an original work prepared by me; that I have behaved in accordance with the scientific ethical principles and rules throughout the stages of preparation, data collection, analysis and presentation of my work; that I have cited the sources of all the data and information that could be obtained within the scope of this study, and included these sources in the references section; and that this study has been scanned for plagiarism with “scientific plagiarism detection program” used by Anadolu University, and that “it does not have any plagiarism” whatsoever. I also declare that, if a case contrary to my declaration is detected in my work at any time, I hereby express my consent to all the ethical and legal consequences that are involved.

Abd Al Rahman ASFOUR

TABLE OF CONTENTS

Page

Page

Page

Page

LIST OF TABLES

Page

LIST OF FIGURES

Page

Page

Page

Page

Page

Page

Page

LIST OF ABBREVIATIONS

Å	: Angstrom
Aβ	: Beta amyloid
AChE	: Acetylcholinesterase
ACh	: Acetylcholine
AD	: Alzheimer's Disease
ATR	: Attenuated total reflection
BChE	: Butyrylcholinesterase
BCh	: Butyrylcholine
BBB	: Blood-brain barrier
CAS	: Catalytic anionic site in acetylcholinesterase
^{13}C NMR	: Carbon-13 nuclear magnetic resonance
CNS	: Central nervous system
J	: Coupling constant
DA	: Dopamine
DMF	: Dimethyl formamide
DMSO-d_6	: Deuterated dimethyl sulfoxide
DMSO	: Dimethyl sulfoxide
FAD	: Flavin adenine dinucleotide
HOMO	: Highest Occupied Molecular Orbital
HRMS	: High-resolution mass spectrometry
h	: Human
IC_{50}	: 50% Inhibitory concentration
IR	: Infra-red
m	: Multiplet
MAO	: Monoamine oxidase
MAOI	: Monoamine oxidase Inhibitor
M.P.	: Melting point
Mwt	: Molecular weigh

m/z	: Mass/charge
NDDs	: Neurodegenerative Disorders
PAS	: Peripheral anionic site in acetylcholinesterase
PD	: Parkinson's Disease
PDB	: Protein data bank
PEA	: Phenethylamine
ppm	: Part per million
^{1}H NMR	: Proton nuclear magnetic resonance
q	: Quartet
ROS	: Reactive Oxygen Species
RT	: Room temperature
5-HT	: Serotonin
s	: Singlet
SSRIs	: Selective serotonin reuptake inhibitors
TEA	: Triethylamine
THF	: Tetrahydrofuran
TLC	: Thin layer chromatography
TMS	: Tetramethylsylane
TPSA	: Topological polar surface area
2D	: Two-dimensional
3D	: Three-dimensional
t	: Triplet
UV	: Ultraviolet

1. INTRODUCTION

Neurodegenerative illnesses, like Parkinson's and Alzheimer's diseases, are characterized by selective or generalized nervous cell malfunction. There are numerous factors, including mitochondrial failure, neuro-inflammatory processes, and oxidative stress, that contribute to the chain of events that results in neuronal malfunction and finally cell death [1–3].

The development of sophisticated medical technology has led to an increase in the average lifespan, particularly among older individuals [4–6]. However, this has also brought about significant societal and complex challenges, notably neurodegenerative disorders (NDDs) [7–9]. NDDs is a broad term encompassing various degenerative neurological conditions that are linked to brain neuron injuries, for which recovery is often difficult or impossible [10–12]. Various neurodegenerative disorders (NDDs), including stroke, depressive illness, Parkinson's disease (PD), Alzheimer's disease (AD), as well as many others, are caused by the selective death of neurons in certain regions of the brain. AD and PD are the most frequent types of NDDs, but the particular areas of the brain affected can vary depending on the disorder, and as of now, there is no absolute curative remedy for these conditions [13]. As a result, altering the disease route by neuroprotective therapy is a critical unmet therapeutic need.

AD is a persistent, neurodegenerative, and deadly brain illness that causes memory loss, attention deficits, and a variety of other cognitive impairments [14]. Alzheimer's disease affects approximately about 47 million people, and the number is growing every year [15]. Unfortunately, due to its complicated etiology, its mechanism has not been fully understood. Despite the fact that the specific causes of AD is unknown, studies find that a number of factors, including oxidative stress, s-protein aggregation, β-amyloid (Aβ) deposits, imbalances in biometals, and deficiencies in acetylcholine (ACh) levels within the cortex and hippocampus regions inside the brain [16].

Monoamine oxidases (MAOs), which are enzymes found in different cells (including liver, nerve terminals, and stomach mucosa), contain flavin adenine dinucleotide (FAD) and are situated in the outside barrier of mitochondria [17, 18] Their function involves the oxidation and deamination of neurotransmitters and biogenic monoamines [19]. MAOs

comprise two distinct isoforms, MAO-B and MAO-A, that have almost 70 percent amino acid series but differ in their specificities towards substrates and inhibitors. Additionally, the genes responsible for encoding these isoforms are found on the X chromosome [20–22]. MAO-A is accountable for breaking down adrenaline, noradrenaline, and serotonin and also is majorly inhibited by clorgyline. In contrast, MAO-B is specifically inhibited by selegiline and it primarily catalyzes the oxidation of β-phenylethylamine and benzylamine. Targeting MAO-B was discovered to have value in the management of neurodegeneration disorders like AD [23, 24]. In addition, blocking the activity of MAO-B has been shown to be effective in managing NDDs like Parkinson's and Alzheimer's disease [25–27], selective MAO-A inhibition has also been shown to be advantageous in the treatment of anxiety and depression. [19,20]. Furthermore, depressive symptoms are frequently linked to NDDs [29]. When monoamine oxidases exist in high levels in neuronal tissue, they generate hydrogen peroxide as a byproduct, which subsequently elevates the productions of reactive oxygen species (ROS). These ROS are significant factor in the development of neurodegenerative disorders. The Inhibitor of MAOs can be a useful treatment for NDDs because they have the potential to prevent oxidative damage [30].

According to studies, the heterocyclic compounds have a variety of biological activities [31]. The thiazole moiety is an essential pharmacophore and intermediary in the production of agro-chemicals and medicines [32–34]. Thiazoles are a kind of heterocyclic structure present in several biologically active substances, including central nervous system (CNS) drugs as Riluzole (anticonvulsant), Talipexole and Pramipexole (antiparkinsonian) (see Figure 1.1) [35]. Additionally, it is utilized in the creation of medications that treat inflammation [36]. Recently, thiazole analogues have also been discovered to have anti-diabetic, anti-glycation, and strong cholinesterase inhibitor properties [37, 38].

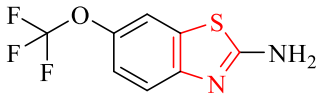

Riluzole (anticonvulsant)

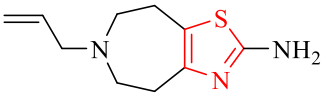

Talipexole (antiparkinsonian)

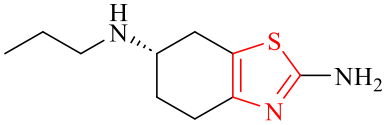

Pramipexole (antiparkinsonian)

Figure 1.1. *CNS drugs containing thiazole ring*

2. LITERATURE REVIEW

2.1. Thiazole Chemistry

The class of azole heterocycles includes thiazoles. The general formula for thiazoles is C_3H_3NS, and they are organic compounds with five aromatic rings. Free thiazole smells like pyridine and is a pale-yellow liquids [39]. Thiazole and its derivatives have industrial applications including agrochemicals and photography. Additionally, they have many pharmacological activity including hepatoprotective, anti-inflammatory, anti-Alzheimer's, anti-hypertensive, antioxidant, and antimicrobial activities (sulfazole, ritonavir, abafungin, and tiazofurin) [2, 40, 41]. Many natural products, including vitamin B and penicillin, have molecules with thiazole moieties as a key structural component. Thus, many forms of thiazole-type heterocyclic structures, such as bicyclic or monocyclic structure synthesized, are discussed in this chapter along with studies of their biological functions. Additionally, it is discussed how to modify thiazole-based compounds at various places to create novel molecules with strong anti-Alzheimer, and anti-Parkinson activity [42, 43].

Since thiazole-containing compounds are useful for making photosensitizers, rubber vulcanizers, sunscreens, chromophores, pigments, catalysts, dyes, sensors, and liquid crystals, interest in their synthesis has been continuously rising [37, 44]. Thiazoles also hold a major position in modern medicinal chemistry because of their numerous uses in the areas of drug discovery and design [45, 46]. They appear as the short-acting sulfa medication sulfathiazole in bacitracin, penicillin antibiotics, and many synthetic medicines [47–50]. They are furthermore utilized nizatidine is an anti-ulcer agent, meloxicam is an anti-inflammatory medicine, and pramipexole is used as an antidepressant, a medicine for HIV/AIDS (ritonavir), and a drug for treating cancer (tiazofurin). Thiazole occurs more frequently in FDA-approved medications than other 5 heterocyclic rings such as furan, azoles, isothiazole, and thiophene. In contrast, Various linked heterocyclic compounds that possess biological activity, including imidazothiazoles, thiazolopyridine, and thiazolopyrimidine, can be produced by subjecting 1,3-thiazoles to various types of reactions. Photocatalysis typically uses thiazole metal complexes [51–53].

Thiazole is an aromatic compound containing nitrogen and sulfur atoms. Electrons in four 2pz orbitals and one 3pz orbital are delocalized. Three carbon atoms and one nitrogen

atom each donate one electron to the ring, while the sulfur atom contributes two electrons. The thiazole ring has a planar structure, in which case the sulfur atom makes a spd hybrid and the calculated π electron densities for each atom are as in Figure 2.1 [54–56].

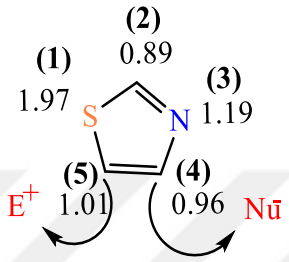

Figure 2.1. *The chemical shift of ring proton*

The excess of π electrons in the thiazole ring is concentrated on heteroatoms. For example, due to the density on the nitrogen, the density of the electron on the carbon 2 has decreased. Because of this, nucleophilic attack occurs on carbon atom 2, while electrophilic attack occurs at position 5. If position 5 is blocked, the attack takes place from position 4 [57, 58].

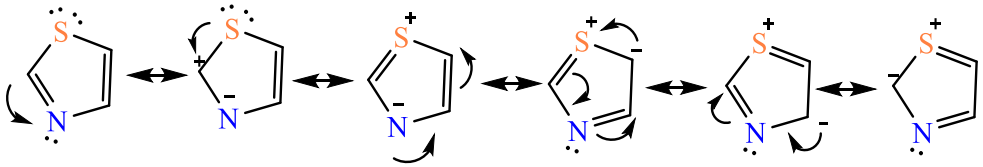

Figure 2.2. *Thiazole resonance structures*

The resonance forms of the thiazole ring are shown in the figure above (Figure 2.2). Due to the d orbitals in the thiazole ring, additional resonance structures exist. Heteroatoms containing unbonded electron pairs have increased the resonance structures of the molecule, and thanks to conjugation, molecules have become more important as optical electroactive

materials. The presence of heteroatom increases electron-hole mobility and enables molecular charge transfer [59].

2.2. 1,3-Thiazole Synthesis Methods

The synthesis of thiazole compounds can be done by several methods. These methods can be classified as shown in Figure 2.3. The first structure (1A) is a very common method. Desired groups can be attached to the 2-, 3-, 4- or 5- positions of the ring by appropriate selection of alkyl, aryl or heterocyclic substituents. This method is named after the German chemist "Hantzsch". Another method (1B), proposed by Tcherniac, is based on the cyclization of α-halo ketones and α-thiocyano ketones obtained from metal thiocyanates to thiazoles [60]. Other processes can be used to synthesize the thiazole ring, but their application is restricted. One of these is the interaction of carbon disulfide with α-aminonitriles or α-aminoamides used by Cook and Heilborn (2). Thiazoles can also be obtained from α-acylamino carbonyls with phosphopentasulfide (3) [61]. They can also be obtained by combining α-mercaptoketone with nitriles (4) or by reaction of α-mercaptoacids or their esters with Schiff bases. In the (5) type synthesis pathway, the thiazole ring can be reached by forming the 5-position of one of the reactants [62].

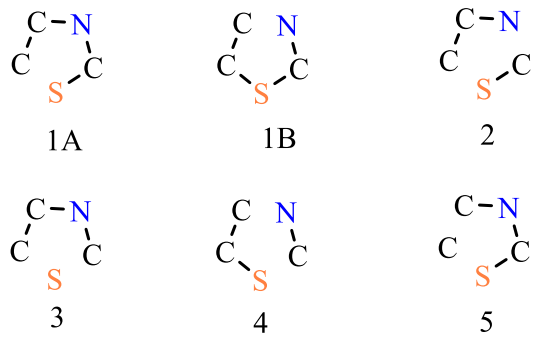

Figure 2.3. *Different types of thiazole ring closure methods*

By using well-known techniques from Hantzsch [63], Cook-Heilbron [64], and Gabriel [65], thiazole ring systems were simply synthesized. Various substances and their derivatives, like thiourea, thioamides, dithiocarbamate or ammonium thiocarbamate, and

their derivatives, may act as a nucleophilic reagent in this reaction. In 1887, Hantzsch created the first straightforward thiazole nucleus [66]. This method of synthesis, which is thought to be the most extensively used one for the production of the thiazole molecule, entails the condensation of haloketones with thioamide and their subsequent cyclization. This method of synthesis, which is thought to be the most extensively used one for the production of the thiazole molecule, entails the condensation of thioamide with haloketones and their subsequent cyclization. On the other hand, by reacting Lawesson's reagent with α-acylaminoketones or stoichiometric quantity of P_2S_5, Gabriel created thiazoles [67]. Additionally, to produce substituted aminothiazoles, Cook-Heilbron employed various techniques, one of which involved the gentle reaction of carbonyl sulfide, isothiocyanates, carbon disulfide, and dithioacids or esters with α-aminonitriles [68]. Thiazole derivatives have recently been produced using a microwave irradiation approach [69] and in the presence of many catalysts [70–73].

2.2.1. The Hantzsch reaction: synthesis from α-halocarbonyl compounds

2.2.1.1 Thioamide-related reactions

Thiazoles with functional groups at positions 2, 4, or 5 include heteroaryl of various types or arylalkyl, aryl, and alkyl were produced by reacting thioamides with various α-halocarbonyl compounds [74, 75] (Figure 2.4).

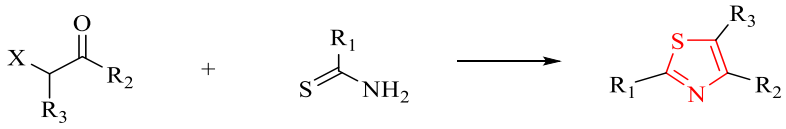

Figure 2.4. *The synthesis of 2-, 4-, 5-trisubstituted thiazoles.*

2.2.1.2 *N*-Substituted thiourea reactions

The interaction of *N*-substituted thiourea with halo-carbonyl compounds results in the production of aminothiazoles that have either one or two substituents [76] (Figure 2.5).

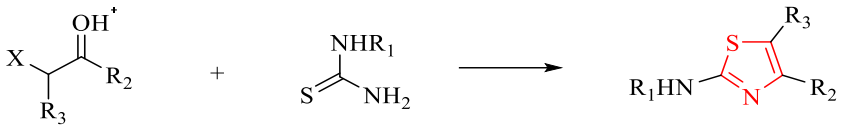

Figure 2.5. *Substituted aminothiazole synthesis.*

2.2.1.3 With esters of thiocarbamic acid reaction

2-Hydroxythiazole derivatives were produced through the reaction of thiocarbamates with α-halocarbonyl compounds to form a condensation product [77, 78] (Figure 2.6).

Figure 2.6. *Production of 2-hydroxythiazoles*

2.2.2. The Cook Heilbron's reaction: Synthesis from molecules containing α-aminonitrile

By strongly interacting the production of 5-aminothiazole with diverse substitutions at position two is accomplished through the interaction of aminonitrile compound with esters and salts of isothiocyanates, dithioacids carbon oxysulfide, and carbon disulfide [79–81].

2.2.2.1 Reaction using carbon dioxide

At order to create 5-amino-thiazoles replaced compound at position two, 2-mercapto-5-amino thiazoles were produced by interaction between of α-aminonitriles with CS_2 to form a condensation product [79, 82] (Figure 2.7).

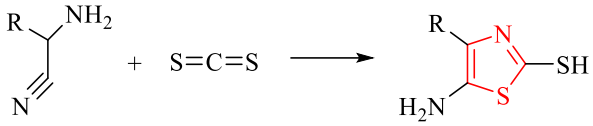

Figure 2.7. *Synthesis of 2-mercapto-5-aminothiazoles.*

2.2.3. Reaction with esters and salts of dithioacids

5-Aminothiazoles were produced in good quantities by reacting α-aminonitriles with the esters or salts of both dithiophenacetic and dithioformic acids [83] (Hata! Başvuru kaynağı bulunamadı.).

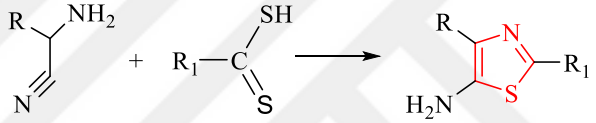

Figure 2.8. *Synthesis of 5-aminothiazole derivative products.*

2.2.4. The Gabriel's reaction: Phosphorus pentasulfide and acylaminocarbonyl compound synthesis and condensation

Gabriel first referred to this reaction in 1910. By the interaction of acylaminoketone with P_2S_5 a significant yield of 2-phenyl-5-alkyl-thiazole was produced [84] (Figure 2.9).

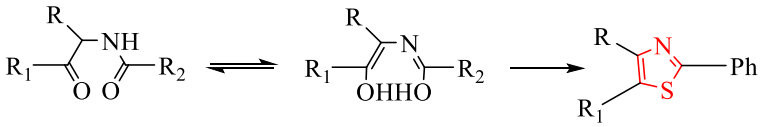

Figure 2.9. *Synthesis of 2-phenyl-5-alkyl-thiazole compounds.*

2.2.5. Synthesis utilizing eco-friendly techniques

2.2.5.1 Utilizing microwave-assisted organic synthesis

Derivatives of thiazoles are usually created under harsh conditions of reaction, leading to the disposal of solvents and catalysts. In order to resolve these issues,, more environmentally-friendly techniques like irradiation of microwave are frequently employed in the synthesis of thiazole derivatives [85]. A quick and efficient method for producing a

variety of thiazoles involves the application of microwave heating in the absence of solvents [69, 86, 87] (Figure 2.10).

2.2.5.2 Aqueous one-pot multicomponent reaction.

H_2O is a suitable solvent for eco-friendly chemical reactions because it is commercially viable, non-toxic, and eco-friendly. The combination of thiourea, phenyl acetylene, and *N*-bromosuccinimide in a three component process resulted in high yields of substituted thiazole derivatives [88](Figure 2.11).

2.2.5.3 Utilizing silica-supported tungstosilisic acid

An environmentally friendly and effective technique has indeed been created for synthesizing a new substituted Hantzsch dericatives of thiazole through a one-pot multicomponent approach. The method involves the reaction of thiourea with 3-(bromoacetyl)-4-hydroxy-6-methyl-2*H*-pyran-2-one and substituted benzaldehydes using silica supported tungsto-silisic acid as a catalyst, either by customary heating or ultrasonic irradiation [86–89] **(**Figure 2.12**).**

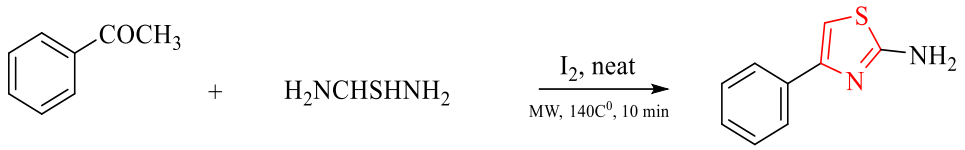

Figure 2.10. *Thiazole synthesis using microwave irradiation.*

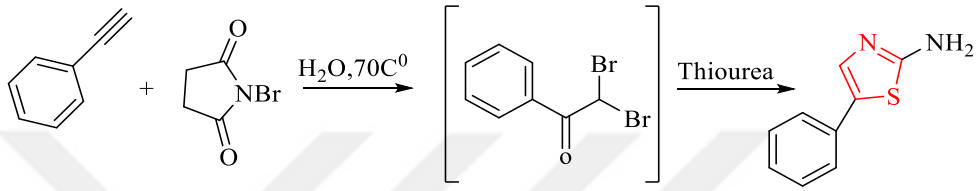

Figure 2.11. *Aqueous synthesis of 2-aminothiazole.*

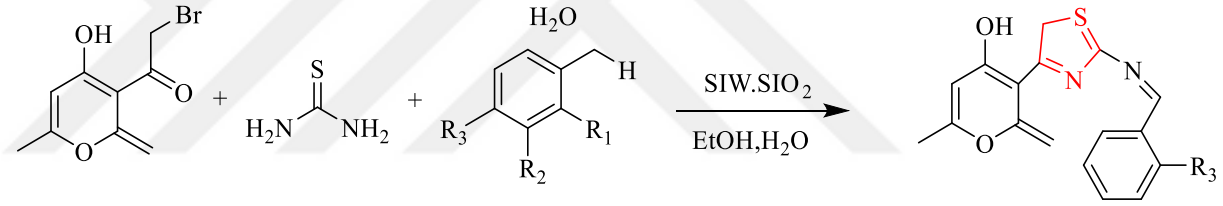

Figure 2.12. *The use of silica in the synthesis of thiazole derivatives.*

2.2.6. Miscellaneous methods

The reaction between thioamides or thioureas and α-chloroglycinate esters led to the discovery of the Hantzsch construction of thiazole derivatives. Targeted substances are synthesized from easily accessible and cheap constructing elements in a non-hazardous to the environment and catalyst-free approach [76] (Figure 2.13).

High yields of numerous 2,5-diarylthiazole derivatives were produced under mild conditions in the CH replacement methods of thiazole, which was catalyzed by the palladium/copper technique in the existing tetrabutylammonium fluoride [90].

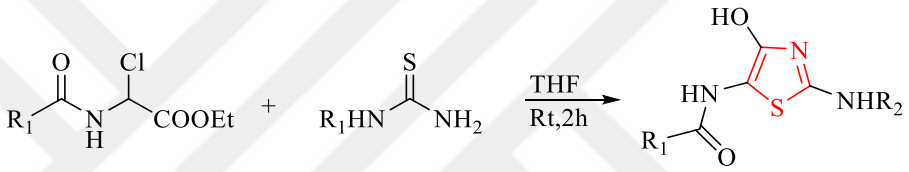

Figure 2.13. *Thiazole derivative synthesis.*

2.2.7. Using oxidizing agents and thiourea

The oxidative reagents, like SO_2Cl_2, HSO_3Cl, $SOCl_2$, S_2Cl_2, SO_3, H_2SO_4, S, and HNO_3 were used to treat the mixes of thiourea and acetophenone. A significant amount of 2-amino-4-phenylthiazole was obtained in all cases [91] (Figure 2.14).

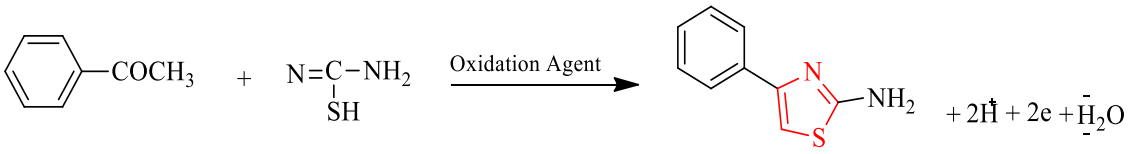

Figure 2.14. *Synthesizing of thiazole derivatives utilizing oxidizing agents.*

2.3. Thiazole Derivatives as Anticholinesterases, Butyrylcholinesterase and Monoamine Oxidase Inhibitors

Mazzone and colleagues synthesized three sets of 2-thiazolylhydrazines in 1992 and evaluated their MAO inhibitory (MAOI) activity using both *in vivo* and *in vitro* methods. In the *in vivo* tests, the researchers measured the changes in pressure of the blood caused by clonidine and tyramine, as well as Hypermotility produced by L-amfetamine. The *in vitro*

assessments involved using a kinuramine fluorimetric assay to determine the effect of the compounds on rat brain mitochondria. All of the examined substances had a significant impact on the evaluation measures *in vivo*. All substances demonstrated MAOI activity in an *in vitro* test at a concentration of $1.10^{(-4)}$ mol. L^{-1}, which was substantial in several situations. The impact of the produced compounds' structures on their biological activity was outlined in the discussion of the findings [92].

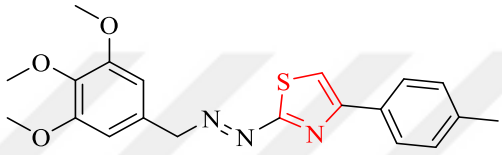

Figure 2.15. *N-(4-p-Tolyl-thiazol-2-yl)-N'-(3,4,5-trimethoxy-benzyl)-hydrazine*

Later in 1995 Raciti *et al.* identified how the chemical structure of various hydrazine-thiazole derivatives affects their ability to inhibit rat liver mitochondria monoamine oxidase. A total of 45 hydrazine-thiazole derivatives were examined, which were categorized into three distinct series and had either arylic or alkylic substitutes for the thiazole ring. Two piperonyl derivatives having a 4-methyl group in the thiazole ring had the best inhibitory efficacy. The study established a link between the activity of MAOs inhibitors and the structure in terms of their hydrophobic, electronic, and steric hindrance characteristics. Additionally, the researchers postulated a hypothetical mechanism of inhibition of enzyme according to the determination of HOMO energy [93].

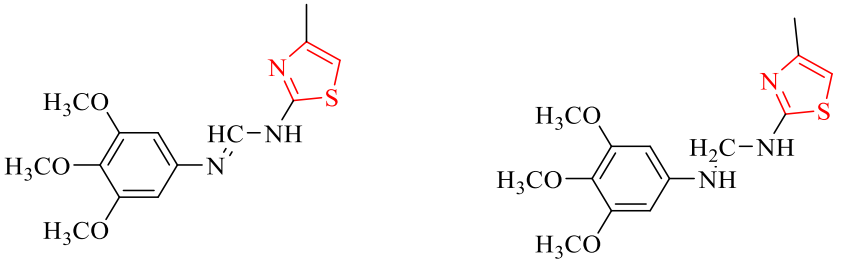

Figure 2.16. *(E)-N-(4-Methylthiazol-2-yl)-N'-(3,4,5-trimethoxyphenyl) formimidamide (Left) N-(4-Methylthiazol-2-yl)-N-(3,4,5-trimethoxyphenyl)methanediamine (Right)*

Andreani *et al*. created a brand-new class of imidazo [2,1-*b*] thiazole compounds in 2005. They were evaluated as AChE inhibitors using a high throughput screening chemiluminescent technique. The lack of quaternization caused the compounds' lack of considerable inhibitory efficacy, which is likely a result of their poor water solubility. The quaternized compounds that corresponded to them were effective inhibitors with action based on the chosen spacer [94].

After three years in 2008, Chimenti *et al.* studied the efficacy of a sequence of 2-methylcyclohexylidene-(4-arylthiazol-2-yl) hydrazones to selectively block the activity of the *h*MAOs. All drugs exhibited enhanced anti-human MAO-B isoform activity, with IC_{50} from 26.81 M (2.74 nM) to 14.20 M (0.26 nM), while pure enantiomers demonstrated stronger activity for the (R) form [95].

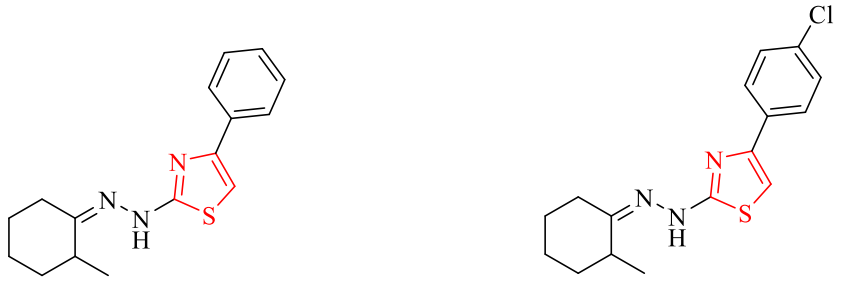

hMAO-A IC_{50} = 41.23 ± 3.96 µM[b]
hMAO-B IC_{50} = 711.23 ± 36.95 nM[b]

hMAO-A IC_{50} = 35.22 ± 1.81 µM[b]
hMAO-B IC_{50} = 13.12 ± 0.51 nM[b]

Figure 2.17. *(Z)-2-[2-(2-Methylcyclohexylidene)hydrazinyl]-4-phenylthiazole (Left) (Z)-4-(4-Chlorophenyl)-2-[2-(2-methylcyclohexylidene)hydrazinyl]thiazole(Right)*

Carradori *et al.* developed a new substructure of hydrazothiazoles in 2013 that act as MAO by merging the thiazole ring of glitazones with the N2H4 component of iproniazid. Glitazones belong to a type of drugs called PPARγ agonists, which have been found to crystallize with *h*MAO-B. The researchers synthesized the occurring compounds and tested their activity *in vitro* against the *h*MAOs isoforms. The study confirmed that all of the substances are effective inhibitor against *h*MAO-B, and the IC_{50} range in the high nanomolar/low micromolar number [96].

*h*MAO-B IC_{50} = 3.34 ± 0.25 µM

*h*MAO-B IC_{50} = 7.18 ± 0.36 µM

Figure 2.18. *(E)-Ethyl 2-[2-(1-(furan-2-yl)ethylidene)hydrazinyl]thiazole-4-carboxylate(Left) (E)-Ethyl 2-[2-(thiophen-2-ylmethylene)hydrazinyl]thiazole-4-carboxylate (Right)*

In 2015, Rahim *et al.* produce a series of 30 thiazole compounds showed strong BChE and AChE inhibitory activity. In comparison to the standard eserine (IC_{50} = 0.850 ± 0001 μM), every analogs showed varying inhibition activity against, by IC_{50} values varying from 1.59 ± 0.01 to 389.25 ± 1.75 μM.

In order to evaluate the potency of BChE inhibition, the IC_{50} values for 4-chlorophenyl and 4-methoxyphenyl substituted derivatives were determined. The results revealed that the IC_{50} value for the 4-chlorophenyl derivative was 1.59 ± 0.01 µM, while the IC_{50} value for the 4-methoxyphenyl derivative was 16.54 ± 0.21 µM. In order the IC_{50} values for 4-chlorophenyl and 4-methoxyphenyl substituted derivatives for BChE inhibition are 1.59 ± 0.01 μM and 16.54 ± 0.21 μM. In addition, the IC_{50} values for 4-chlorophenyl and 4-methoxyphenyl substituted derivatives for AChE inhibition are 21.3 ± 0.50 μM and 48.2 ± 0.06 μM, subsequently [97].

AChE: IC_{50} = 21.3 ± 0.50 µM
BChE: IC_{50} = 1.59 ± 0.01 µM

AChE: IC_{50} = 48.2 ± 1.06 µM
BChE: IC_{50} = 16.54 ± 0.21 µM

Figure 2.19. *(E)-4-[[2-(4-(4-Chlorophenyl)thiazol-2-yl)hydrazono]methyl]benzene-1,2-diol* (left) *(E)-4-[[2-(4-(4-Methoxyphenyl)thiazol-2-yl)hydrazono]methyl]benzene-1,2-diol (Right)*

Sun *et al.* developed a novel class of thiazole acetamides in 2016. These substances were evaluated for their capacity to inhibit BChE and AChE *in vitro* in the goal of treating AD. The 4-methoxyphenyl substituted derivative was discovered as the one that demonstrated the highest level of effectiveness in inhibiting AChE had an IC_{50} rate of 3.14 ± 0.16 µM. Furthermore, this specific compound exhibited a selectivity index of 2.94 towards BChE in comparison to the other synthesized compounds [98].

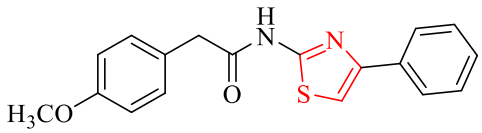

AChE: IC_{50} = 3.14 ± 0.16 µM

BChE: IC_{50} = 9.24 ± 0.32 µM

Figure 2.20. *2-(4-Methoxyphenyl)-N-(4-phenylthiazol-2-yl)acetamide*

In 2017, Abbas and others write a novel. To locate newer and unique pharmacophores in purpose of treat of NDDs such as PD, the bis-iminothiazolidinone compounds were evaluated *in vitro* inhibition against MAO-B & MAO-A enzymes. The majority of the developed compounds demonstrated strong MAO inhibitory effectiveness. The IC_{50} value was 0.001 μM, compound (2*E*,2'*E*)-dimethyl 2,2'-((2*Z*,2'Z)-3,3'-(1,4-phenylene)bis(4-oxo-2-(pentanoylimino)thiazolidin-3-yl-5-ylidene))diacetate was shown to be the most effective MAO-A inhibitor, having a 4-fold higher inhibiting potency than the original (Clorgyline, whose IC_{50} value is 0.0045 μM). MD study shed light on the interactions between enzymes and inhibitors and explained the observed inhibition of monoamine oxidases [99].

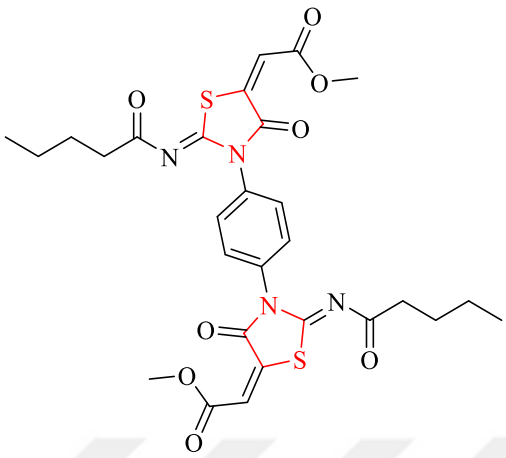

MAO-A IC_{50} = 0.001 ± 0.0001 µM,
MAO-B IC_{50} = 0.51 ± 0.02 µM,

Figure 2.21. *(2E,2'E)-Dimethyl 2,2'-[(2Z,2'Z)-3,3'-(1,4-phenylene)bis(4-oxo-2-(pentanoylimino)thiazolidin-3-yl-5-ylidene)]diacetate*

Also, during 2017, Atli and Özkay synthesized several new thiazole-hydrazones, which included 4-phenylthiazole and 4-(2,4-difluorophenyl). These compounds were subsequently characterized and examined via utilizing the *in vitro* fluorometric methodology to determine their capacity to inhibit *h*MAO-B and A. The SI were determined as IC_{50} MAO-A and B. One of the compounds, 2,4-dichlorophenyl, demonstrated a promising ability t to inhibit *h*MAO-A, with an IC_{50} =1.20 µM. Moreover, this compound exhibited an effective SI of 0.04 against *h*MAO-A [100].

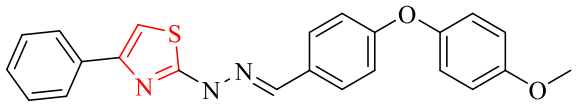

hMAO-A IC_{50} = 8.54± 0.39 µM,
hMAO-B IC50 = 50.43± 2.48 µM,
SI = 0.17 forward MAO-A

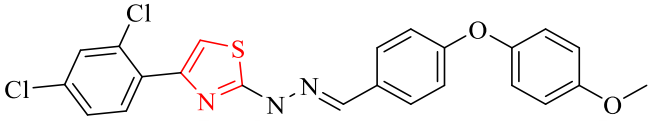

hMAO-A IC_{50} = 1.20 ± 0.08µM,
hMAO-B IC_{50} = 33.47 ± 1.98µM,
SI = 0.04 forward MAO-A

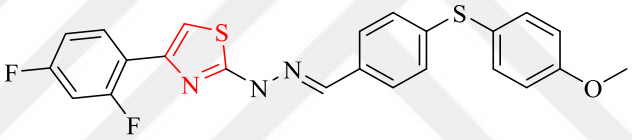

*h*MAO-A IC50 = 26.74 ± 1.53 µM,
*h*MAO-B IC50 = 279.70 ±13.27 µM,
SI = 0.10 forward MAO-A

Figure 2.22. *(E)-2-[2-(4-(4-Methoxyphenoxy)benzylidene)hydrazinyl]-4-phenylthiazole (Up) (E)-4-(2,4-Dichlorophenyl)-2-[2-(4-(4-methoxyphenoxy)benzylidene)hydrazinyl]thiazole (middle) (E)-4-(2,4-Difluorophenyl)-2-[2-(4-((4-methoxyphenyl)thio)benzylidene) hydrazinyl]thiazole (Down)*

Later In 2018, Tripathi and *et al.* developed a series of semicarbazone derivatives of 2-amino-5-nitrothiazole and studied their abilities to inhibit MAOs, AChE, and BChE. by IC_{50} =0.212 M with a SI =331.04, the compound 4 [1-(1-(4-bromophenyl)ethylidene)-4-(5-nitrothiazol-2-yl)semicarbazide] was shown to be the best promising candidate against MAO-B. In order compounds 21 and 17 were shown to have the most impact against acetylcholinesterase and butyrylcholinesterase, with IC_{50} = 0.264 mM and 0.024 mM. Compound 21 is 1-(5-bromo-2-oxoindolin-3-ylidene)-4-(5-nitrothiazol-2-yl)semicarbazide, while compound 17 is 1-((4-chlorophenyl)(phenyl) compounds [101].

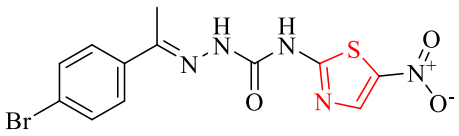

MAO-B IC_{50} = 0.212 µM, SI 331.04

Figure 2.23. *2-[1-(4-Bromophenyl)ethylidene)-N-(5-nitrothiazol-2-yl]hydrazinecarboxamide*

In 2019, Secci and colleagues developed a modern set of 4-[3-nitrophenyl] thiazol-2-yl hydrazone derivatives, which synthetically produced and tested their inhibiting results against *h*MAOs. To establish stable SAR, The N_1 of the hydrazone was modified by the researchers by adding several un/substituted hetero/aromatic substituents [102].

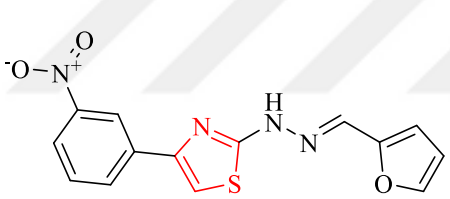

MAO-A IC_{50} = 8.98 ± 0.621 µM,
MAO-B IC_{50} = 0.095 ± 0.0043 µM,
SI^b = 95

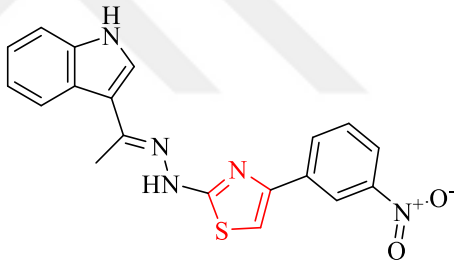

MAO-A IC_{50} = 28.1 ± 3.32 µM,
MAO-B IC_{50} = 4.52 ± 0.915 µM,
SI^b = 6.2

Figure 2.24. *(E)-2-[2-(Furan-2-ylmethylene)hydrazinyl)-4-(3-nitrophenyl]thiazole (Left) (E)-2-[2-(1-(1H-Indol-3-yl)ethylidene)hydrazinyl]-4-(3-nitrophenyl)thiazole (Right)*

In 2020, Sağlık et al. synthesized a novel compound series and evaluated their inhibitory effects on both BChE and AChE. While all compounds showed some inhibitory effect on BChE, the 2-methoxy substituted derivative was found to be the most effective compound against AChE among the series, by an IC_{50} = 0.028 ± 0.001 μM, showing similar characteristics of inhibition to the standard drug donepezil [103].

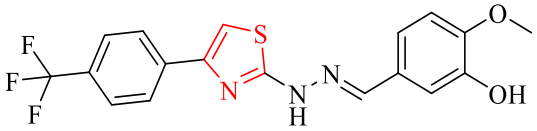

AChE: IC_{50} = 0.028 ± 0.001 µM

Figure 2.25. *(E)-2-Methoxy-5-[(2-(4-(4-(trifluoromethyl)phenyl)thiazol-2-yl)hydrazono)methyl]phenol*

Also, in 2020 Ghotbi *et al.* produced a novel containing thiazole and pyridinium. In order the most effective AChE inhibitory actions were demonstrated by 2-bromobenzyl and 2-fluorobenzyl substituted derivative at sub micromolar concentration ranges (IC_{50} = 0.69 ± 0.06 μM, and 0.40 ± 0.04 μM). The majority of the new compounds had a medium to minor levels of BChE inhibition, suggesting that they selectively inhibit AChE [104].

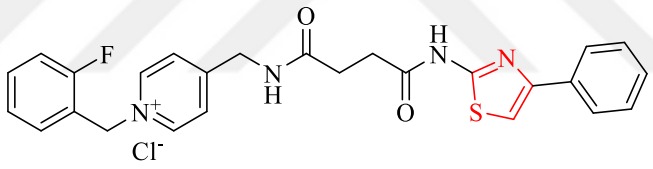

AChE: IC_{50} = 0.40 ± 0.04 µM

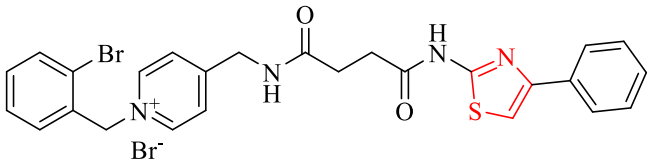

AChE: IC_{50} = 0.69 ± 0.06 µM
BChE: IC_{50} = 50.90 ± 9.38 µM

Figure 2.26. *1-(2-Fluorobenzyl)-4-[[4-oxo-4-((4-phenylthiazol-2-yl)amino)butanamido] methyl]pyridin-1-ium chloride* (*Up*) *1-(2-Bromobenzyl)-4-[[4-oxo-4-((4-phenylthiazol-2-yl)amino)butanamido]methyl]pyridin-1-ium* (*Down*)

After that in 2021 Aya Y. Hemaida *et al.* produced a novel of nineteen new thiazole-derivatives *in vitro* as an inhibitor of AChE with corresponding IC_{50} =103.24 nM and 108.94 nM, the compounds R(CH_3) - R′/Ar (3,4-$(CH_3O)_2C_6H_3$) and R (CH_3) - R′/Ar (4-$CH_3OC_6H_4$) produced significant AChE inhibitory actions [105].

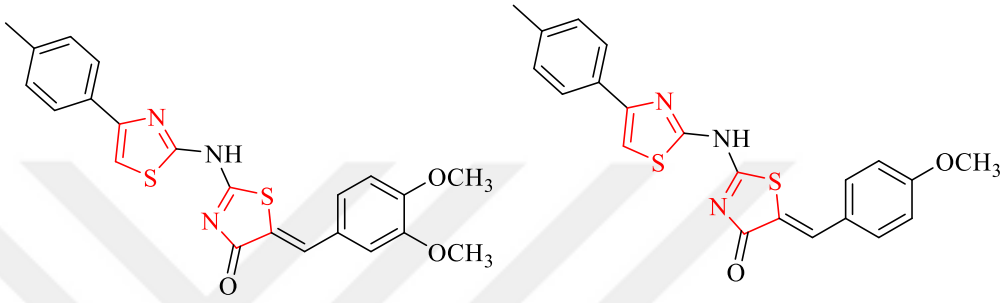

AChE: IC_{50} = 103.24 ± 2.8 nM AChE: IC_{50} = 108.94 ± 3 nM

Figure 2.27. *(Z)-5-(3,4-Dimethoxybenzylidene)-2-[(4-(p-tolyl)thiazol-2-yl)amino]thiazol-4(5H)-one (left) (Z)-5-(4-Methoxybenzylidene)-2-[(4-(p-tolyl)thiazol-2-yl)amino]thiazol-4(5H)-one (Right)*

In 2022, a number of benzimidazole-based thiazole compounds were created by Rafaqat Hussain and *et al.*, and their ability to inhibit cholinesterase enzymes was tested. The analogues showed strong inhibitory activity against both BChE and AChE, having IC_{50} that range from 0.20 ± 0.050 μM to 14.20 ± 0.10 μM and from 0.10 ± 0.05 to 11.10 ± 0.30 μM respectively. These values were compared to the commonly used medication Donepezil. The analogues with R1 (2-NO_2), R2 (4-OH), and R1 (3,4-Cl), R2 (3,4-Cl) were shown being the strongest AChE and BChE enzyme inhibition in the series, respectively [106].

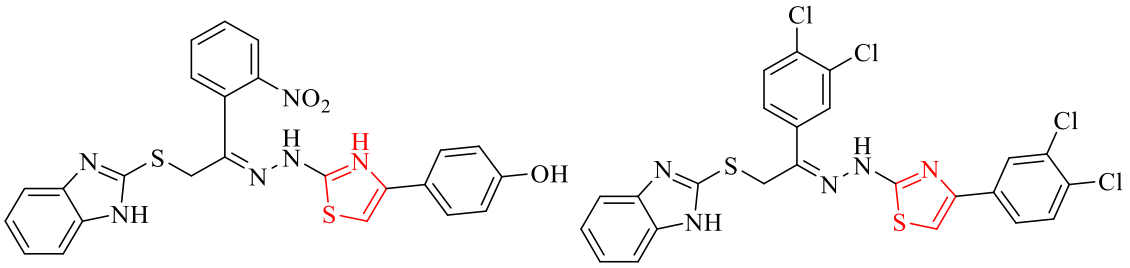

AChE: IC_{50} = 0.20 _ 0.050 µM
BChE: IC_{50} = 0.50 ± 0.050 µM

AChE: IC_{50} = 0.10 ± 0.05 µM
BChE: IC_{50} = 0.20 ± 0.05 µM

Figure 2.28. *(E)-4-[2-[2-(2-((1H-Benzimidazol-2-yl)thio)-1-(2-nitrophenyl)ethylidene)hydrazinyl]thiazol-4-yl]phenol (left) (E)-2-[2-[2-((1H-benzimidazol-2-yl)thio)-1-(3,4-dichlorophenyl) ethylidene)hydrazinyl]-4-(3,4-dichlorophenyl]thiazole (Right)*

Meiyang Xi *et al*. synthesized 33 analogs and evaluated their capacity to inhibit BChE and AChE. Among the analogs, one of them, named *N*-isobutyl-*N*-[2-(p-tolyloxymethyl)thiazol-4-yl)methyl]benzodioxole-5-carboxamide (1), was found to be a selective inhibitor of BChE [107].

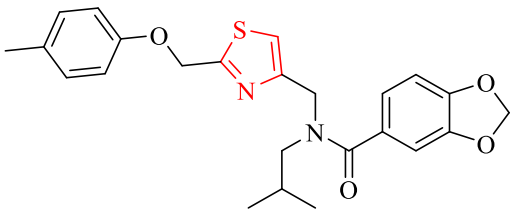

BChE: IC_{50} = 1.28 ± 0.27 µM

Figure 2.29. *N-Isobutyl-N-[[2-((p-tolyloxy)methyl)thiazol-4-yl]methyl]benzodioxole-5-carboxamide*

3. MATERIALS AND REAGENTS

3.1. Chemicals Reagents

Acetic acid	: Carlo Erba, France
2-Mercapto-1-methylimidazole	: abcr, Germany
4-Aminoacetophenone	: Sigma-Aldrich, Germany
Acetyl chloride	: Merck-Schuchardt, Germany
Bromine	: Merck, Germany
Acetone	: Merck, Germany
Tetrahydrofuran (THF)	: Sigma-Aldrich, Germany
Potassium carbonate	: Merck, Germany
Ethanol	: Merck, Germany
2-Chloropropionyl chloride	: Merck, Germany
N,*N*-Dimethylformamide (DMF)	: Sigma-Aldrich, Germany
Triethylamine (TEA)	: Merck, Germany
Thiourea	: Sigma-Aldrich, Germany
2-Mercapto-1-methytetrazole	: Sigma-Aldrich, Germany
5-Chloro-2-mercaptobenzothiazole	: Sigma-Aldrich, Germany
2-Mercapto-5-methy-1,2,3-thiadiazole	: Alfa Aesar, USA
2-Mercapto-5-nitrobenzimidazole	: Sigma-Aldrich, Germany
2-Mercaptobenzimidazole	: J&K Scientific GmbH, Germany
2-Mercaptobenzothiazole	: Acros Organics, Belgium
3-Mercapto-4-methyl-4*H*-1,2,4-triazole	: TCI, Belgium
2-Mercaptobenzoxazole	: Acros Organics, Belgium
2-Mercapto-5-chlorobenzoxazole	: Sigma-Aldrich, Germany
2-Mercaptopyrimidine	: Sigma-Aldrich, Germany
2-Mercapto-5-methylbenzoxazole	: Sigma-Aldrich, Germany

3.2. Instruments and Tools

Lamb Ultraviolet (UV)	: Camag, Cabinet, Switzerland
Analytical balance (electronic)	: Shimadzu, Libror EB-330 HU, Japan
Mass spectrometer	: Shimadzu, LCMS-IT-TOF, Japan
Microplate reader	: BioTek-Synergy H1, USA
Nuclear magnetic resonance spectrometer	: Bruker, UltraShield 400 MHz, USA
Robotic pipetting table	: BioTek- Precision XS, USA
Vortex	: Wisemix, Korea
Sterile cabinet	: Class II TypeA2 (CHC-222A2-60), Korea
Robotic pipetting table	: Biotek Precision XS robotic, USA
Melting point system	: IA9000 Digital Melting Point Apparatus, UK

4. METHODOLOGY

4.1. Chemical Synthesis Methods

4.1.1. Method A: Synthesis of *N*-(4-Acetylphenyl) acetamide

In an ice bath, 4-aminoacetophenone (5 g, 0.036 mol), (1 equivalent), TEA (1.5 equivalent), and THF as a solvent (200 mL), were added to the reaction flask. Acetyl chloride (3.07 ml, 0.043 mol), (1.2 equivalent) was diluted with THF solvent in the dropping funnel and then dropped into the reaction flask for approximately three hours. TLC was used to confirm that the reaction had ended, then we poured the mixture into a glass dish, the solvent and TEA were evaporated under the fume hood, and distilled water was used to wash and filter the precipitated part, then left to dry.

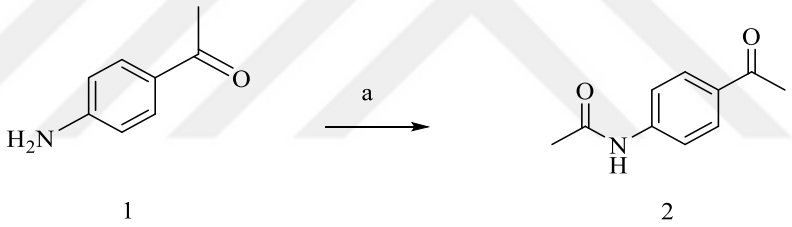

Figure 4.1. *Method A: Synthesis of N-(4-acetylphenyl)acetamide*

4.1.2. Method B: *N*-[4-(2-Bromoacetyl) phenyl]acetamide

We added *N*-(4-acetylphenyl)acetamide (5.5 g, 0.031 mol) (1 equivalent) into a round flask with 1-2 drops of HBr, and acetic acid (200 mL) as solvent. Br_2 (1.91 ml, 0.037 mol) (1.2 equivalents) and acetic acid in the dropping funnel on the balloon were dropped into the reaction for about three hours. TLC was used to confirm that the reaction had ended. After that the product was added to ice water with continuous stirring and then filtered and left to dry.

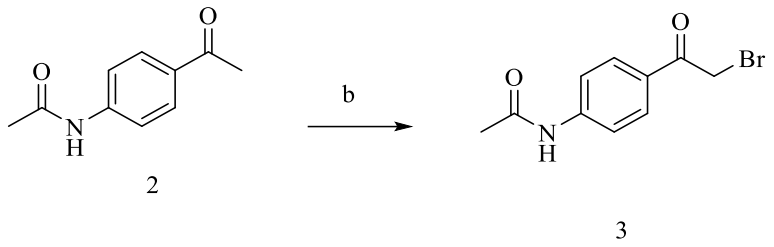

Figure 4.2. *Method B: Synthesis of N-(4-(2-bromoacetyl)phenyl)acetamide*

4.1.3. Method C: *N*-[4-(2-Aminothiazol-4-yl)phenyl]acetamide

N-[4-(2-Bromoacetyl)phenyl]acetamide (8.45 g, 0.033 mol) (1 equivalent) and thiourea (2.51 g, 0.033 mol) (1 equivalent) were added in a round flask with ethanol as a solvent (100 mL) and the reaction was boiled for about two hours under reflux. When the reaction was finished, the substance was poured into the beaker because of that the ethanol was permitted to evaporate under a fume hood, then the substance was scraped from the beaker and placed on the filter paper, washed with a little ethanol then left to dry.

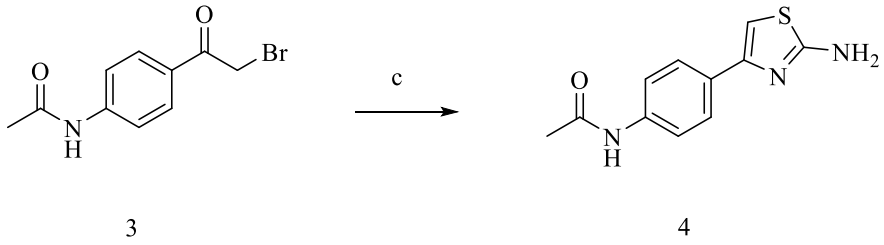

Figure 4.3. *Method C: Synthesis of N-[4-(2-aminothiazol-4-yl)phenyl]acetamide*

4.1.4. Method D: *N*-[4-(4-Acetamidophenyl) thiazol-2-yl]-2-chloropropanamide

N-(4-(2-Aminothiazol-4-yl)phenyl)acetamide (6.26 g, 0.027 mol) (1 equivalent), TEA (3.38 ml, 0.032 mol) (1.2 equivalent), and THF (200 mL) as solvent are mixed into the reaction flask and the reaction placed in ice bath. 2-Chloropropionyl chloride (4.5 ml, 1.2 eq) was diluted with THF solvent in the dropping funnel and then dropped into the reaction flask for approximately three hours. TLC was used to confirm that the reaction had ended, then we

poured the mixture into a glass dish, the solvent and TEA are evaporated under the fume hood, and distilled water was used to wash and filter the precipitated part, then left to dry.

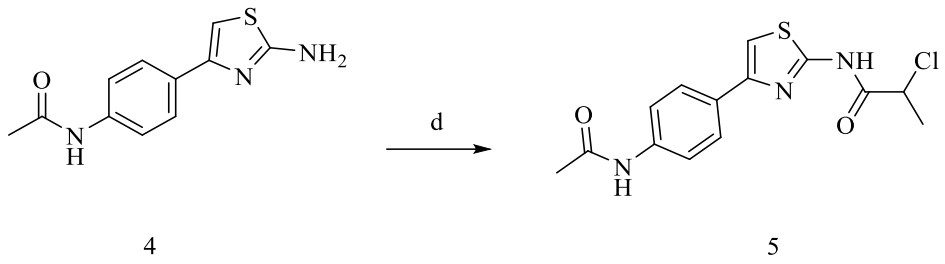

4 5

Figure 4.4. *Method D: Synthesis of N-[4-(4-acetamidophenyl) thiazol-2-yl]-2-chloropropanamide*

4.1.5. Method E: *N*-[4-(4-Acetamidophenyl)thiazol-2-yl]-2-(heteroarylthio) propanamide

N-[4-(4-Acetamidophenyl)thiazol-2-yl]-2-chloropropanamide (0.25 g, 0.00077 mol) (1 equivalent), various heterocyclic mercaptan derivative (1 equivalent), and potassium carbonate (1 equivalent) in acetone (40 mL) solvent for one day at room temperature are mixed. TLC was used to confirm that the reaction had ended, and then poured into the beaker to allow evaporation of the acetone under the fume hood. Distilled water was used to wash the compounds and dried. It was crystallized by ethanol.

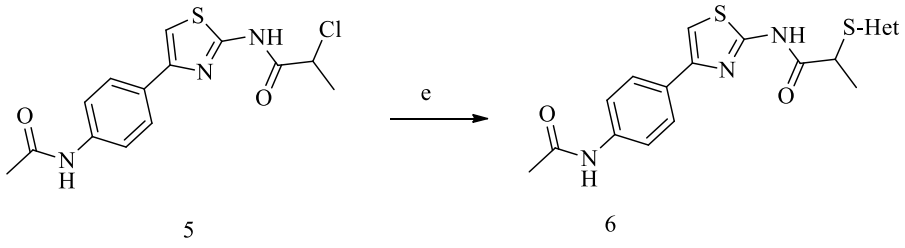

5 6

Figure 4.5. *Method E: Synthesis of N-[4-(4-acetamidophenyl)thiazol-2-yl]-2-(heteroarylthio)propanamide*

4.2. Chemical Analysis

4.2.1. Thin layer chromatography (TLC) studies

Thin Layer Chromatography (TLC) was used to evaluate each compound during and after the reactions. In thin layer chromatography, 20x20 sized, silicagel 60 F_{254} coated aluminum plates were used. Ultraviolet (UV) lamps with 366 nm and 254 wavelengths were used to determine the spots. The plate was then immersed in a mobile phase made up of various concentrations of ethyl acetate/chloroform or petroleum ether mixture (1:1, 3:1, and 1:9).

Under UV light, the advancement of the reaction was evaluated by comparing reaction sample spots to reactant spots at the beginning (254 nm and 366 nm).

4.2.2. Infra-red (IR) spectrometry

The IR spectra of the created substances were taken in Perkin Elmer Spectrum Two FT-IR Spectrometer device by direct compression method after the compounds were finely powdered in an agate mortar and dried in a vacuum oven.

4.2.3. High-resolution mass spectroscopy (HRMS)

Mass spectra of compounds were taken in high resolution (HRMS) on a Shimadzu LCMS-IT-TOF (Shimadzu, Tokyo, Japan) instrument.

4.2.4. ^{1}H-NMR spectral acquisition

^{1}H-NMR spectra of compounds were taken in Bruker 400 MHz Ultra Shield NMR by adding TMS (tetramethyl silane) internal standard in a solution of 20-30 mg of substance in hexadeutero dimethylsulfoxide (DMSO-d_6).

4.2.5. ^{13}C-NMR spectral acquisition

^{13}C-NMR spectra of the compounds were taken on the Bruker 100 MHz UltraShield NMR instrument.

4.3. Melting Point Determination

All substances were added in powder form up to 0.5 cm in height into capillary tubes, and the Electrothermal IA 9100 Melting Point Instrument accustomed to calculating the materials' melting points.

4.4. Determination of Anticholinesterase Activity

The produced substances were examined for their inhibiting effects on acetylcholinesterase and butyrylcholinesterase using the modified Ellman's spectrometric method in 96-well plates. The pipetting procedures were conducted by the Biotek Precision XS robotic system in Winooski, VT, USA. The BioTek-Synergy H1 microplate reader, also located in Winooski, VT, USA, determined the inhibition percentage at a wavelength of 412 nm. All solutions were adjusted to a temperature range of 20-25°C before analysis

In each well of the 96-well plates, a mixture consisting of 140 µL of PO_4^{3-} buffer (0.1 M, pH = 8), 20 µL of 5,5′-dithiobis-(2-nitrobenzoic acid) DTNB (0.01 M), 20 µL of either electric eel AChE or equine serum BChE in 1% gelatin solution at 2.5 U/mL, 20 µL of inhibitor solution in 2% aqueous DMSO, and 10 µL of substrate solution (0.075 M acetylthiocholine iodide (ATC) or butyrylthiocholine iodide (BTC)) was added, resulting in a 210 µL mixture. To evaluate enzyme inhibitory activity, prescreening assessments were conducted at concentrations of 10^{-3} M and 10^{-4} M, and the outcomes were reported as percentages. Tacrine and Donepezil were used as standard compounds BChE for and AChE inhibitory activity, respectively.

To prepare the enzyme-inhibitor solutions, the enzyme, inhibitor, and chromogenic reagent DTNB have been added to the PO_4^{3-} buffer and brooded at 25°C for 15 minutes. The substrate solution (ATC or BTC) was then added to the mixture. The resulting yellow color's absorbance was measured for 5 minutes at 412 nm. A control solution lacking inhibitors was

also prepared. The inhibition percentage was calculated using formula (**I**), taking into account the absorbance difference values, and the control and inhibitor readings were adjusted using blank readings [108, 109].

$$\% \, inhibition = \frac{[(\mathrm{A(C)}-\mathrm{A(B)})-(\mathrm{A(I)}-\mathrm{A(B)})]}{(A(C)-A(B))} * 100 \quad \textbf{(I)}$$

A(B) and A(C) represent the distinction in absorbance measurements for the blank and control, respectively.

Blank (B). Inhibitor and substrate free well.

A(I): Absorbance measurement difference for inhibitors.

The control (C) is an inhibitor-free well.

4.4.1. AChE and BChE enzyme solutions preparation

By dissolving the AChE and BChE enzymes in water, a 1% gelatin solution was created. The enzymes were dissolved in gelatine solution to reach a 500 U/mL concentration. To make a 5 U/mL stock solution, 100 mL of H_2O were combined with one mL of the enzyme solution.in a Measuring flask, then split into 0.7 mL parts and kept at -20°C. The portions of enzyme solution were thawed and allowed to reach room temperature before use. Each aliquot was then diluted with water to a concentration of 2.5 U/mL by filling the 0.7 mL container to 1.4 mL with water.

4.5. Determination of MAO Inhibitory Activity

To assess the potential of the synthesized compounds in inhibiting MAO isoenzymes, an *in vitro* fluorometric technique was employed. The procedure involved creating a solution mixture of tyramine (200 µL,100 mM), Ampliflu™ Red (200 µL, 20 mM), and horseradish peroxidase (200 U/mL, 100 µL) in PO_4^{3-} buffer. Further, solutions of inhibitors in 2% DMSO (10^-3 - 10^-9 M) and remerging *h*MAO-B (0.64 U/mL) and *h*MAO-A (0.5 U/mL) enzymes in phosphate buffer were freshly prepared. The total solution volume was calibrated to 10 mL [110].

The hMAO-A or hMAO-B enzyme solutions and inhibitor solutions (20 L/well) were mixed on a 96-well micro test plate to begin the experiment, which was then incubated for 30 minutes at 37 °C. The working solution was then added (100 L/well) and the plate was incubated once more for 30 minutes. Ex/Em=535/587 nm was used to quantify fluorescence at 5-minute intervals. When a 3 percent H_2O_2 solution (20 mM, 100 L/well) was used in place of enzyme solutions, the fluorescence of the plate was measured to determine the inhibitory impact of the produced compounds on horseradish peroxidase. Additionally, by combining inhibitor and working solutions, non-enzymatic inhibition of the compounds was assessed [108, 109].

The % inhibition was determined using the equation, and all study was carried out in quadruplicate. The % inhibition was determined using the equation, and all study was carried out in quadruplicate **(II),**

$$\%\ inhibition = \frac{[(\mathrm{FCt2}-\mathrm{FCt1})-(\mathrm{FIt2}-\mathrm{FIt1})]}{FCt2-FCt1} * 100 \quad \textbf{(II)}$$

FCt2 refers to the fluorescence detected in a control well at time t2, while FCt1 refers to the fluorescence detected in the same well at time t1. FIt2 refers to the fluorescence detected in an inhibitor well at time t2, while FIt1 refers to the fluorescence detected in the same well at time t1.

4.5.1. Preparation of MAO enzymes solutions

Recombinant *h*MAO-A and *h*MAO-B enzyme solutions were produced by dissolving the enzymes in phosphate buffer solution followed by modifying the final volumes to 10 mL to reach concentrations of 0.5 U/mL and 0.64 U/mL, respectively.

4.6. Prediction of the Pharmacokinetic Profile

SwissADME is its ability to predict the bioavailability of a compound. The tool employs several algorithms to expect the ADME properties of a compound. These algorithms consider factors such as lipophilicity, molecular size, and the presence of functional groups

to predict the pharmacokinetic behavior of a compound *in vivo*. SwissADME also provides information on the potential toxicity of a compound. The platform includes a toxicity prediction module that uses statistical models to predict the toxicity of a compound based on its chemical structure. The toxicity prediction module provides information on the potential risks associated with a compound, such as carcinogenicity, mutagenicity, and hepatotoxicity [111–114].

4.7. Molecular Docking (MD) and Molecular Dynamics Simulations (MDSs)

The binding links of the most active AChE inhibitors (**5d**, **5e**, and **5j**) were visualized by molecular docking simulations using the Schrödinger Maestro interface. The Protein Data Bank (PDB) website was utilized to obtain the X-ray crystal structures of *h*AChE (PDB ID: 4EY7) [115], Protocol of the Schrödinger Suite 2020's Protein Preparation Wizard was utilized to prepare the protein for docking. The LigPrep module was used to prepare the ligands by assigning specific atom types and protonation conditions at pH 7.4±1.0, adding hydrogen atoms, and determining bond orders. Standard precision docking mode in the Glide module was employed to conduct docking simulations and generate the grid [116, 117].

Molecular Dynamics Simulations (MDSs) have become an essential computational technique for assessing the stability of ligands in drug-receptor complexes' active sites over a period [118]. In our investigation, we used MDSs for 5 nanoseconds to ensure the stability of the hits discovered from the docking result [109]. To perform these simulations, we utilized the Desmond application [119] We used the Schrodinger Suite's typical force field (OPLS3e), along an intermolecular potential that can be transferred and a three points (TIP3P) H_2O model, in our study. Energy minimization was applied to the complex [120], and sodium and Chloride ions were employed to neutralize the system. We then utilized the Desmond application to determine the RMSF, RMSD, and Rg values [119].

5. RESULTS AND DISCUSSION

5.1. Synthesis of the Targeted Compounds

5.1.1. Synthesis of *N*-(4-acetylphenyl) acetamide (1)

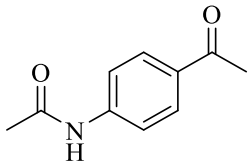

Figure 5.1.*Molecular structure of compound (1)*

N-(4-Acetylphenyl) acetamide 1 was synthesized according to method A. White crystals, compound **1** yield: 88%, measured M.P.=169 °C, literature melting point= 171 °C

5.1.2. Synthesis of *N*-(4-(2-bromoacetyl) phenyl) acetamide (2)

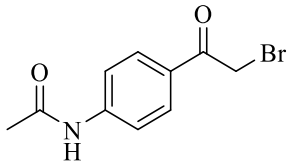

Figure 5.2.*Molecular structure of compound (2)*

N-(4-(2-Bromoacetyl)phenyl)acetamide **2** was synthesized according to method B. Brown crystals, compound **2** yield: 82%, measured M.P.=145 °C, literature melting point= 188 °C [121].

5.1.3. Synthesis of *N*-[4-(2-aminothiazol-4-yl) phenyl] acetamide (3)

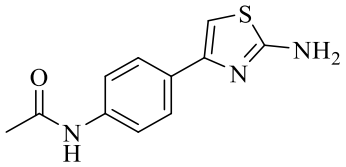

Figure 5.3.*Molecular structure of compound (3)*

N-[4-(2-Aminothiazol-4-yl)phenyl]acetamide **3** was synthesized according to method C. Brown crystals, compound **3** yield: 76%, measured M.P.=283-285 °C, literature melting point= 240-243 °C [122].

5.1.4. Synthesis of *N*-[4-(4-acetamidophenyl)thiazol-2-yl]-2-chloropropanamide (4)

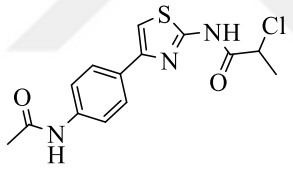

Figure 5.4. *Molecular structure of compound (4)*

N-[4-(4-Acetamidophenyl)thiazol-2-yl]-2-chloropropanamide **4** was synthesized according to method D. Yellow crystals, compound **4** yield: 89%, measured M.P.=184-186 °C.

5.1.5. *N*-[4-(4-Acetamidophenyl)thiazol-2-yl]-2-[(heteroaryl)thio]propanamide derivatives (5a-5l)

The compounds synthesized according to method E.

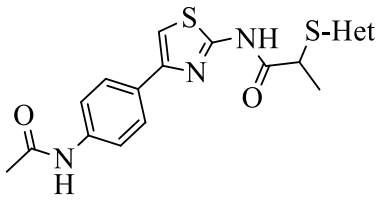

Figure 5.5. *The general molecular structure of derivatives*

5.1.5.1 *N*-[4-(4-Acetamidophenyl)thiazol-2-yl)-]2-((1-methyl-1*H*-imidazole-2 yl)thio)propanamide (5a)

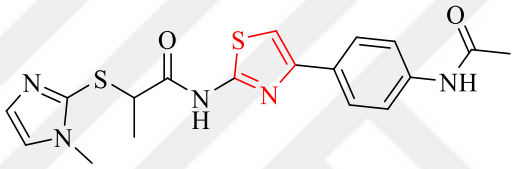

Figure 5.6. *Molecular structure of compound* ***5a***

Physical Characteristics: Material appearance: powder, **Color**: pale yellow, **Yield**: 88%. **M.P. :**134 °C.

IR (ATR) υ_{max} (cm^{-1}): 3174-3115 (N-H stretching) 2976-2929 (C-H stretching), 1668 (C=O stretching, amide), 1541-1408 (C=N stretching, and C=C stretching), 1062-1278 (C-N stretching).

^{1}H-NMR (400 MHz, DMSO-d_6, ppm) *δ:* 1.44 (3H, d, *J*= 6.97 Hz, CH_3), 2.06 (3H, s, $COCH_3$), 3.59 (3H, s, N-CH_3), 4.15 (1H, q, *J*= 6.95 Hz, CH), 7.03 (1H, s, im-H_4), 7.34 (1H, s, im-H_5), 7.52 (1H, s, thiazole), 7.64 (2H, d, *J*= 8.52 Hz, Ph-$H_{2,6}$) , 7.81 (2H, d, *J*= 8.54 Hz, Ph-$H_{3,5}$), 10.05 (1H, brs, N<u>H</u>$COCH_3$), 12.59 (1H, brs, NH)

^{13}C-NMR (100 MHz) (DMSO-d_6) δ (ppm): 17.66 (CH<u>C</u>H_3), 24.51(CO<u>C</u>H_3), 33.69 (NCH_3), 45.52 (CH), 107.51 (thi-C_5), 119.47 (Ph-$C_{3,5}$), 124.84 (Ph-$C_{2,6}$), 126.55 (Ph-C_1), 129.53 (im-$C_{4,5}$), 137.57 (Ph-C_4), 139.49 (Ph-C_4), 149.32 (im-C_2), 158.00 (thi-C_2), 168.80 (<u>C</u>OCH_3), 170.52 (CO).

HRMS (ESI) (*m/z*): [M + 1]$^{+}$: Calculated for $C_{18}H_{19}N_5O_2S_2$: 401.1053; found: 401.1029.

DOPNALAB

	Item	Value
	Acquired Date&Time	22.12.2022 15:15:24
	Acquired by	System Administrator
	Filename	C:\Users\dopnalab\Desktop\MASAÜSTÜ\LEYLA YURTDAŞ\abdurrahman\AB-M\AB-M1.1.isp
	Spectrum name	AB-M1.1
	Sample name	AB-M1
	Sample ID	
	Option	
	Comment	
	No. of Scans	15
	Resolution	4 [cm-1]
	Apodization	Happ-Genzel

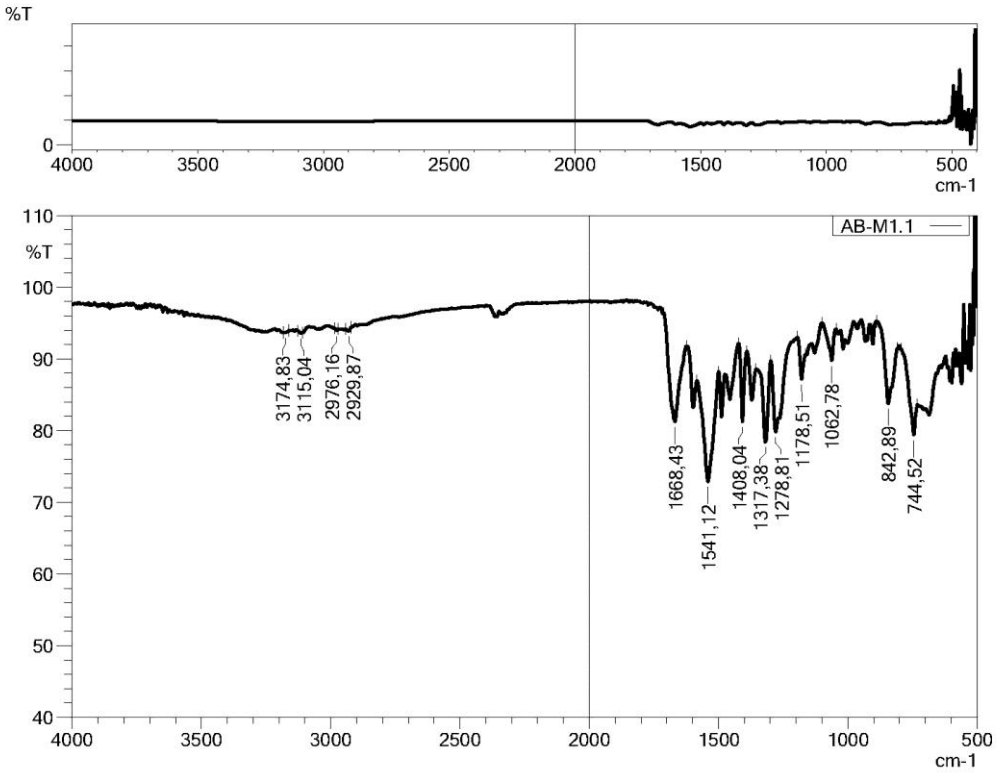

Figure 5.7. *The infrared spectrum of compound **5a***

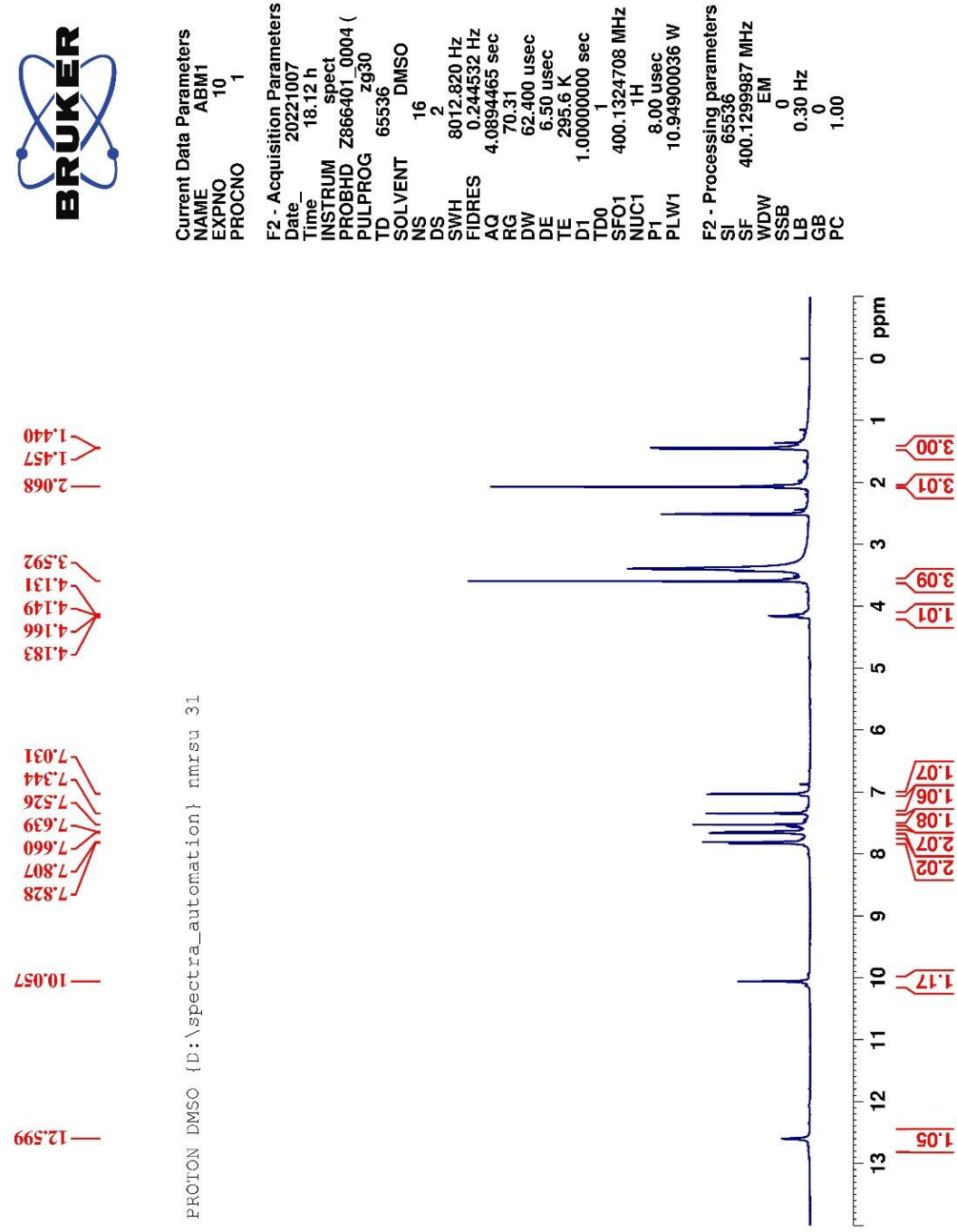

Figure 5.8. *^{1}H-NMR spectrum of compound **5a***

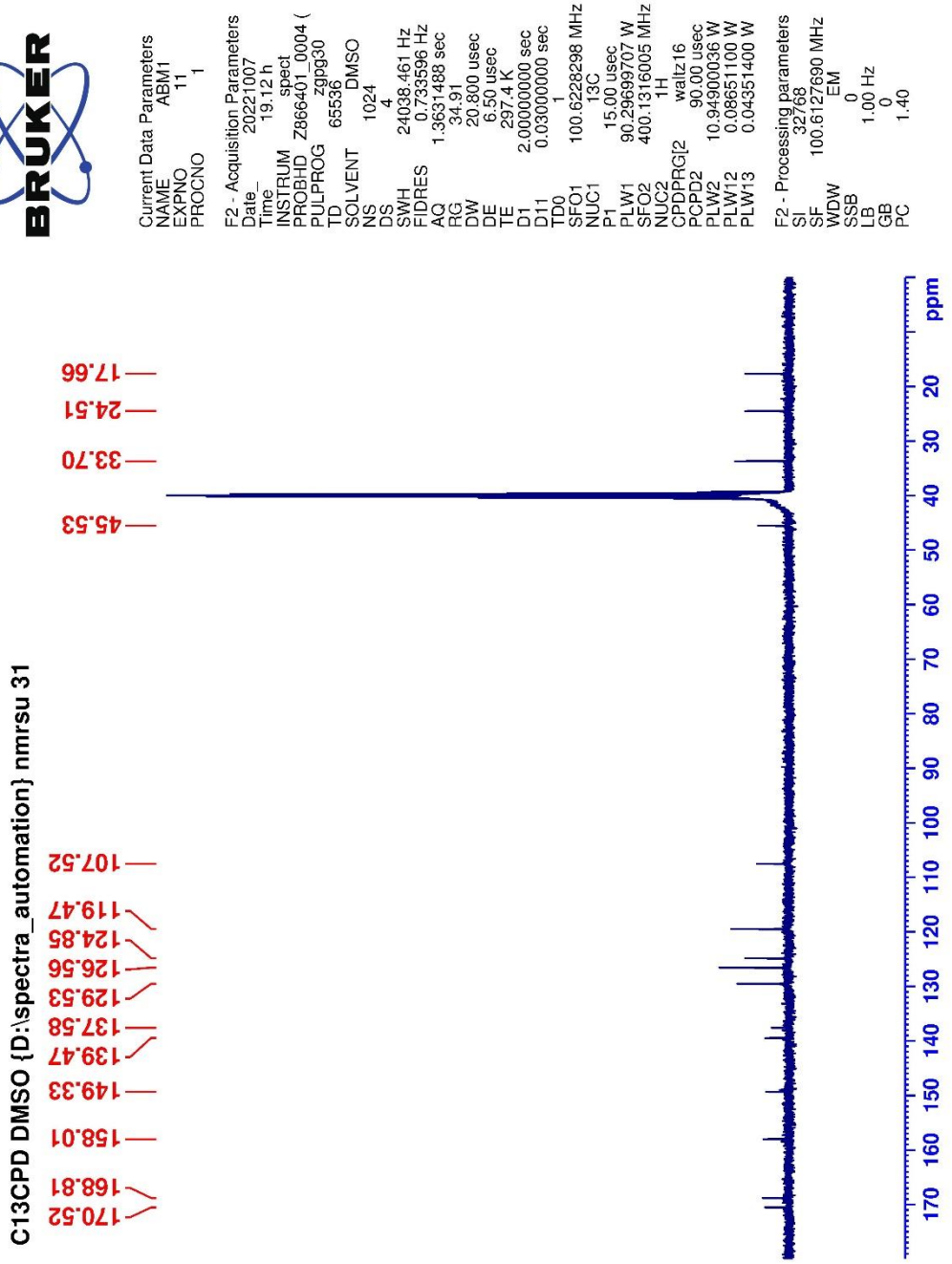

Figure 5.9. *^{13}C-NMR spectrum of compound* ***5a***

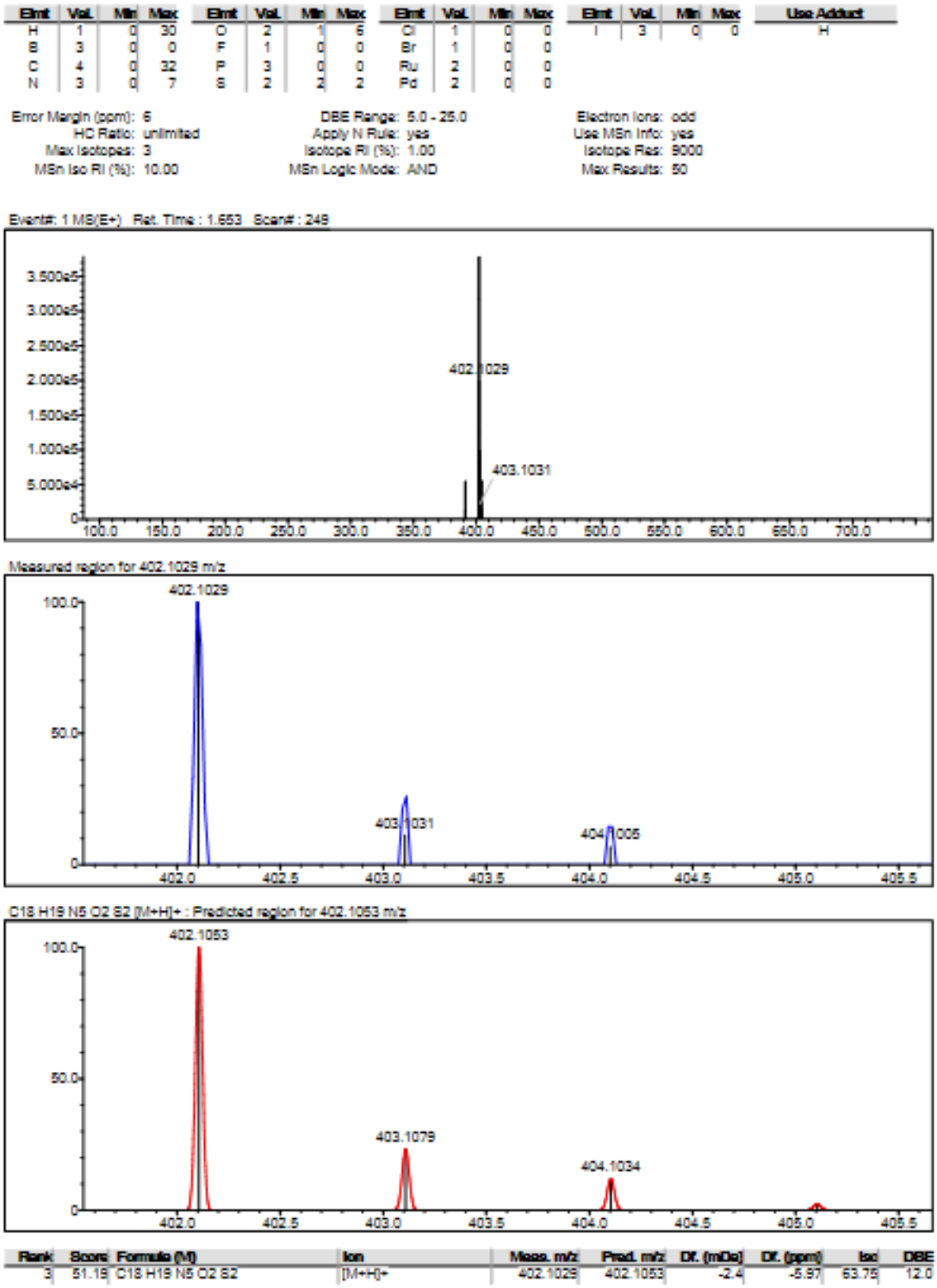

Figure 5.10 *HRMS of compound* ***5a***

5.1.5.2 *N*-[4-(4-Acetamidophenyl)thiazol-2-yl)-]2-[(1-methyl-1*H*-tetrazol-5-yl)thio]propanamide (5b)

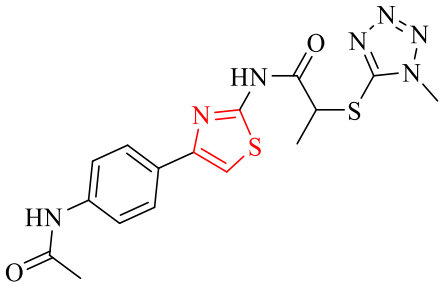

Figure 5.11. *Molecular structure of compound* ***5b***

Physical Characteristics: Material appearance: powder, **Color**: pale yellow, **Yield**: 72%. **M.P:** 151 °C.

IR (ATR) υ_{max} (cm^{-1}): 3304-3184 (N-H stretching), 3116-2978 (C-H stretching), 1668 (C=O stretching, amide), 1541-1408 (C=N stretching, and C=C stretching), 1267 (C-N stretching).

^{1}H-NMR (400 MHz, DMSO-*d_6*, ppm) *δ:*1.63 (3H, d, *J*= 6.99 Hz, CH_3), 2.06 (3H, s, $COCH_3$), 3.97 (3H, s, N-CH_3), 4.60 (1H, q, *J*= 6.98 Hz, CH), 7.56 (1H, s, thiazole), 7.65 (2H, d, *J*= 8.21 Hz, Ph-$H_{2,6}$), 7.82 (2H, d, *J*= 8.21 Hz, Ph-$H_{3,5}$), 10.05 (1H, brs, N<u>H</u>$COCH_3$), 12.68 (1H, brs, NH)

^{13}C-NMR (100 MHz) (DMSO-*d_6*) δ (ppm): 18.72 (CH<u>C</u>H_3), 24.51(CO<u>C</u>H_3), 34.35(NCH_3), 46.22 (CH), 107.79 (thi-C_5), 119.48 (Ph-$C_{3,5}$), 126.57 (Ph-$C_{2,6}$), 129.43 (Ph-C_1), 139.52 (Ph-C_4), 149.42 (thi-C_4), 151.89 (tetrazole-C_5), 157.80 (thi-C_2), 168.81 (<u>C</u>OCH_3), 169.51 (CO).

HRMS (ESI) (*m/z*): [M + 1]$^{+}$: Calculated for $C_{16}H_{17}N_7O_2S_2$ 404.0958.; found: 404.0950.

DOPNALAB

	Item	Value
	Acquired Date&Time	22.12.2022 15:22:08
	Acquired by	System Administrator
	Filename	C:\Users\dopnalab\Desktop\MASAÜSTÜ\LEYLA YURTDAŞ\abdurrahman\AB-M\AB-M2.1.isp
	Spectrum name	AB-M2.1
	Sample name	AB-M2
	Sample ID	
	Option	
	Comment	
	No. of Scans	15
	Resolution	4 [cm-1]
	Apodization	Happ-Genzel

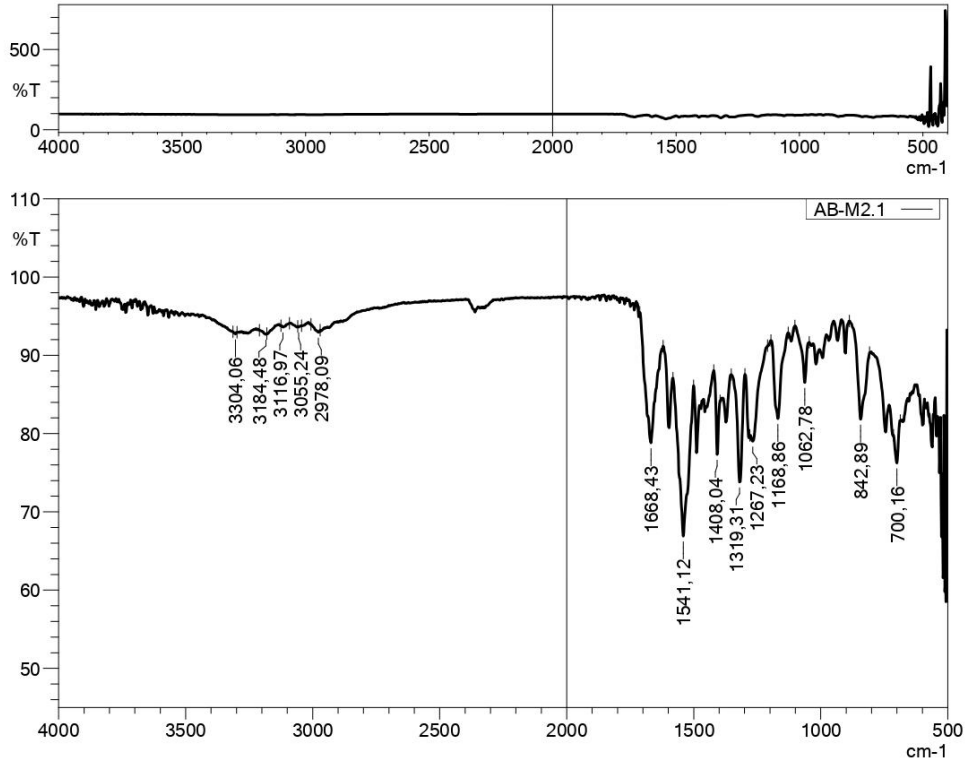

Figure 5.12. *The infrared spectrum of compound* ***5b***

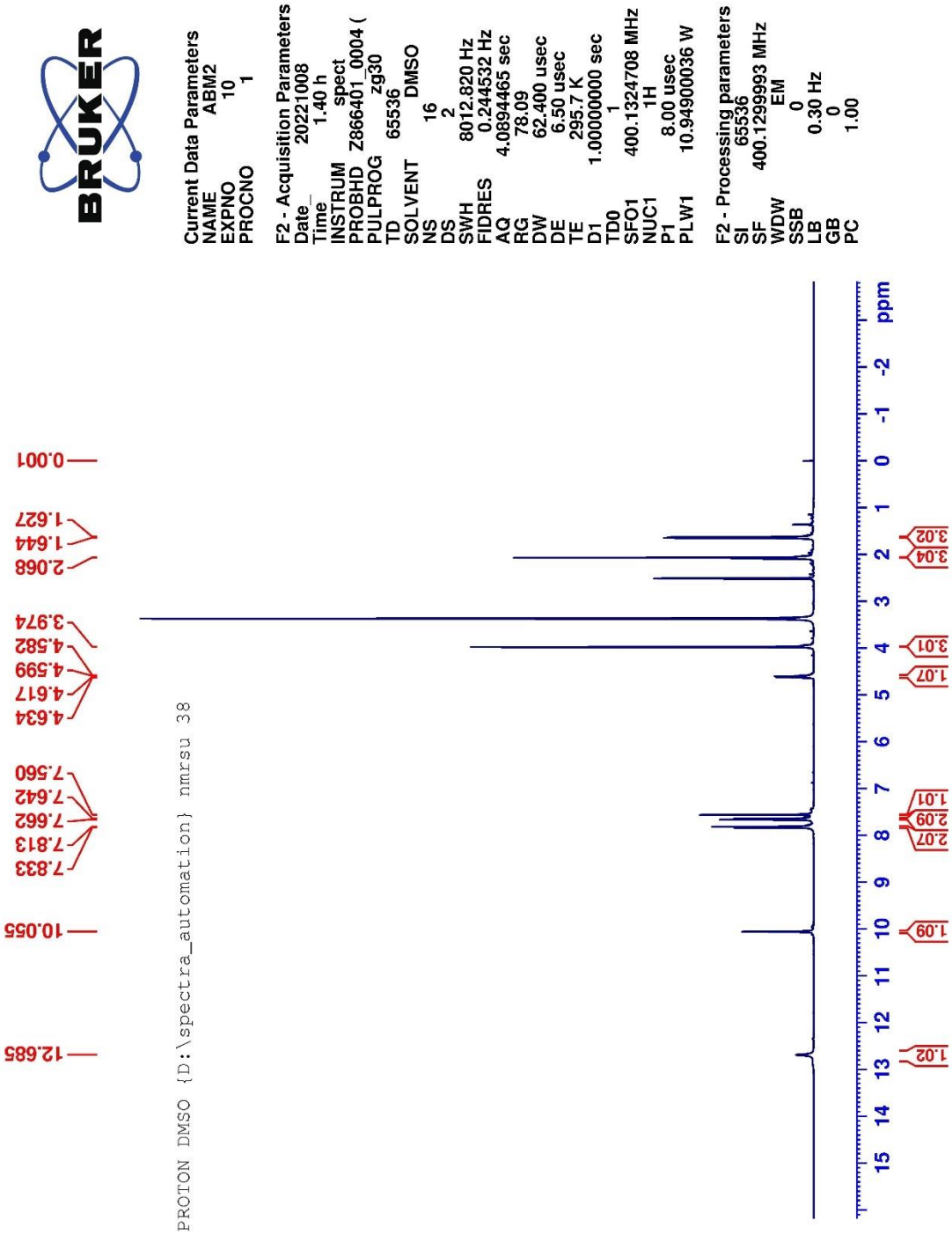

Figure 5.13**.[1]HRMS of compound **5b

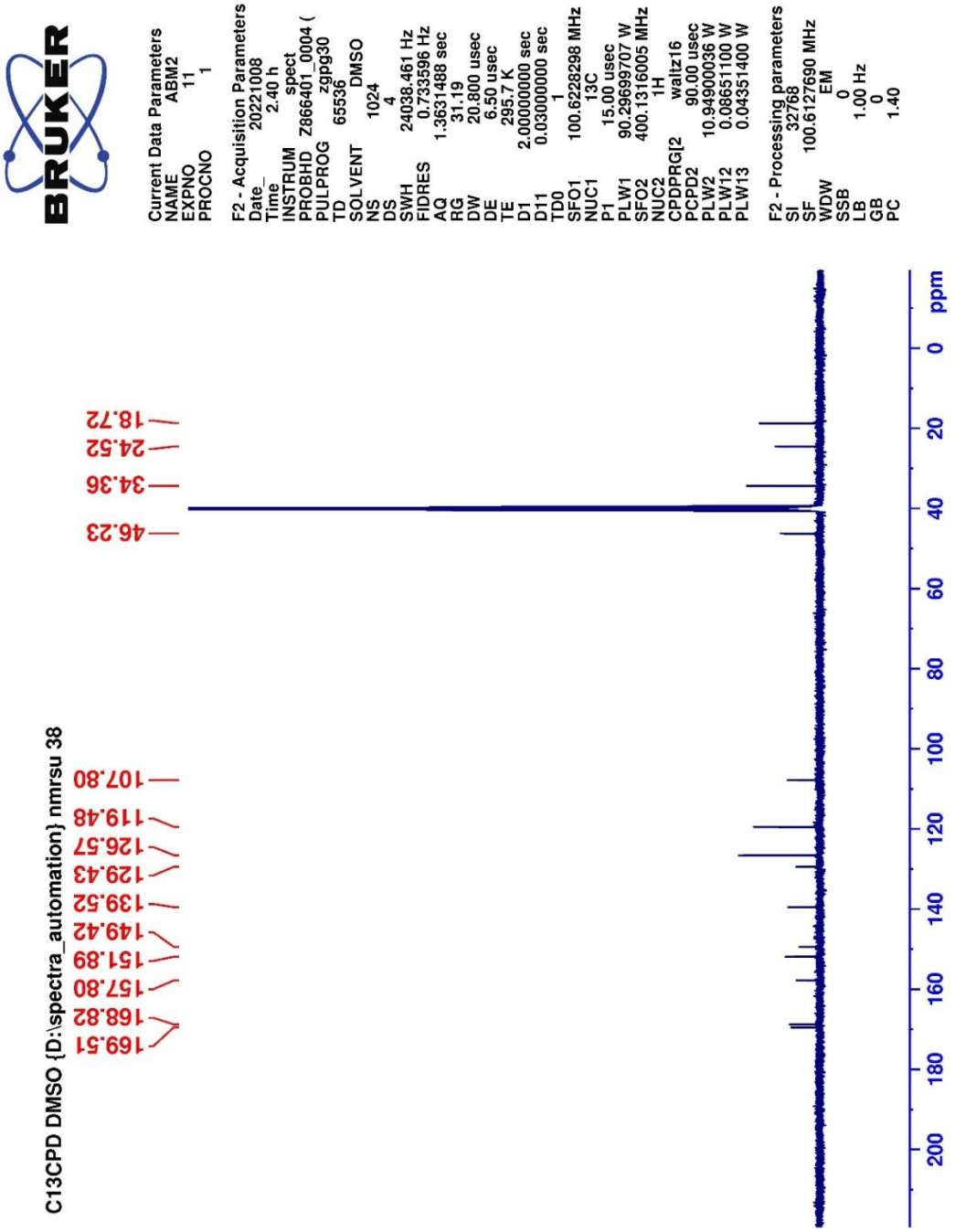

Figure 5.14.*[13]C-NMR spectrum of compound **5b***

Formula Predictor Report - ABM-2_337.lcd

Data File: C:\LabSolutions\Data\Analiz\Asaf\ABM-2_337.lcd

Elmt	Val.	Min	Max	Elmt	Val.	Min	Max	Elmt	Val.	Min	Max	Elmt	Val.	Min	Max	Use Adduct
H	1	0	30	O	2	1	3	Cl	1	0	0	I	3	0	0	H
B	3	0	0	F	1	0	0	Br	1	0	0					
C	4	0	32	P	3	0	0	Ru	2	0	0					
N	3	0	7	S	2	1	2	Pd	2	0	0					

Error Margin (ppm): 5
HC Ratio: unlimited
Max Isotopes: 3
MSn Iso RI (%): 10.00

DBE Range: 5.0 - 25.0
Apply N Rule: yes
Isotope RI (%): 1.00
MSn Logic Mode: AND

Electron Ions: odd
Use MSn Info: yes
Isotope Res: 9000
Max Results: 50

Event#: 1 MS(E+) Ret. Time : 2.053 Scan# : 309

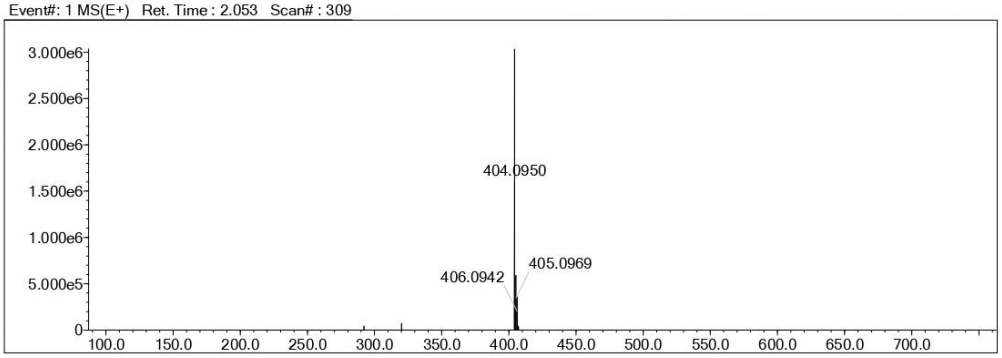

Measured region for 404.0950 m/z

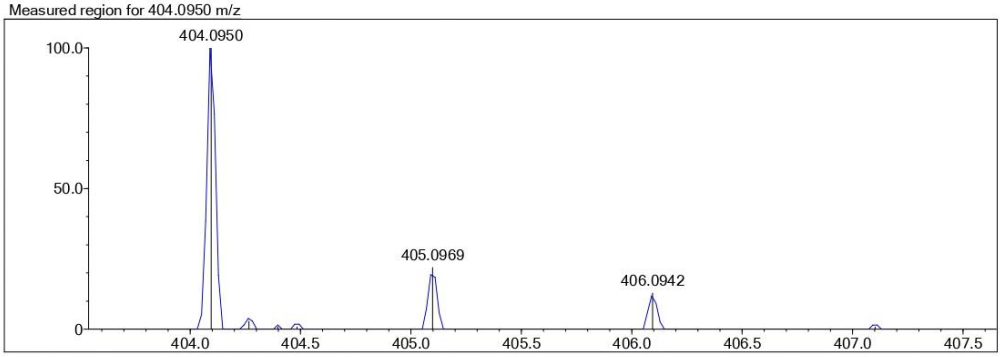

C16 H17 N7 O2 S2 [M+H]+ : Predicted region for 404.0958 m/z

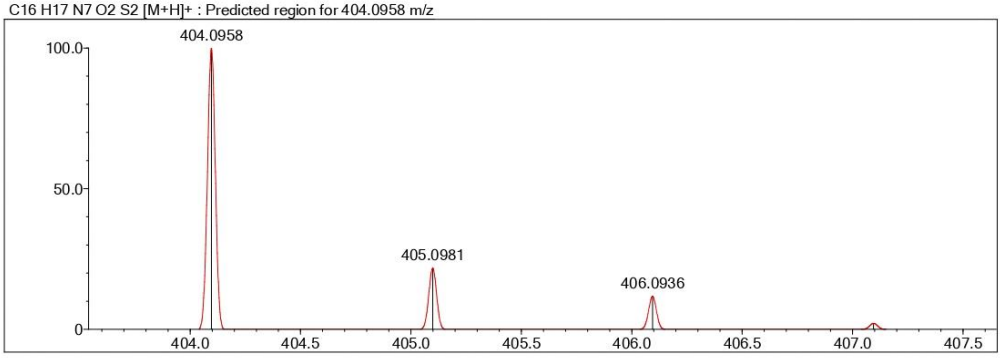

Rank	Score	Formula (M)	Ion	Meas. m/z	Pred. m/z	Df. (mDa)	Df. (ppm)	Iso	DBE
1	72.00	C16 H17 N7 O2 S2	[M+H]+	404.0950	404.0958	-0.8	-1.98	73.81	12.0

Figure 5.15.*HRMS of compound* ***5b***

5.1.5.3 *N*-[4-(4-Acetamidophenyl)thiazol-2-yl)-]2-[(5-chlorobenzothiazol-2-yl)thio]propanamide (5c)

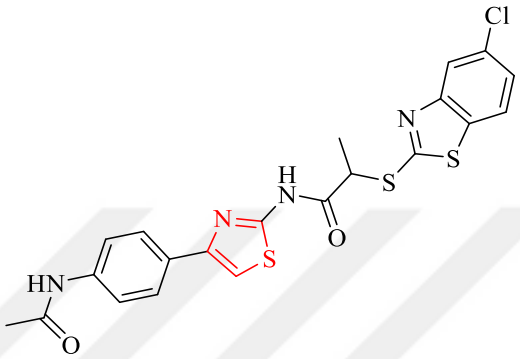

Figure 5.16. *Molecular structure of compound* ***5c***

Physical Characteristics: Material appearance: powder, **Color**: brown, **Yield**: 72%. **M.P.:** 180 °C.

IR (ATR) υ_{max} (cm^{-1}): 3228-3180 (N-H stretching), 3084-2981 (C-H stretching), 1681 (C=O stretching, amide), 1597-1406 (C=N stretching, and C=C stretching), 1178-1010 (C-N stretching).

^{1}H-NMR (400 MHz, DMSO-*d*$_6$, ppm) *δ:* 1.73 (3H, d, *J*= 6.94 Hz,CH_3), 2.08 (3H, s, $COCH_3$), 4.96 (1H, q, *J*= 6.94 Hz, CH) , 7.44 (1H, d, *J*= 8.23 Hz, bt-H_6) , 7.56 (1H, s, thiazole -H_5), 7.67 (2H, d, *J*= 8.33 Hz, Ph-$H_{2,6}$), 7.85 (2H, d, *J*= 8.39 Hz, Ph-$H_{3,5}$) , 7.92 (1H, s, bt-H_4), 8.08 (1H, d, *J*= 8.57 Hz, bt-H_7), 10.07 (1H, s, N<u>H</u>$COCH_3$), 12.81 (1H, s, NH)

^{13}C-NMR (100 MHz) (DMSO-*d*$_6$) δ (ppm): 18.83 ($CH\underline{C}H_3$), 24.51($CO\underline{C}H_3$), 46.62 (CH), 107.75 (thi-C_5), 119.49 (Ph-$C_{3,5}$), 121.22 (bt-C_4), 123.85 (bt-C_6), 125.28 (bt-C_7), 126.58 (Ph-$C_{2,6}$), 129.46 (ph-C_1), 131.78 (bt-C_5), 134.17 (bt-C_{7a}), 139.51 (ph-C_4), 149.41 (thi-C_4), 153.81 (bt-C_{3a}), 157.92 (thi-C_2), 167.59 (bt-C_2), 168.81 ($\underline{C}OCH_3$), 169.60 (CO).

HRMS (ESI) (*m/z*): [M + 1]$^{+}$: Calculated for $C_{21}H_{17}N_4O_2S_3Cl$: 489.0275; found: 489.0278.

DOPNALAB

	Item	Value
	Acquired Date&Time	22.12.2022 15:37:13
	Acquired by	System Administrator
	Filename	C:\Users\dopnalab\Desktop\MASAÜSTÜ\LEYLA YURTDAŞ\abdurrahman\AB-M\AB-M4.1.isp
	Spectrum name	AB-M4.1
	Sample name	AB-M4
	Sample ID	
	Option	
	Comment	
	No. of Scans	15
	Resolution	4 [cm-1]
	Apodization	Happ-Genzel

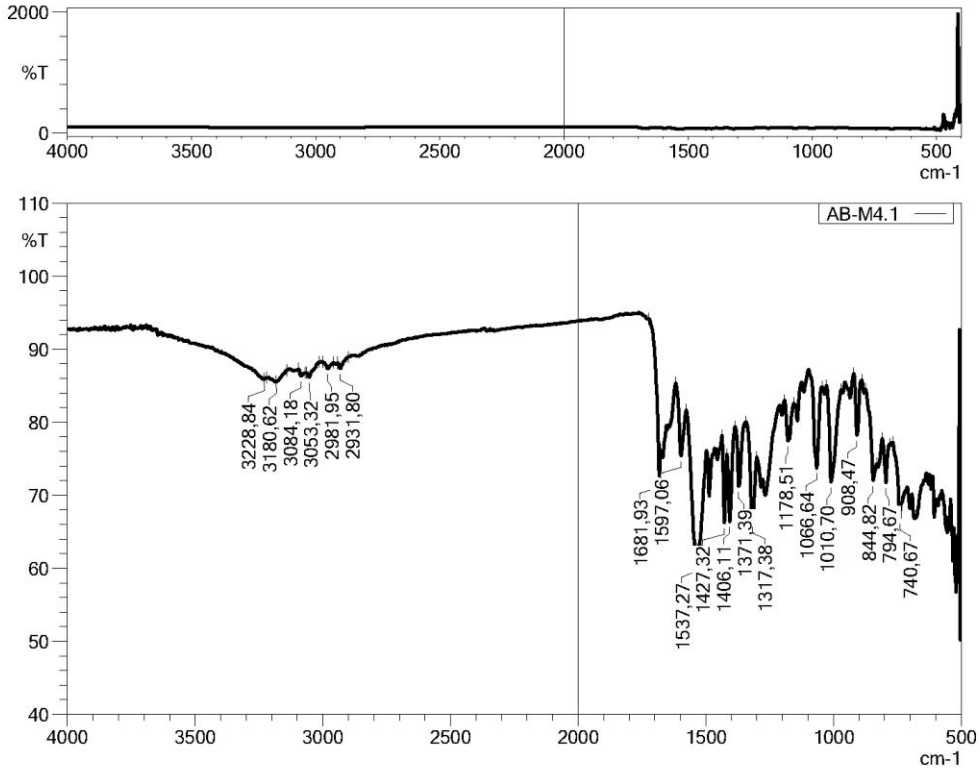

Figure 5.17. *The infrared spectrum of compound* ***5c***

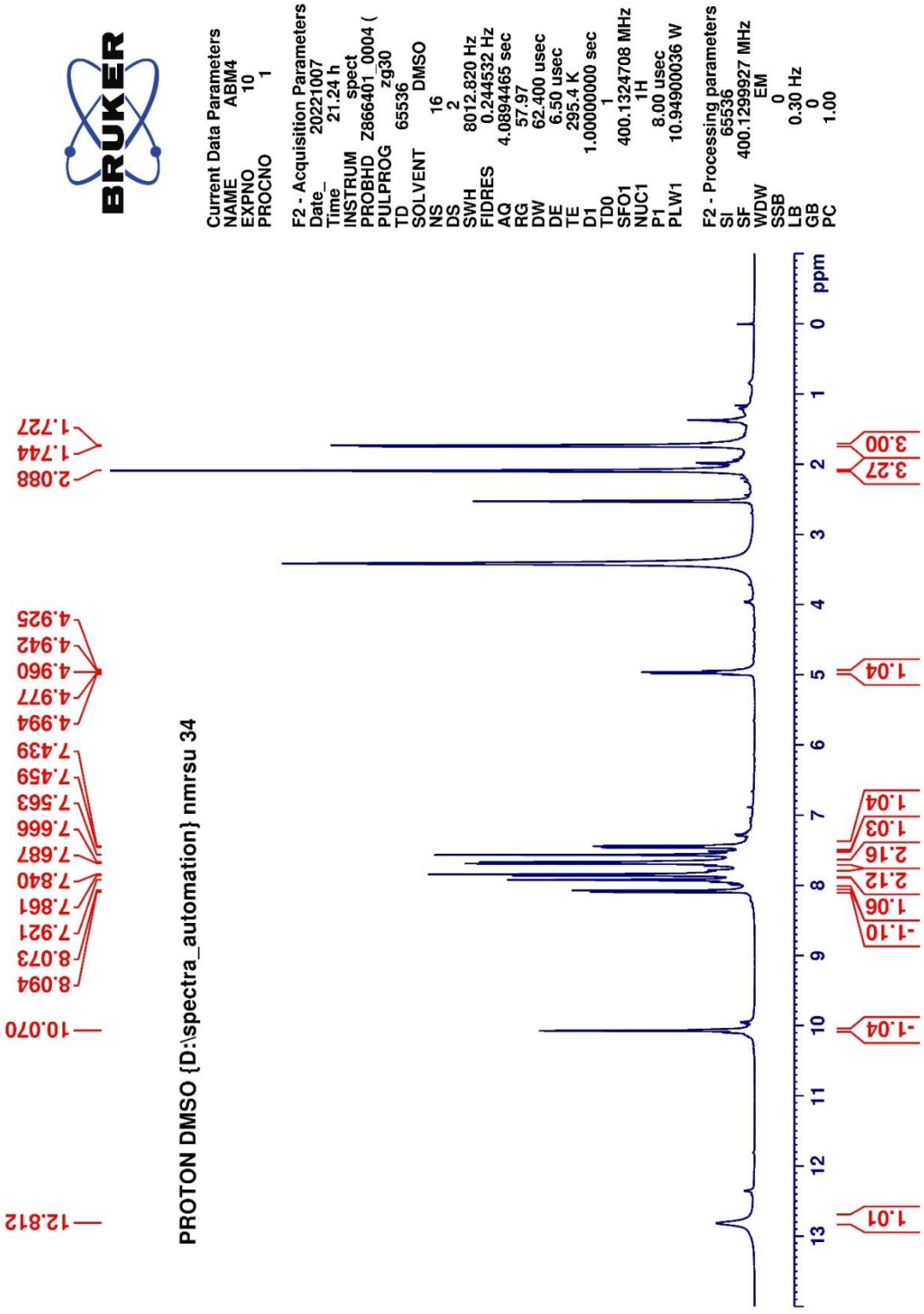

Figure 5.18. *^{1}H-NMR spectrum of compound **5c***

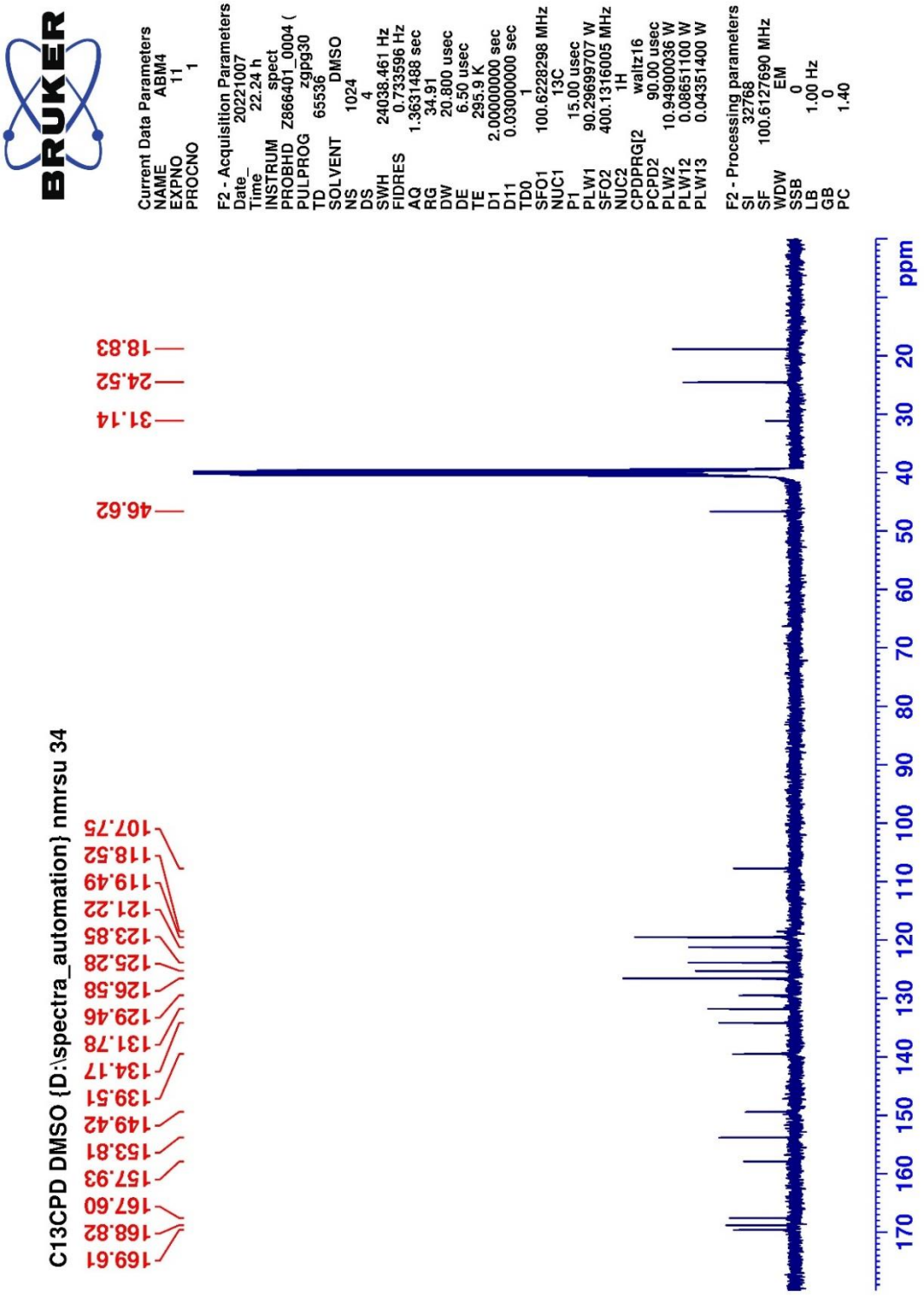

Figure 5.19.*[13]C-NMR spectrum of compound **5c***

Formula Predictor Report - AB-M4_349.lcd

Page 1 of 1

Data File: C:\LabSolutions\Data\Analiz\Asaf\AB-M4_349.lcd

Elmt	Val.	Min	Max	Elmt	Val.	Min	Max	Elmt	Val.	Min	Max	Elmt	Val.	Min	Max	Use Adduct
H	1	0	30	O	2	0	4	S	2	2	3	Ru	2	0	0	H
C	4	0	30	F	1	0	0	Cl	1	1	1	Pd	2	0	0	
N	3	0	6	P	3	0	0	Br	1	0	0	I	3	0	0	

Error Margin (ppm): 5
HC Ratio: unlimited
Max Isotopes: 3
MSn Iso RI (%): 10.00

DBE Range: 5.0 - 25.0
Apply N Rule: yes
Isotope RI (%): 1.00
MSn Logic Mode: AND

Electron Ions: odd
Use MSn Info: yes
Isotope Res: 9000
Max Results: 50

Event#: 1 MS(E+) Ret. Time : 4.760 -> 4.760 Scan# : 715 -> 715

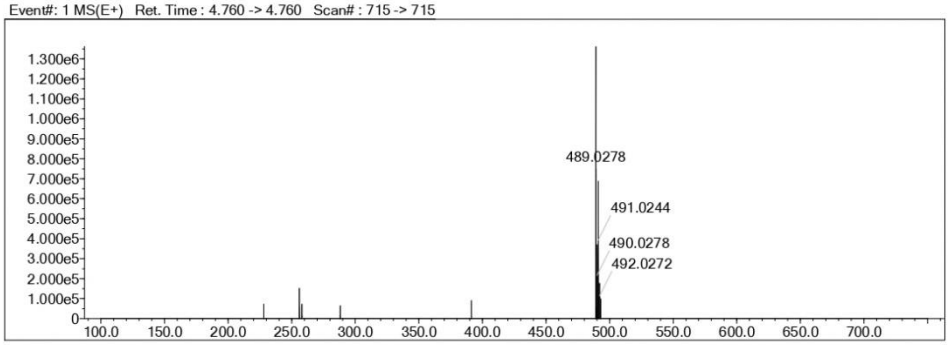

Measured region for 489.0278 m/z

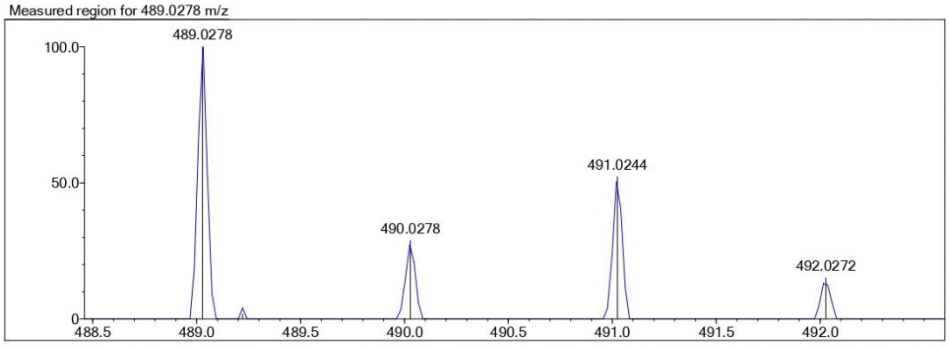

C21 H17 N4 O2 S3 Cl [M+H]+ : Predicted region for 489.0275 m/z

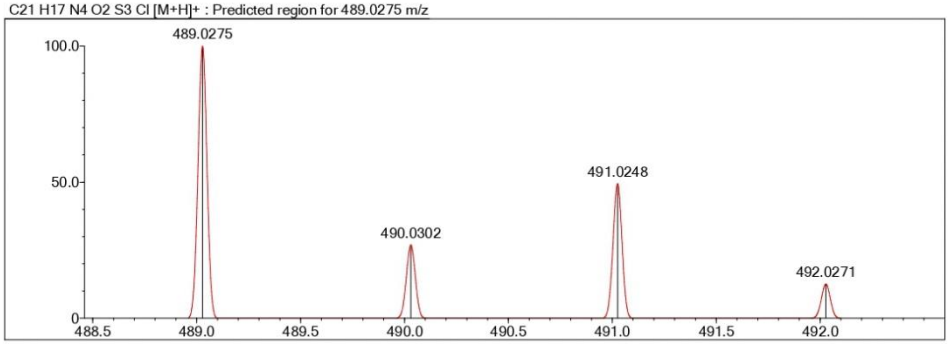

Rank	Score	Formula (M)	Ion	Meas. m/z	Pred. m/z	Df. (mDa)	Df. (ppm)	Iso	DBE
1	96.53	C21 H17 N4 O2 S3 Cl	[M+H]+	489.0278	489.0275	0.3	0.61	96.53	15.0

Figure 5.20. *HRMS of compound* ***5c***

5.1.5.4 *N*-[4-(4-Acetamidophenyl)thiazol-2-yl)-]2-[(5-methyl-1,3,4-thiadiazol-2-yl)thio]propanamide (5d)

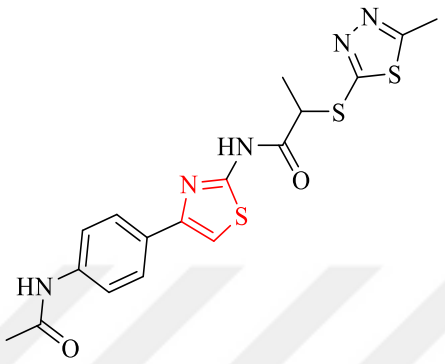

Figure 5.21. *Molecular structure of compound* ***5d***

Physical Characteristics: Material appearance: powder, **Color**: light brown, **Yield**: 93%. **M.P.**: 140-143 °C.

IR (ATR) υ_{max} (cm^{-1}): 3234-3180 (N-H stretching), 3084-2848 (C-H stretching), 1688 (C=O stretching), 1597-1427 (C=N stretching, and C=C stretching), 1178-1010 (C-N stretching).

^{1}H-NMR (400 MHz, DMSO-d_6, ppm) δ: 1.61 (3H, d, *J*= 6.98 Hz, $\underline{CH}_3CHCO$), 2.07 (3H, s, $COCH_3$), 2.69 (3H, s, CH_3), 4.70 (1H, q, *J*= 6.96 Hz, CH), 7.54 (1H, s, thiazole-H_5), 7.65 (2H, d, *J*= 8.46 Hz, Ph-$H_{2,6}$), 7.83 (2H, d, *J*= 8.51 Hz, Ph-$H_{3,5}$), 10.04 (1H, s, $N\underline{H}COCH_3$), 12.68 (1H, s, NH).

^{13}C-NMR (100 MHz) (DMSO-d_6) δ (ppm): 15.71 ($\underline{C}H_3CHCO$), 18.41 (CH_3), 24.51 ($CO\underline{C}H_3$), 46.43 (CH), 107.69 (thi-C_5), 119.49 (Ph-$C_{3,5}$), 126.57 (Ph-$C_{2,6}$), 129.48 (Ph-C_1), 139.50 (Ph-C_4), 149.38 ($N\underline{C}HCH_3$), 157.92 (thi-C_4), 162.41 (thiadiazole-C_2), 167.42 (thi-C_2), 168.81 ($\underline{C}OCH_3$), 169.72 (CO).

HRMS (ESI) (*m/z*): [M + 1]$^{+}$: Calculated for $C_{17}H_{17}N_5O_2S_3$: 420.0617; found 420.0613.

DOPNALAB

	Item	Value
	Acquired Date&Time	22.12.2022 15:41:44
	Acquired by	System Administrator
	Filename	C:\Users\dopnalab\Desktop\MASAÜSTÜ\LEYLA YURTDAŞ\abdurrahman\AB-M\AB-M5.1.isp
	Spectrum name	AB-M5.1
	Sample name	AB-M5
	Sample ID	
	Option	
	Comment	
	No. of Scans	15
	Resolution	4 [cm-1]
	Apodization	Happ-Genzel

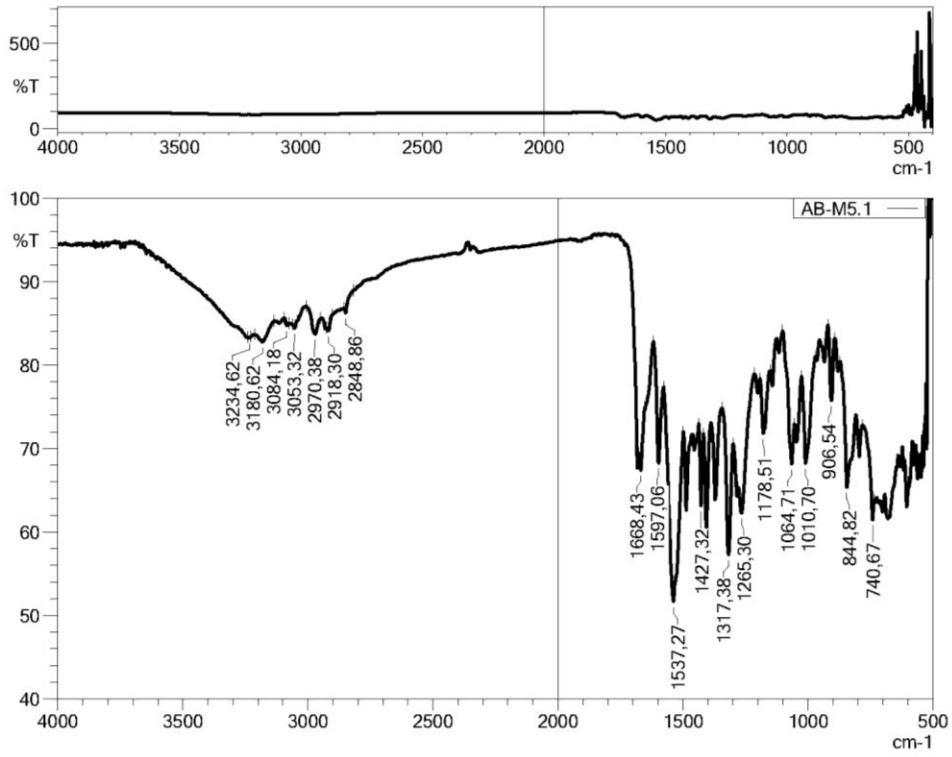

Figure 5.22.*The infrared spectrum of compound* ***5d***

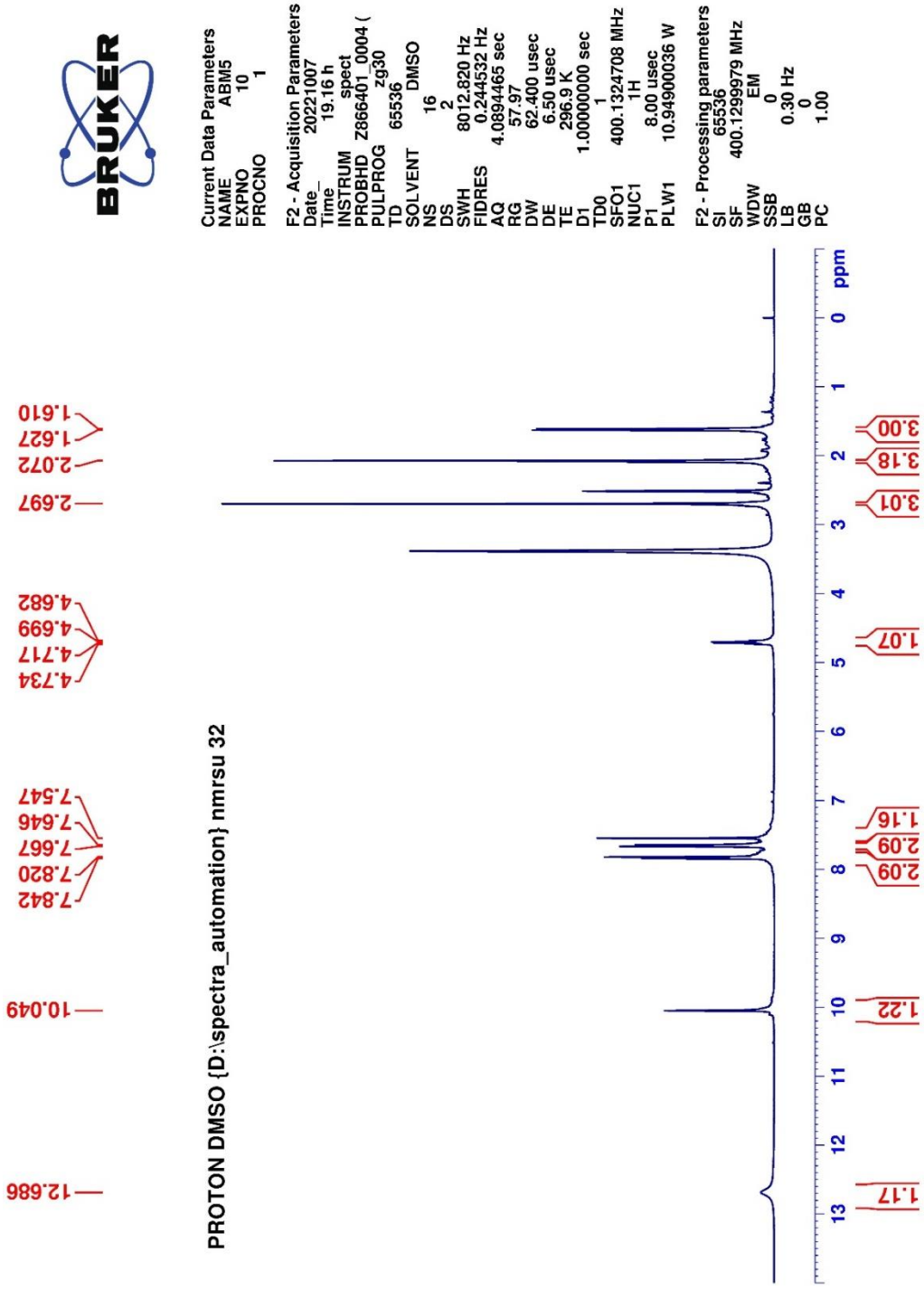

Figure 5.23. *^{1}H-NMR spectrum of compound **5d***

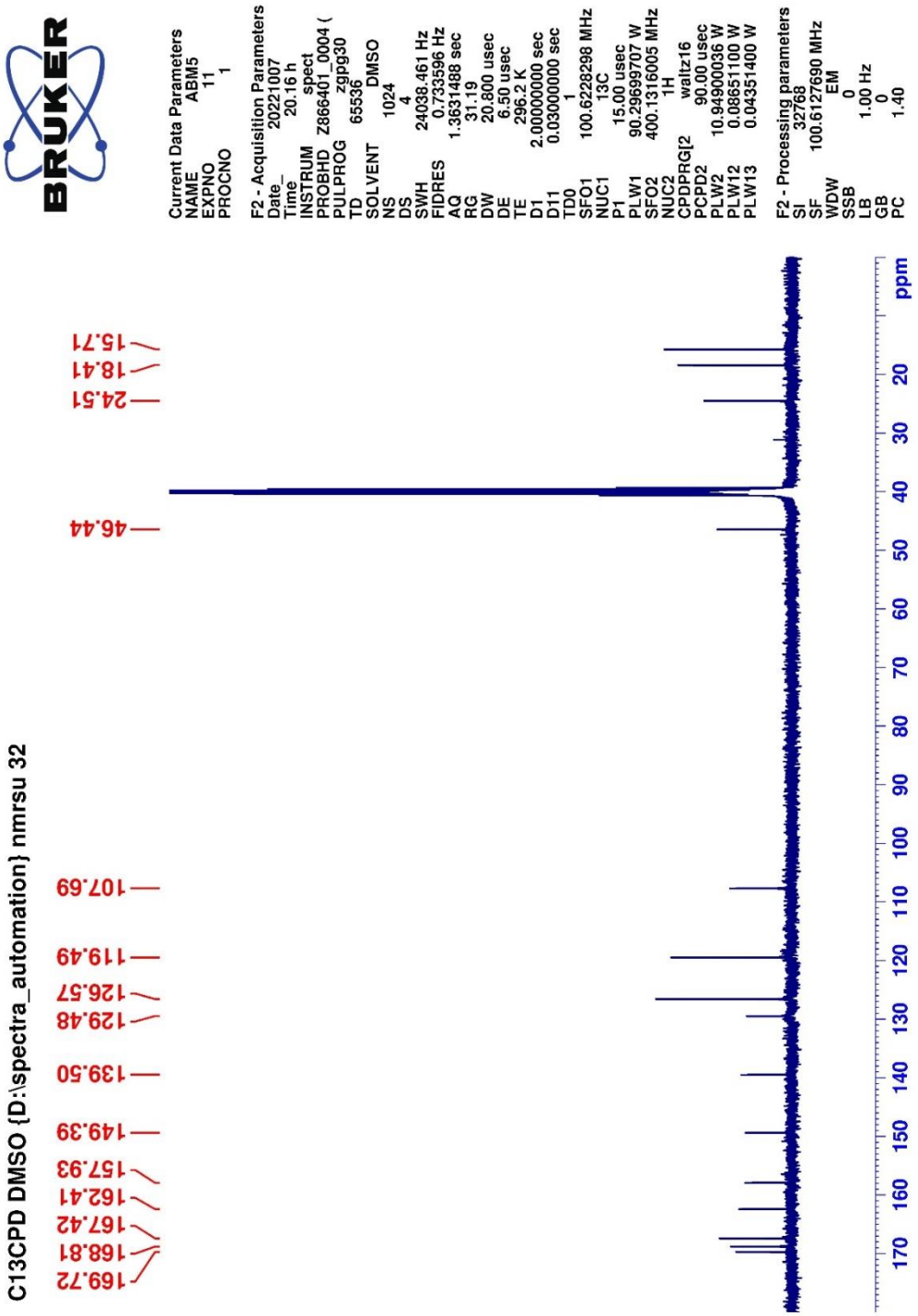

Figure 5.24. *^{13}C-NMR spectrum of compound* ***5d***

Formula Predictor Report - AB-M5_350.lcd

Page 1 of 1

Data File: C:\LabSolutions\Data\Analiz\Asaf\AB-M5_350.lcd

Elmt	Val.	Min	Max	Elmt	Val.	Min	Max	Elmt	Val.	Min	Max	Elmt	Val.	Min	Max	Use Adduct
H	1	0	30	O	2	0	4	S	2	3	3	Ru	2	0	0	H
C	4	0	30	F	1	0	0	Cl	1	0	0	Pd	2	0	0	
N	3	0	5	P	3	0	0	Br	1	0	0	I	3	0	0	

Error Margin (ppm): 5
HC Ratio: unlimited
Max Isotopes: 3
MSn Iso RI (%): 10.00

DBE Range: 5.0 - 25.0
Apply N Rule: yes
Isotope RI (%): 1.00
MSn Logic Mode: AND

Electron Ions: odd
Use MSn Info: yes
Isotope Res: 9000
Max Results: 50

Event#: 1 MS(E+) Ret. Time : 2.147 Scan# : 323

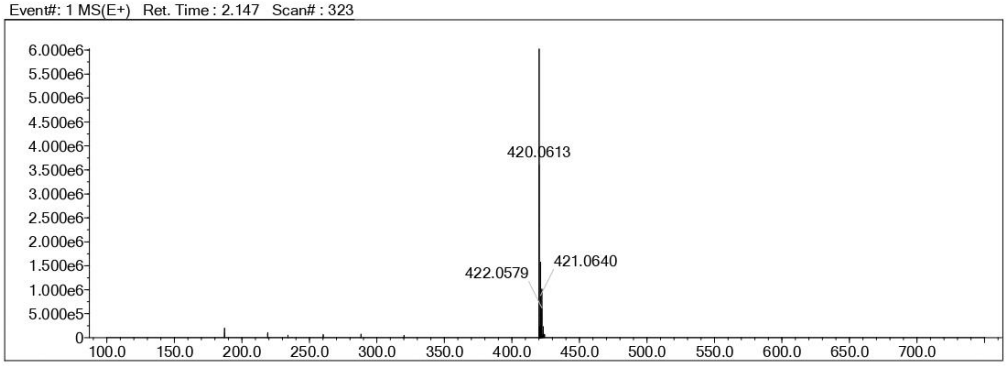

Measured region for 420.0613 m/z

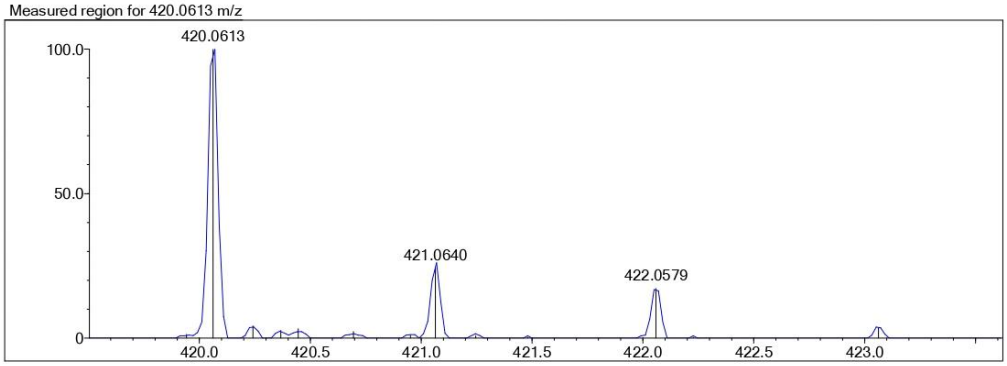

C17 H17 N5 O2 S3 [M+H]+ : Predicted region for 420.0617 m/z

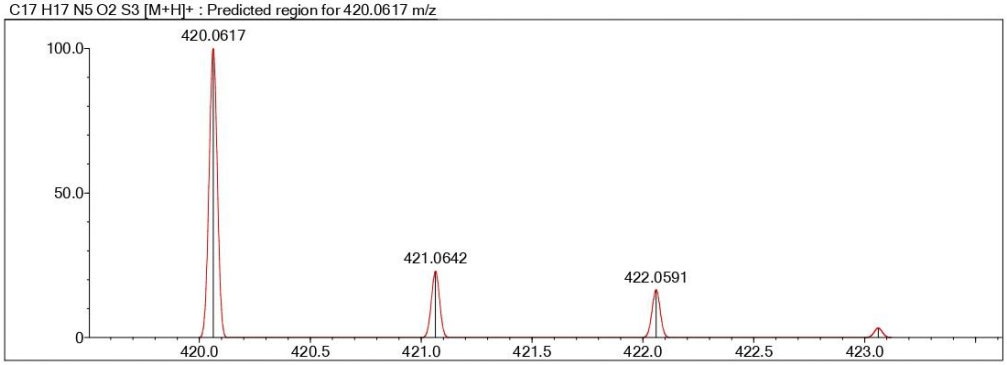

Rank	Score	Formula (M)	Ion	Meas. m/z	Pred. m/z	Df. (mDa)	Df. (ppm)	Iso	DBE
1	100.00	C17 H17 N5 O2 S3	[M+H]+	420.0613	420.0617	-0.4	-0.95	100.00	12.0

Figure 5.25.*HRMS of compound **5d***

5.1.5.5 *N*-[4-(4-Acetamidophenyl)thiazol-2-yl]-2-[(5-nitro-1*H*-benzimidazol-2-yl)thio]propanamide (5e)

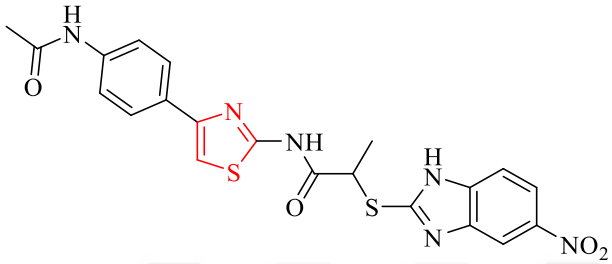

Figure 5.26. *Molecular structure of compound* ***5e***

Physical Characteristics: Material appearance: powder, **Color**: dark orange, **Yield**: 91%. **M.P** :177 °C.

IR (ATR) υ_{max} (cm^{-1}): 3080-3063 (N-H stretching), 2972-2931 (C-H stretching), 1681-1688 (C=O stretching, amide), 1405-1539 (C=N stretching, and C=C stretching), 1371 (N=O stretching), 1178-1008 (C-N stretching).

^{1}H-NMR (400 MHz, DMSO-d_6, ppm) δ: 1.67 (3H, d, *J*= 7.03 Hz, CH_3), 2.07 (3H, s, $COCH_3$), 4.90 (1H, q, *J*= 7.00 Hz, CH), 7.52 (1H, s, thiazole-H_5), 7.58 (1H, d, *J*= 8.38 Hz, benzimidazole -H_7), 7.65 (2H, d, *J*= 8.38 Hz, Ph-$H_{2,6}$), 7.83 (2H, d, *J*= 8.41 Hz, Ph-$H_{3,5}$), 8.02 (1H, d, benzimidazole -H_6), 8.33 (1H, s, benzimidazole -H_4), 10.06 (1H, s, $NHCOCH_3$, NH).

^{13}C-NMR (100 MHz) (DMSO-d_6) δ (ppm): 18.35 (CH_3), 24.50 ($CO\underline{C}H_3$), 44.13 (CH), 107.41 (thi-C_5), 110.89 (benzimidazole -C_7), 114.11 (benzimidazole -C_4), 117.11 (benzimidazole -C_5), 119.46 (Ph-$C_{3,5}$), 126.53 (Ph-$C_{2,6}$), 129.50 (Ph-C_1), 141.71 (Ph-C_4, benzimidazole -C_{7a}), 146.77 (benzimidazole -$C_{6,3a}$), 149.28 (benzimidazole -C_2), 158.01 (thi -C_4), 158.08 (thi -C_2), 168.80 ($\underline{C}OCH_3$), 170.61 (CO).

HRMS (ESI) (*m/z*): [M + 1]$^{+}$: Calculated for $C_{21}H_{18}N_6O_4S_2$: 483.0894; found 483.0904.

DOPNALAB

	Item	Value
	Acquired Date&Time	22.12.2022 15:58:21
	Acquired by	System Administrator
	Filename	C:\Users\dopnalab\Desktop\MASAÜSTÜ\LEYLA YURTDAŞ\abdurrahman\AB-M\AB-M7.1.isp
	Spectrum name	AB-M7.1
	Sample name	AB-M7
	Sample ID	
	Option	
	Comment	
	No. of Scans	15
	Resolution	4 [cm-1]
	Apodization	Happ-Genzel

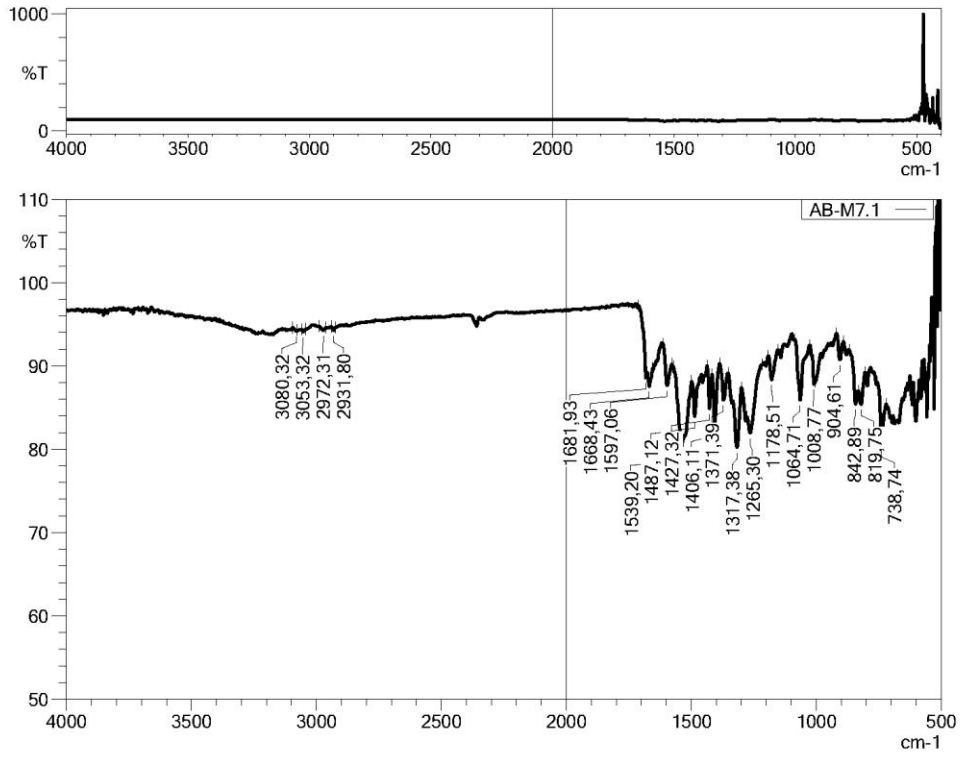

Figure 5.27. *The infrared spectrum of compound* ***5e***

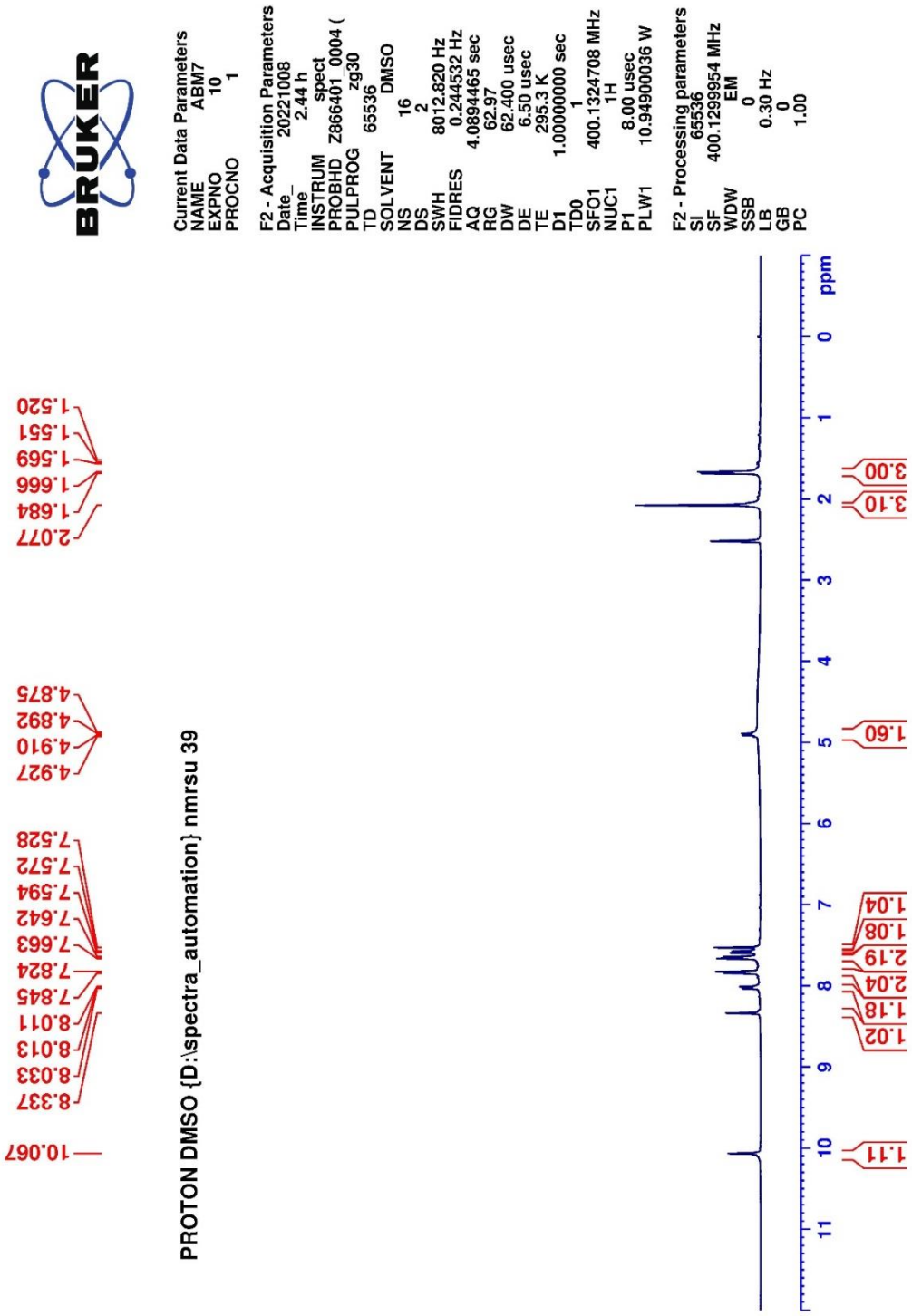

Figure 5.28.*[1]H-NMR spectrum of compound **5e***

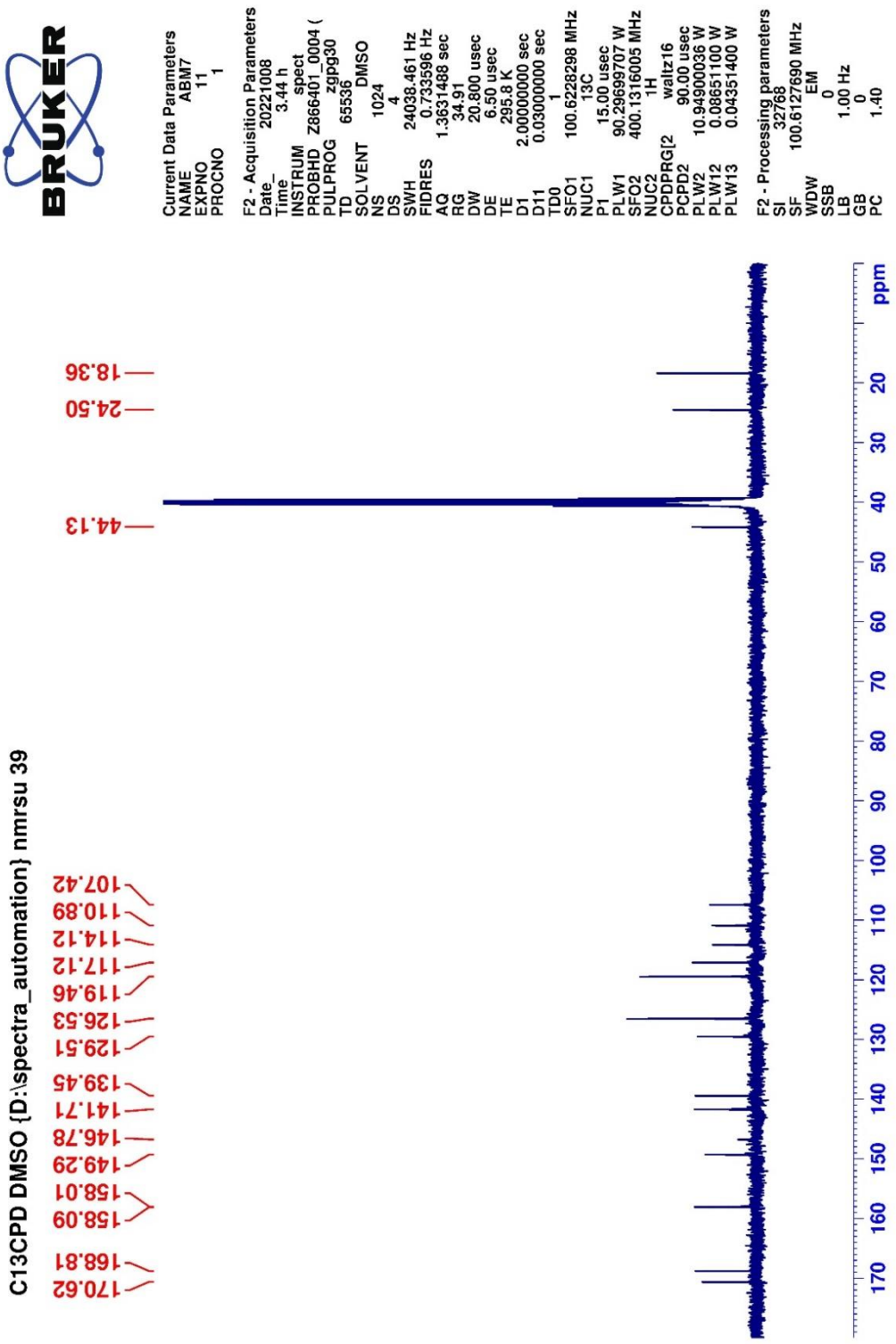

Figure 5.29. *^{13}C-NMR spectrum of compound **5e***

Formula Predictor Report - AB-M7B_356.lcd

Data File: C:\LabSolutions\Data\Analiz\Asaf\AB-M7B_356.lcd

Elmt	Val.	Min	Max	Elmt	Val.	Min	Max	Elmt	Val.	Min	Max	Elmt	Val.	Min	Max	Use Adduct
H	1	0	30	O	2	0	4	S	2	1	2	Ru	2	0	0	H
C	4	0	30	F	1	0	0	Cl	1	0	0	Pd	2	0	0	
N	3	0	8	P	3	0	0	Br	1	0	0	I	3	0	0	

Error Margin (ppm): 5
HC Ratio: unlimited
Max Isotopes: 3
MSn Iso RI (%): 10.00

DBE Range: 0.0 - 30.0
Apply N Rule: yes
Isotope RI (%): 1.00
MSn Logic Mode: AND

Electron Ions: both
Use MSn Info: yes
Isotope Res: 9000
Max Results: 50

Event#: 1 MS(E+) Ret. Time : 2.160 Scan# : 325

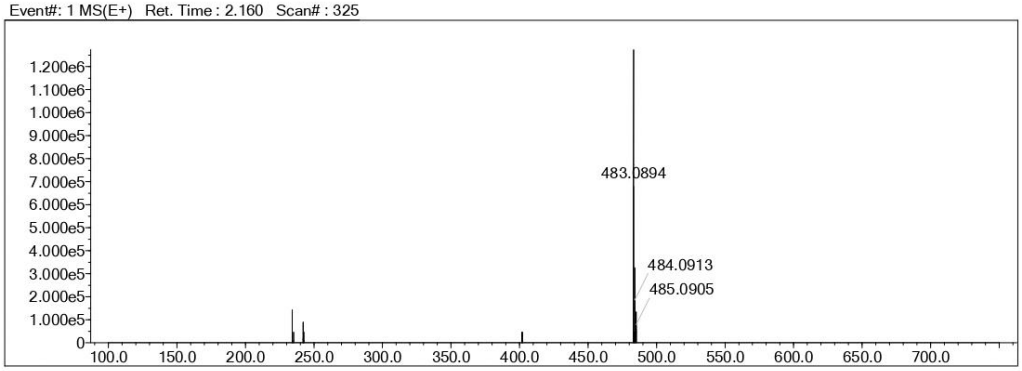

Measured region for 483.0894 m/z

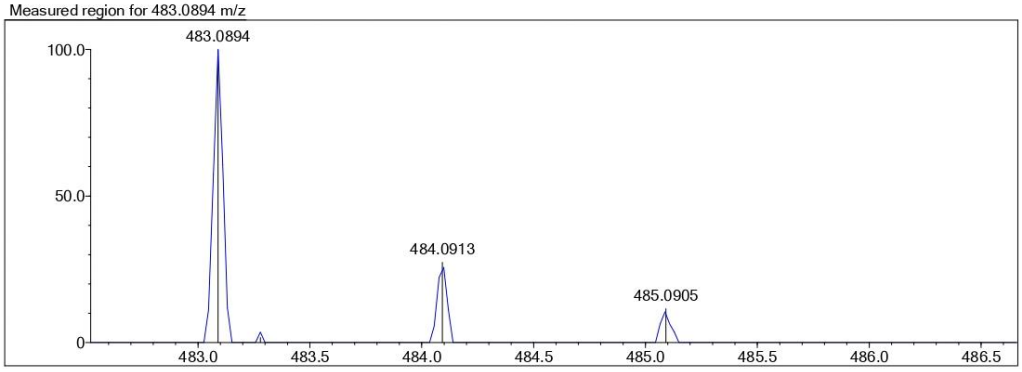

C21 H18 N6 O4 S2 [M+H]+ : Predicted region for 483.0904 m/z

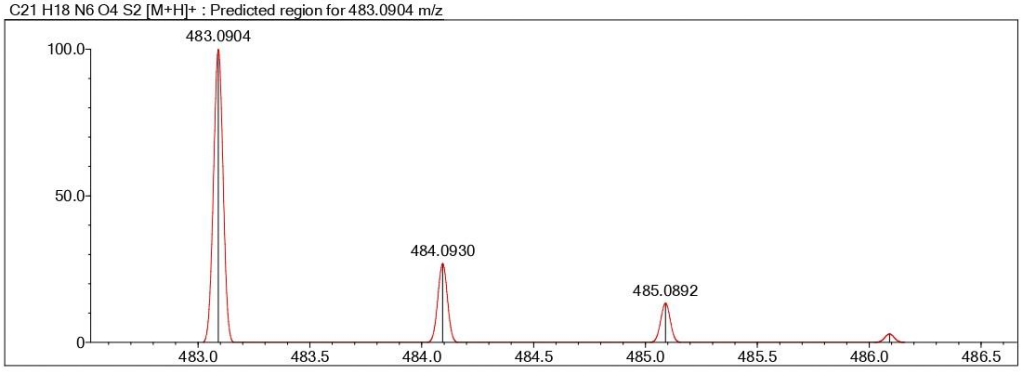

Rank	Score	Formula (M)	Ion	Meas. m/z	Pred. m/z	Df. (mDa)	Df. (ppm)	Iso	DBE
1	83.92	C21 H18 N6 O4 S2	[M+H]+	483.0894	483.0904	-1.0	-2.07	86.23	16.0

Figure 5.30.*HRMS of compound* ***5e***

5.1.5.6 2-[(1*H*-Benzimidazol-2-yl)thio]-*N*-[4-(4-acetamidophenyl)thiazol-2-yl]propanamide (5f)

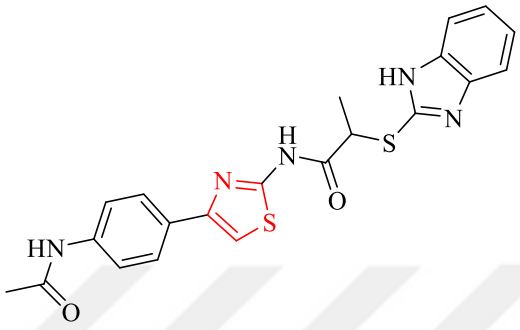

Figure 5.31. *Molecular structure of compound **5f***

Physical Characteristics: Material appearance: powder, **Color**: pale yellow, **Yield**: 70%. **M.P.:** 149 °C.

IR (ATR) υ_{max} (cm^{-1}): 3063 (N-H stretching), 2974-2961 (C-H stretching), 1668 (C=O stretching, amide), 1597-1406 (C=N stretching, and C=C stretching), 1094-1008 (C-N stretching).

^{1}H-NMR: (400 MHz, DMSO-d_6, ppm) δ: 1.66 (3H, d, *J*= 6.98 Hz, CH_3), 2.07 (3H, s, $COCH_3$), 4.83 (1H, q, *J*= 6.86 Hz, CH), 7.15 (2H, brs, benzimidazole-$H_{5,6}$), 7.51 (3H, brs, thiazole-H_5, benzimidazole-$H_{5,6}$), 7.66 (2H, d, *J*= 8.42 Hz, Ph-$H_{3,5}$), 7.83 (2H, d, *J*= 8.42 Hz, Ph-$H_{2,6}$), 10.09 (1H, s, NH).

^{13}C-NMR (100 MHz) (DMSO-d_6) δ (ppm): 18.86 (CH_3), 24.50($CO\underline{C}H_3$), 44.92 (CH), 107.41 (thi-C_5), 109.95 (benzimidazole-$C_{4,7}$), 119.48 (Ph-$C_{3,5}$), 122.12 (benzimidazole-$C_{5,6}$), 122.76 (), 126.53 (Ph-$C_{3,5}$), 129.61 (Ph-C_1), 132.71 (Ph-C_4), 139.42 (benzimidazole-C_2),149.07 (benzimidazole-C_{7a}), 149.25 (benzimidazole-C_{3a}), 158.59 (thi-C_4) 168,56 (thi-C_2),168.82 ($\underline{C}OCH_3$), 170,74 (CO).

HRMS (ESI) (*m/z*): [M + 1]$^{+}$: Calculated for $C_{21}H_{19}N_5O_2S_2$: 438.1053; found 438.1045.

DOPNALAB

	Item	Value
	Acquired Date&Time	22.12.2022 16:03:49
	Acquired by	System Administrator
	Filename	C:\Users\dopnalab\Desktop\MASAÜSTÜ\LEYLA YURTDAŞ\abdurrahman\AB-M\AB-M8.1.isp
	Spectrum name	AB-M8.1
	Sample name	AB-M8
	Sample ID	
	Option	
	Comment	
	No. of Scans	15
	Resolution	4 [cm-1]
	Apodization	Happ-Genzel

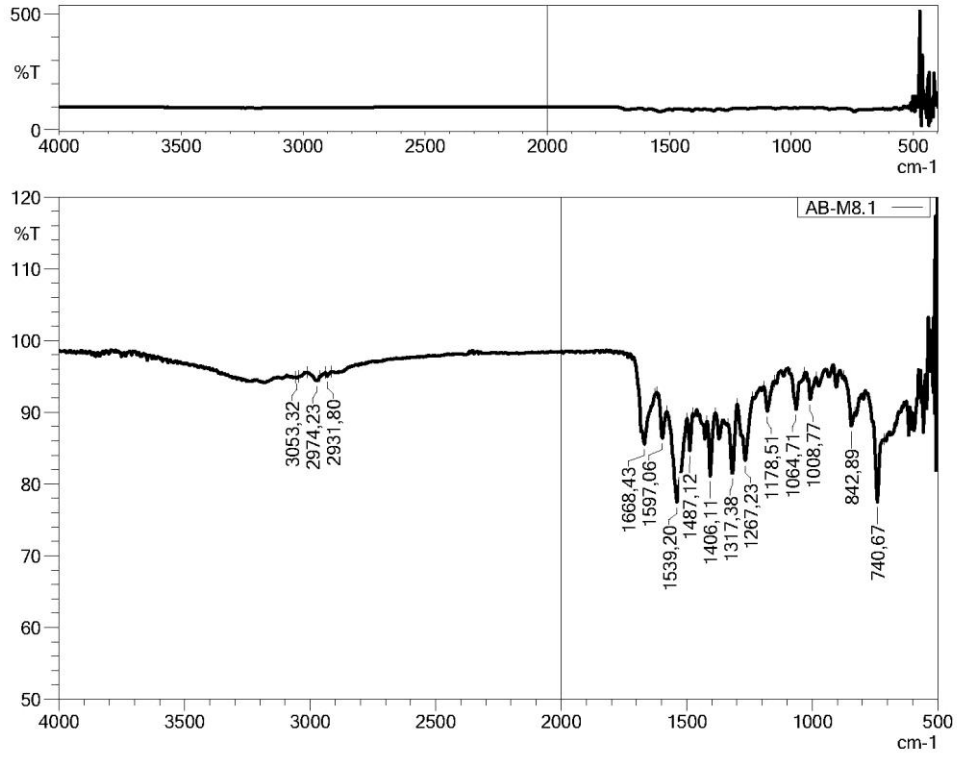

Figure 5.32.*The infrared spectrum of compound* ***5f***

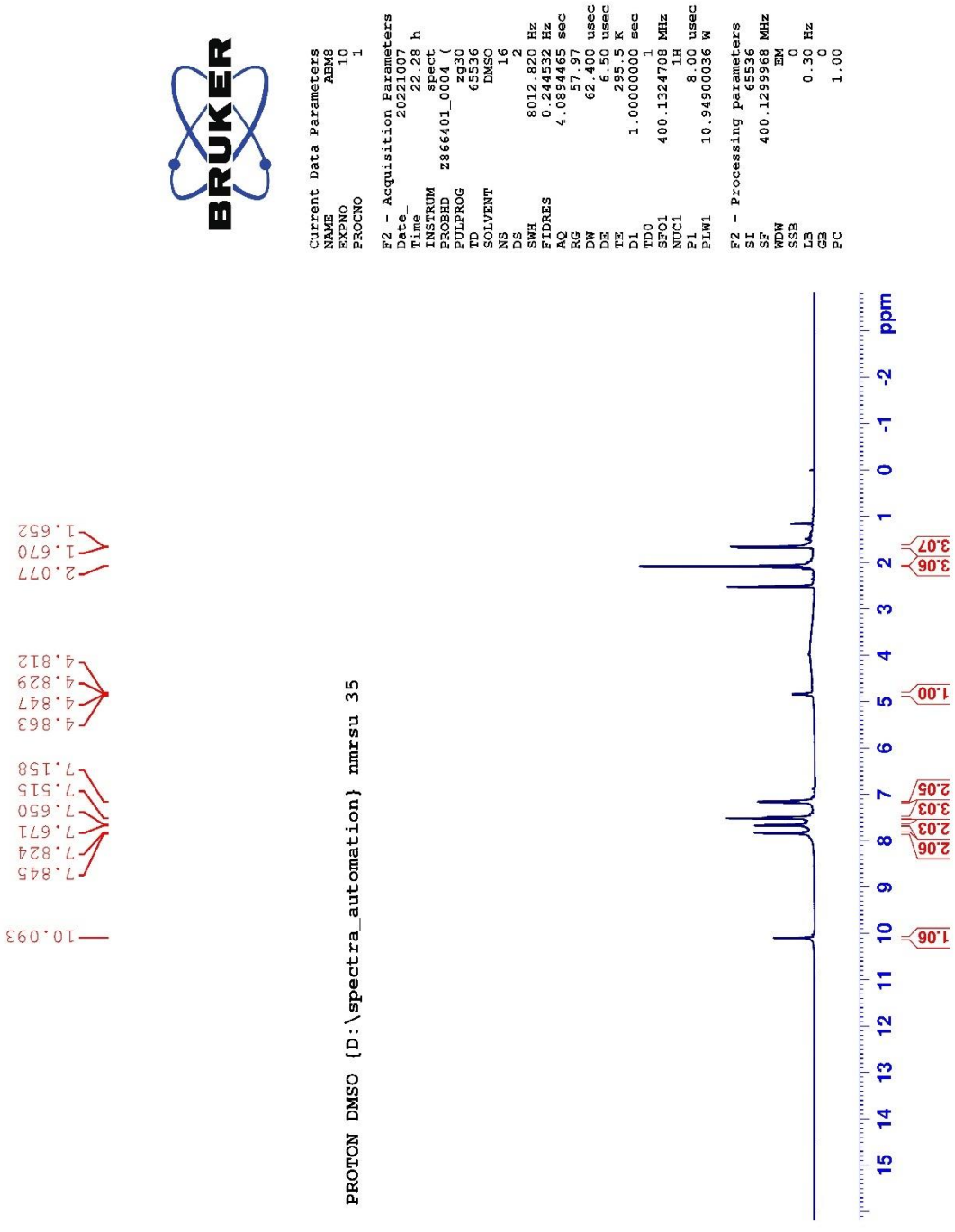

Figure 5.33..*[1]H-NMR spectrum of compound **5f***

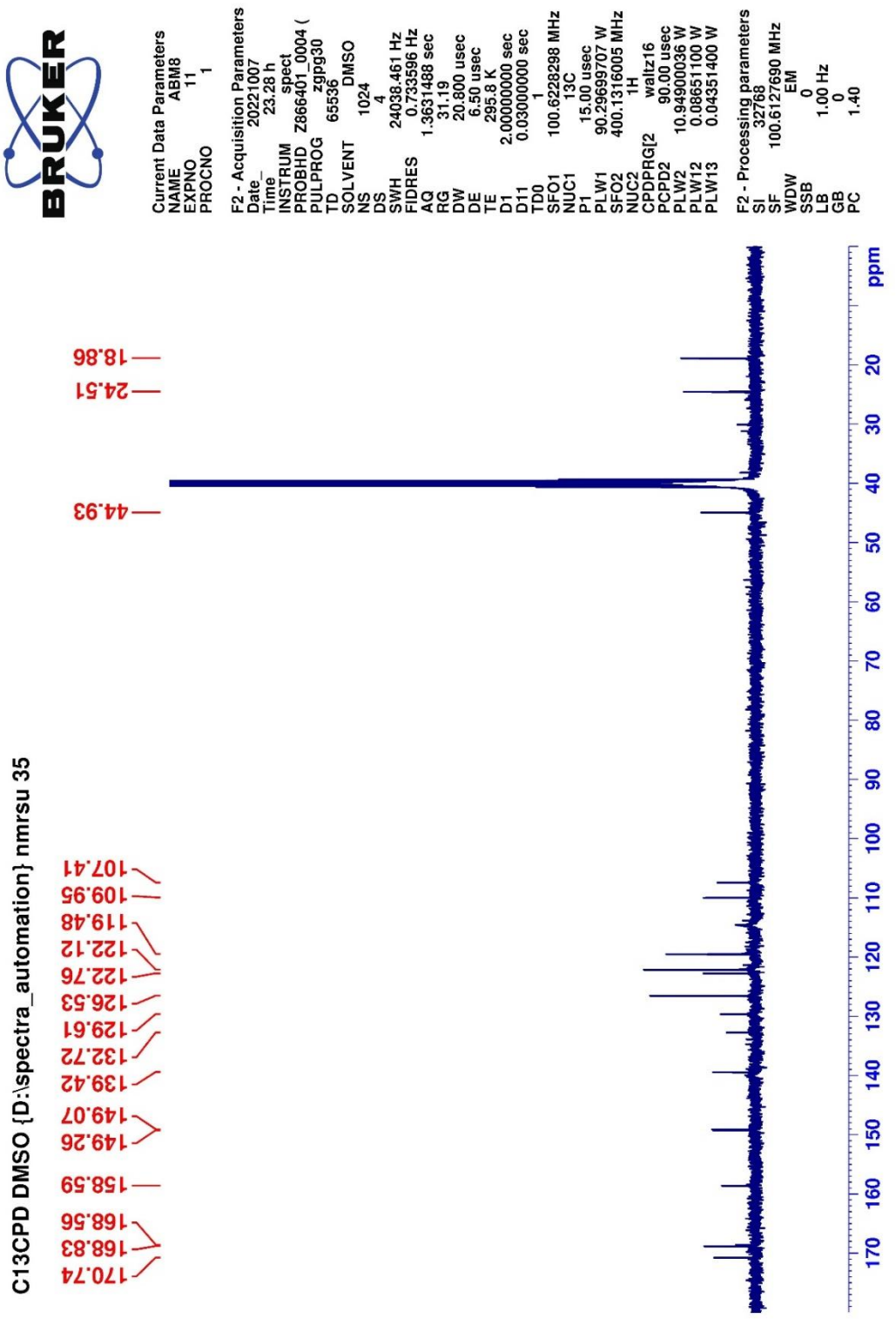

Figure 5.34.*[13]C-NMR spectrum of compound **5f***

Formula Predictor Report - AB-M8_353.lcd

Data File: C:\LabSolutions\Data\Analiz\Asaf\AB-M8_353.lcd

Elmt	Val.	Min	Max	Elmt	Val.	Min	Max	Elmt	Val.	Min	Max	Elmt	Val.	Min	Max	Use Adduct
H	1	0	30	O	2	0	4	S	2	2	2	Ru	2	0	0	H
C	4	0	30	F	1	0	0	Cl	1	0	0	Pd	2	0	0	
N	3	0	6	P	3	0	0	Br	1	0	0	I	3	0	0	

Error Margin (ppm): 5
HC Ratio: unlimited
Max Isotopes: 3
MSn Iso RI (%): 10.00

DBE Range: 5.0 - 25.0
Apply N Rule: yes
Isotope RI (%): 1.00
MSn Logic Mode: AND

Electron Ions: odd
Use MSn Info: yes
Isotope Res: 9000
Max Results: 50

Event#: 1 MS(E+) Ret. Time : 2.467 Scan# : 371

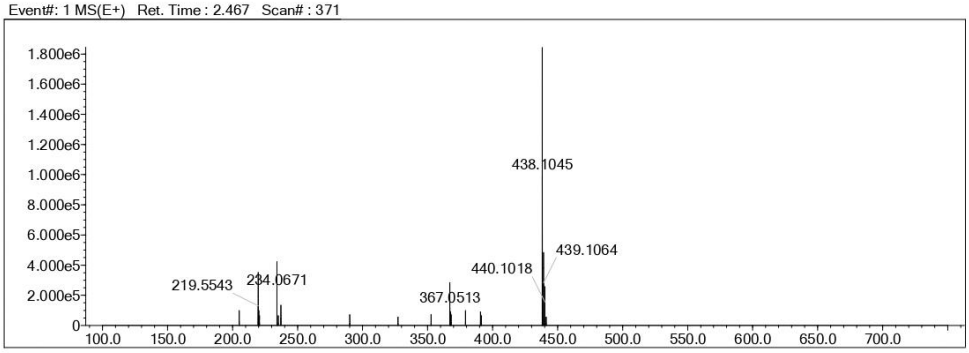

Measured region for 438.1045 m/z

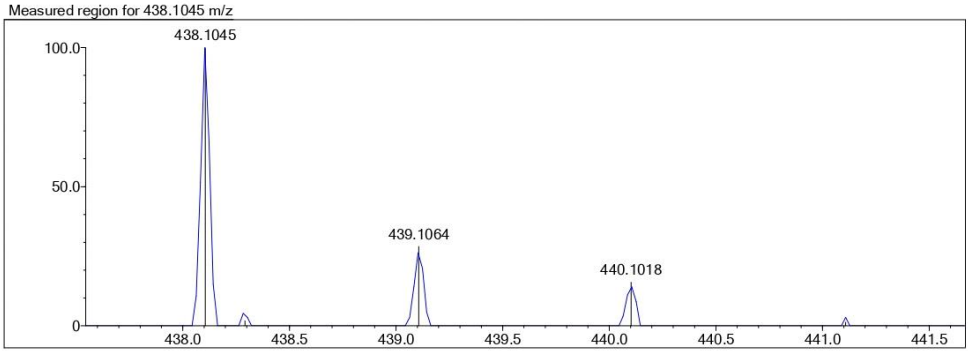

C21 H19 N5 O2 S2 [M+H]+ : Predicted region for 438.1053 m/z

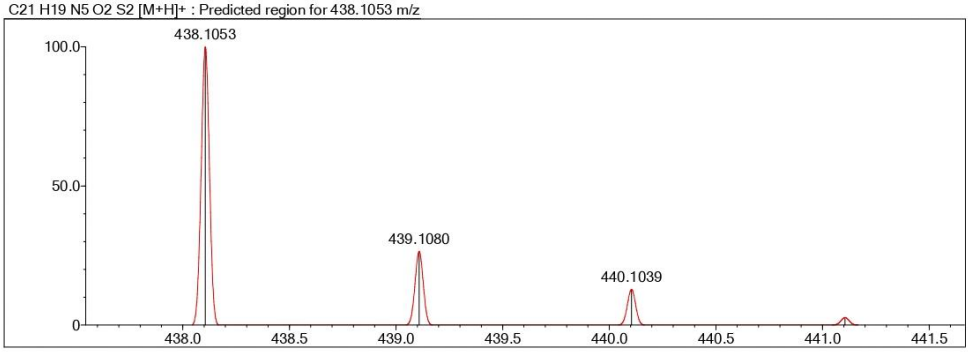

Rank	Score	Formula (M)	Ion	Meas. m/z	Pred. m/z	Df. (mDa)	Df. (ppm)	Iso	DBE
1	91.67	C21 H19 N5 O2 S2	[M+H]+	438.1045	438.1053	-0.8	-1.83	93.61	15.0

Figure 5.35.*HRMS of compound* ***5f***

5.1.5.7 *N*-[4-(4-Acetamidophenyl)thiazol-2-yl]-2-(benzothiazol-2-ylthio)propanamide (5g)

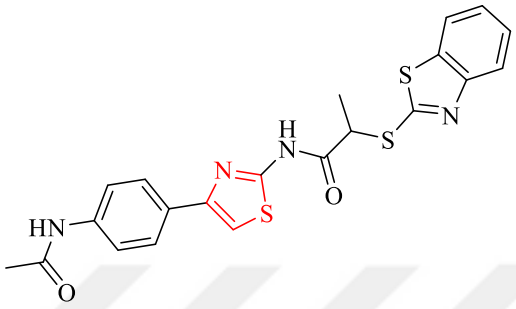

Figure 5.36. *Molecular structure of compound* ***5g***

Physical Characteristics: Material appearance: powder, **Color**: light brown, **Yield**: 76%. **M.P:** 190 °C.

IR (ATR) υ_{max} (cm^{-1}): 3244-3107 (N-H stretching), 3059 - 2988 (C-H stretching), 1687 (C=O stretching, amide), 1663-1423 (aromatic C=N stretching and C=C stretching), 1236-1002 (C-N stretching).

^{1}H-NMR: (400 MHz, DMSO-d_6, ppm) δ: 1.71 (3H, d, *J*= 6.99 Hz, CH_3), 2.07 (3H, brs, $COCH_3$), 4.95 (1H, q, *J*= 7.03 Hz, CH), 7.39 (1H, t, *J*= 7.60 Hz, benzothiazole-H_5), 7.48 (1H, t, *J*= 7.67 Hz, benzothiazole-H_6), 7.55 (1H, s, thiazole-H_5), 7.65 (2H, d, *J*= 8.53 Hz, Ph-$H_{2,6}$), 7.84-7.87 (3H, m, *J*= 8.52 Hz, benzothiazole-H_4, Ph-$H_{3,5}$), 8.04 (1H, d, *J*= 7.95 Hz, benzothiazole-H_7). 10.05 (1H, s, N<u>H</u>$COCH_3$). 12.78 (1H, s, NH).

^{13}C-NMR (100 MHz) (DMSO-d_6) δ (ppm): 18.83 (CH_3), 24.52(CO<u>C</u>H_3), 46.47(CH), 107.73 (thiazole -C_5), 119.49 (Ph-$C_{3,5}$), 121.84 (benzothiazole-C_4), 122.44 (benzothiazole-C_7), 125.31(benzothiazole-C_6), 126.58 (Ph-$C_{2,6}$), 126.98 (benzothiazole-C_5), 129.48 (Ph-C_1), 135.41 (benzothiazole-C_{7a}), 139.50 (Ph-C_4), 149.39 (thiazole -C_4), 152.96 (benzothiazole-C_{3a}), 157.97 (thiazole -C_2), 164.66 (benzothiazole-C_9), 168.82 (<u>C</u>OCH_3), 169.80 (CO).

HRMS (ESI) (*m/z*): [M + 1]$^{+}$: Calculated for $C_{21}H_{18}N_4O_2S_3$: 455.0665; found 455.0665.

DOPNALAB

	Item	Value
	Acquired Date&Time	22.12.2022 16:07:54
	Acquired by	System Administrator
	Filename	C:\Users\dopnalab\Desktop\MASAÜSTÜ\LEYLA YURTDAŞ\abdurrahman\AB-M\AB-M9.1.isp
	Spectrum name	AB-M9.1
	Sample name	AB-M9
	Sample ID	
	Option	
	Comment	
	No. of Scans	15
	Resolution	4 [cm-1]
	Apodization	Happ-Genzel

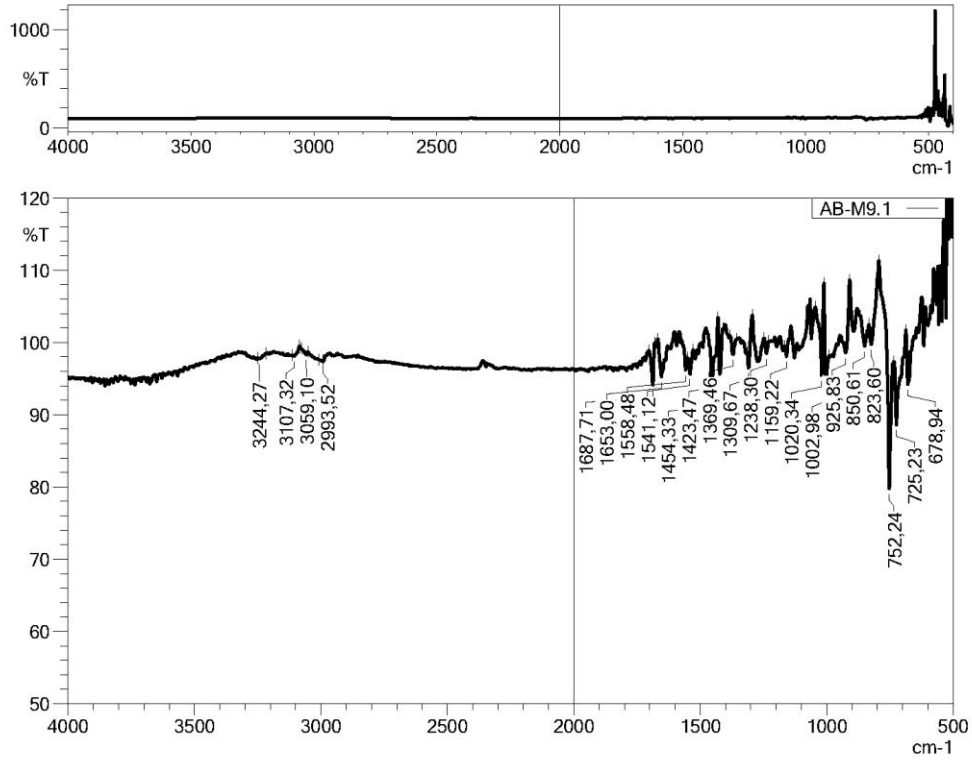

Figure 5.37. *The infrared spectrum of compound **5g***

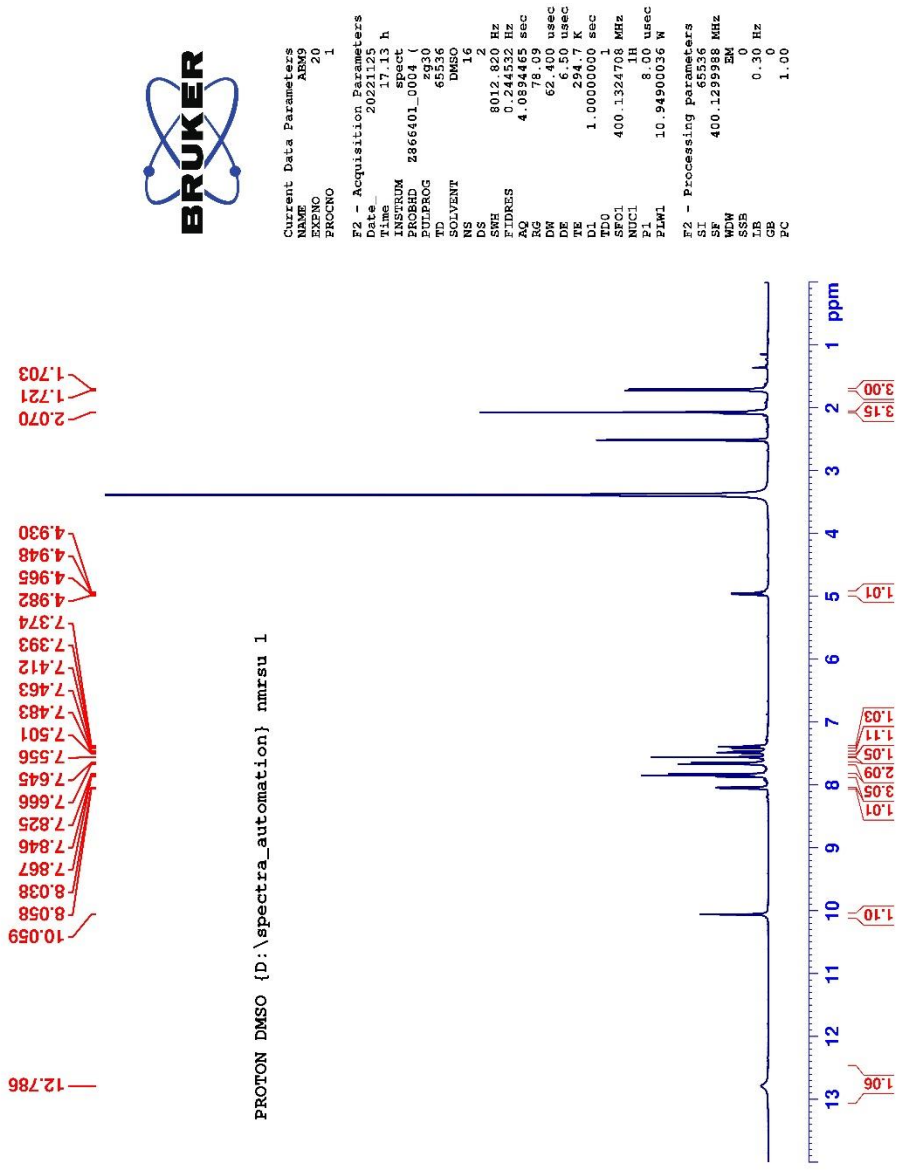

Figure 5.38. *[1]H-NMR spectrum of compound **5g***

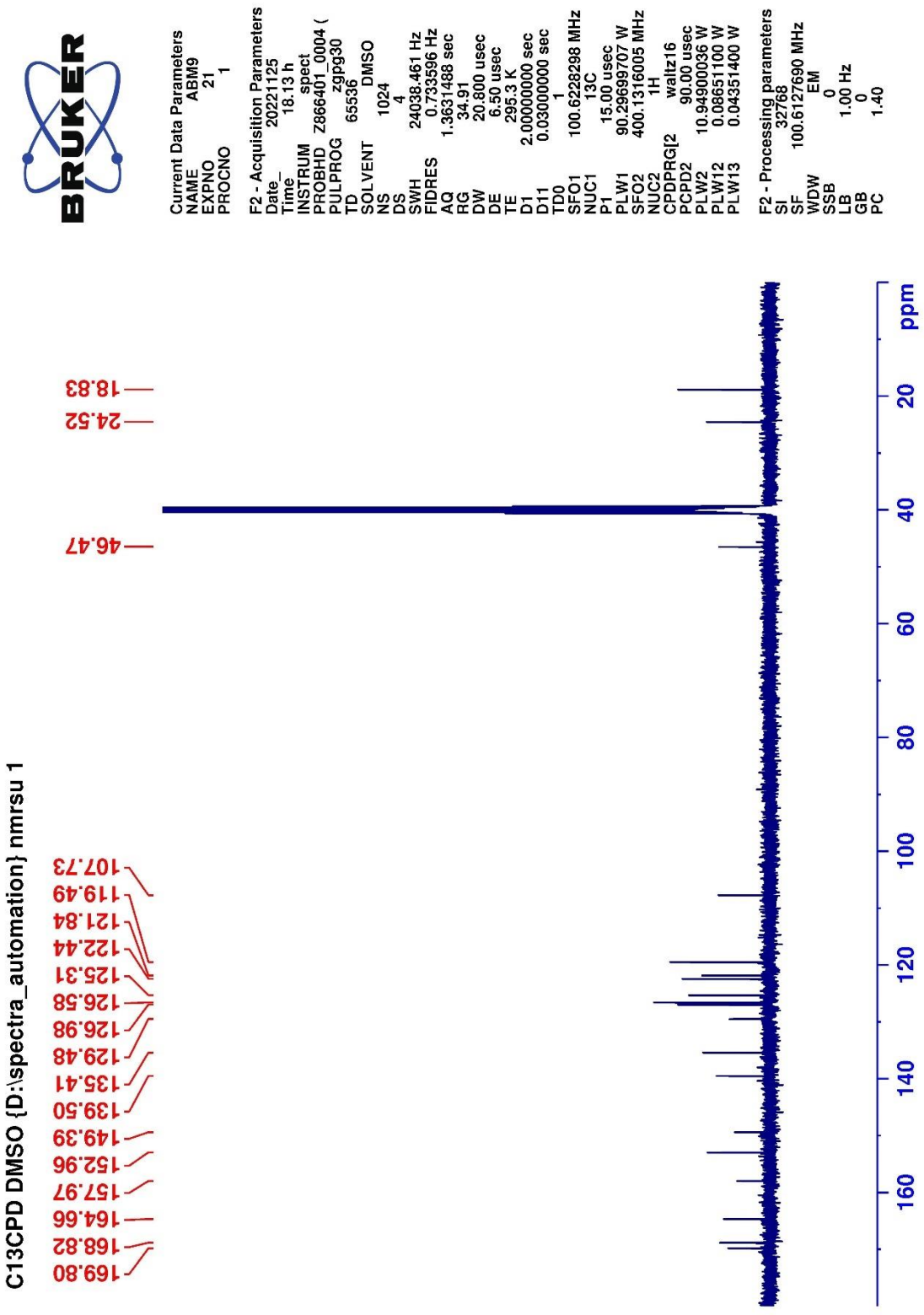

Figure 5.39. *^{13}C-NMR spectrum of compound **5g***

Formula Predictor Report - AB-M9_354.lcd

Page 1 of 1

Data File: C:\LabSolutions\Data\Analiz\Asaf\AB-M9_354.lcd

Elmt	Val.	Min	Max	Elmt	Val.	Min	Max	Elmt	Val.	Min	Max	Elmt	Val.	Min	Max	Use Adduct
H	1	0	30	O	2	0	4	S	2	3	3	Ru	2	0	0	H
C	4	0	30	F	1	0	0	Cl	1	0	0	Pd	2	0	0	
N	3	0	6	P	3	0	0	Br	1	0	0	I	3	0	0	

Error Margin (ppm): 5
HC Ratio: unlimited
Max Isotopes: 3
MSn Iso RI (%): 10.00

DBE Range: 5.0 - 25.0
Apply N Rule: yes
Isotope RI (%): 1.00
MSn Logic Mode: AND

Electron Ions: odd
Use MSn Info: yes
Isotope Res: 9000
Max Results: 50

Event#: 1 MS(E+) Ret. Time : 3.200 -> 4.467 Scan# : 481 -> 671

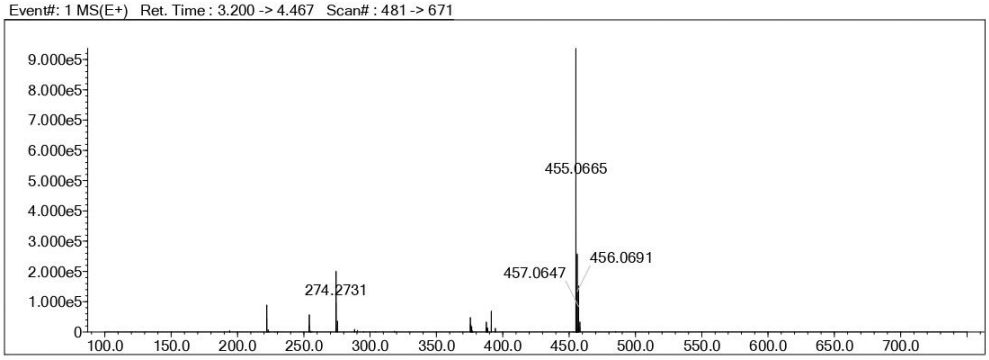

Measured region for 455.0665 m/z

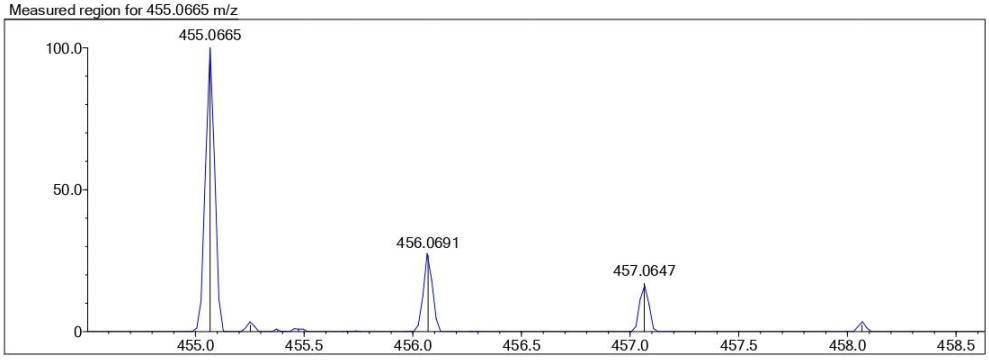

C21 H18 N4 O2 S3 [M+H]+ : Predicted region for 455.0665 m/z

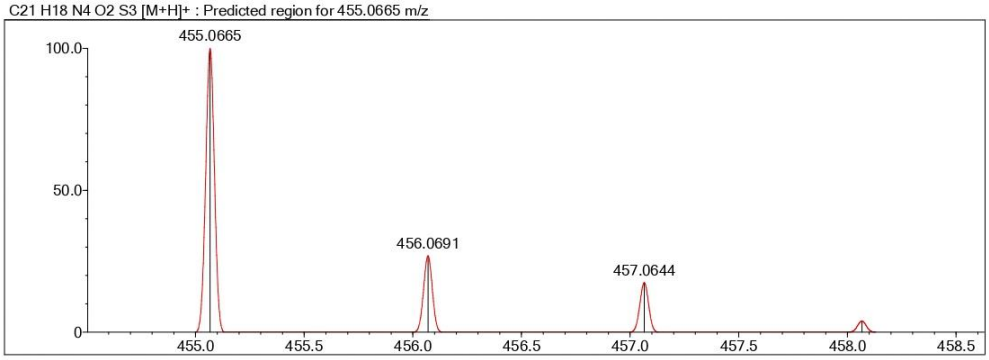

Rank	Score	Formula (M)	Ion	Meas. m/z	Pred. m/z	Df. (mDa)	Df. (ppm)	Iso	DBE
1	100.00	C21 H18 N4 O2 S3	[M+H]+	455.0665	455.0665	0.0	0.00	100.00	15.0

Figure 5.40. *HRMS of compound **5g***

5.1.5.8 *N*-[4-(4-Acetamidophenyl)thiazol-2-yl]-2-[(4-methyl-1*H*-1,2,4-triazol-3-yl)thio]propanamide (5h)

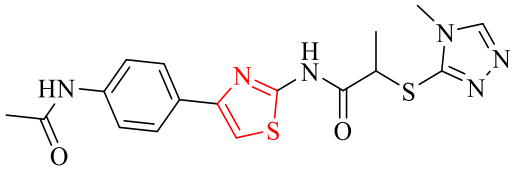

Figure 5.41. *Molecular structure of compound* ***5h***

Physical Characteristics: Material appearance: powder, **Color**: pale yellow, **Yield**: 81%. **M.P:** 201 °C.

IR (ATR) υ_{max} (cm^{-1}): 3246-3176 (N-H stretching), 3115-2931 (C-H stretching), 1666 (C=O stretching, amide), 1566-1406 (C=N stretching, and C=C stretching), 1176-1060 (C-N stretching).

^{1}H-NMR (400 MHz, DMSO-d_6, ppm) δ: 1.52 (3H, d, *J*= 6.83 Hz, C$\underline{H}_3$CHCO), 2.07 (3H, s, $COCH_3$), 3.58 (3H, s, CH_3), 4.31 (1H, q, *J*= 6.84 Hz, CH), 7.54 (1H, s, thiazole-H_5), 7.65 (2H, d, *J*= 8.05 Hz, Ph-$H_{2,6}$), 7.82 (2H, d, *J*= 7.96 Hz, Ph-$H_{3,5}$), 8.65 (1H, s, NCH), 10.05 (1H, s, N$\underline{H}$$COCH_3$), 12.57 (1H, s, NH).

^{13}C-NMR (100 MHz) (DMSO-d_6) δ (ppm): 18.08 ($\underline{C}H_3CHCO$), 24.51($CO\underline{C}H_3$), 31.49 (CH_3), 45.32 (CH), 107.64 (thiazole-C_5), 119.48 (Ph-$C_{3,5}$), 126.56 (Ph-$C_{2,6}$), 129.48 (Ph-C_1), 139.48 (Ph-C_4), 147.00 (triazole-C_3), 147.20 (triazole-C_5), 149.38 (thiazole-C_4), 157.91 (thiazole-C_2), 168.82 ($\underline{C}OCH_3$), 170.07 (CO).

HRMS (ESI) (*m/z*): [M + 1]$^{+}$: Calculated for $C_{17}H_{18}N_6O_2S_2$: 403.1005; found 403.1008.

DOPNALAB

	Item	Value
	Acquired Date&Time	22.12.2022 16:14:42
	Acquired by	System Administrator
	Filename	C:\Users\dopnalab\Desktop\MASAÜSTÜ\LEYLA YURTDAŞ\abdurrahman\AB-M\AB-M10.1.is
	Spectrum name	AB-M10.1
	Sample name	AB-M10
	Sample ID	
	Option	
	Comment	
	No. of Scans	15
	Resolution	4 [cm-1]
	Apodization	Happ-Genzel

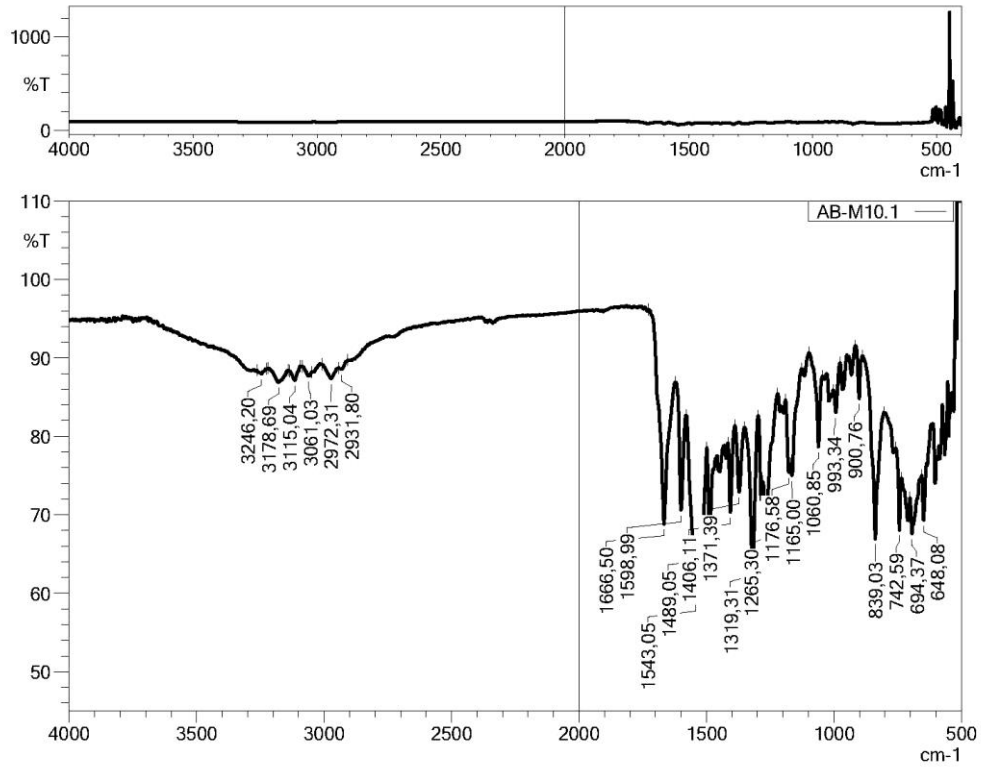

Figure 5.42.*The infrared spectrum of compound* ***5h***

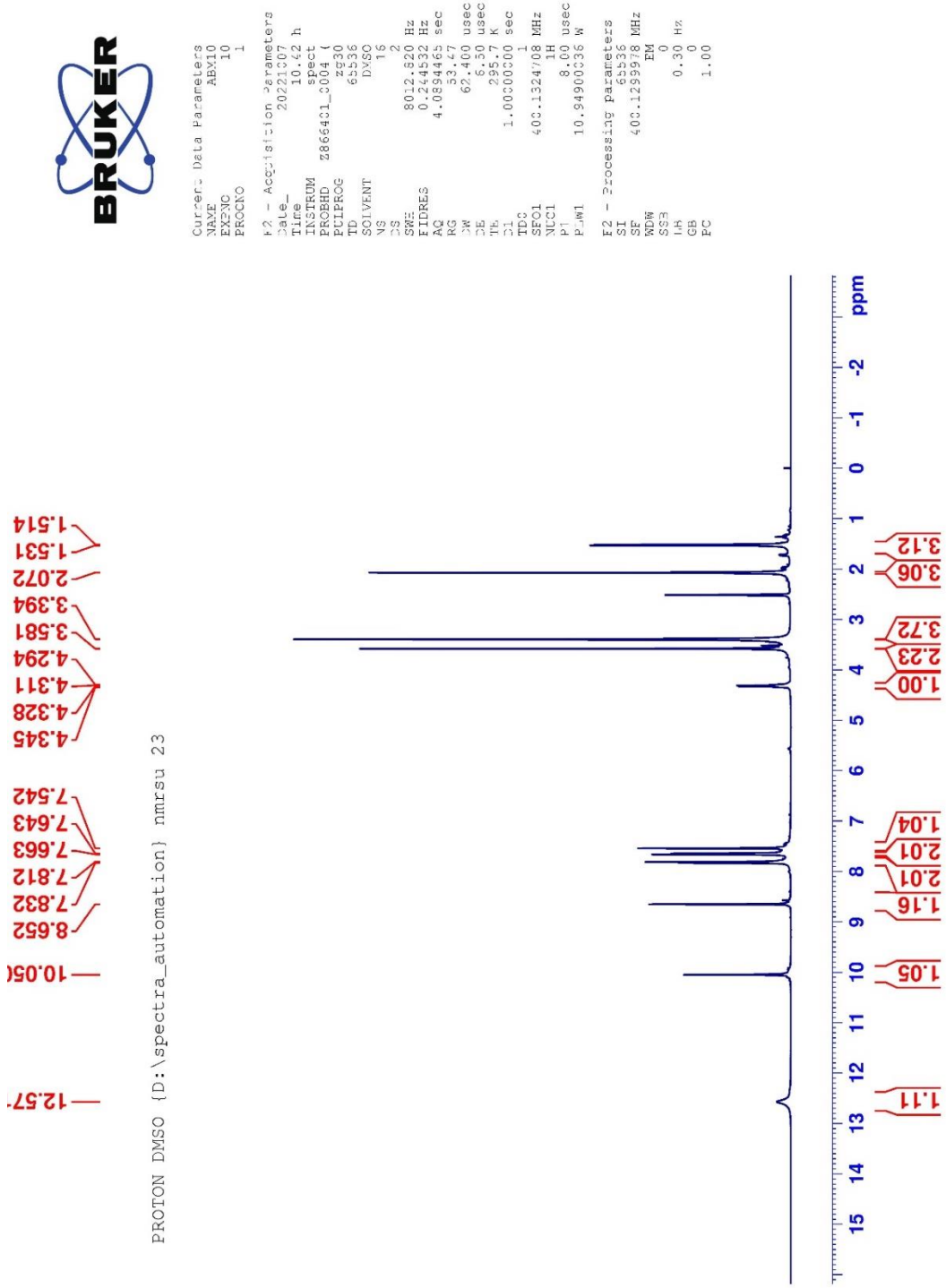

Figure 5.43. *[1]H-NMR spectrum of compound **5h***

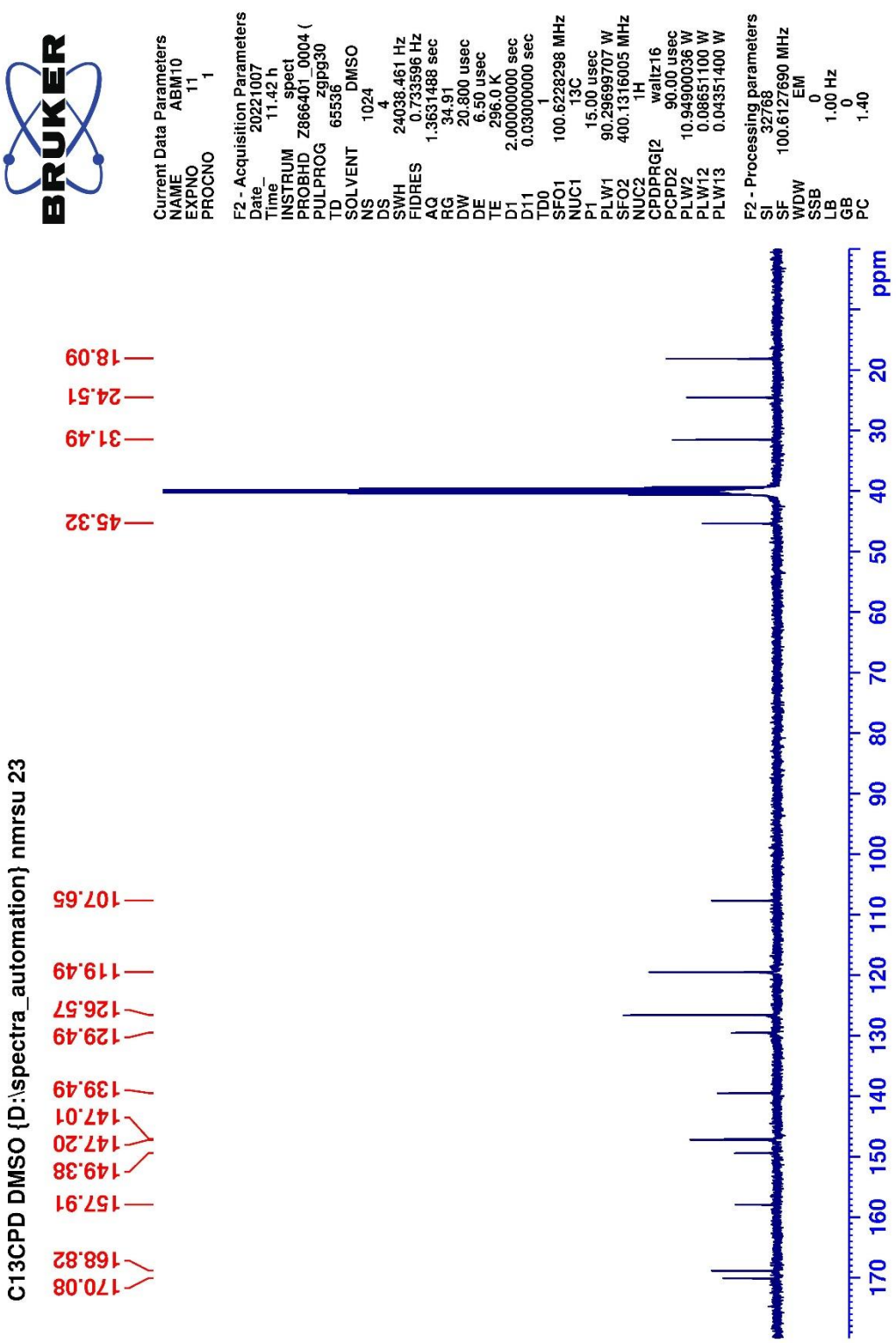

Figure 5.44. *^{13}C-NMR spectrum of compound **5h***

Formula Predictor Report - AB-M10_355.lcd

Data File: C:\LabSolutions\Data\Analiz\Asaf\AB-M10_355.lcd

Elmt	Val.	Min	Max	Elmt	Val.	Min	Max	Elmt	Val.	Min	Max	Elmt	Val.	Min	Max	Use Adduct
H	1	0	30	O	2	0	4	S	2	2	2	Ru	2	0	0	H
C	4	0	30	F	1	0	0	Cl	1	0	0	Pd	2	0	0	
N	3	0	6	P	3	0	0	Br	1	0	0	I	3	0	0	

Error Margin (ppm): 5
HC Ratio: unlimited
Max Isotopes: 3
MSn Iso RI (%): 10.00

DBE Range: 5.0 - 25.0
Apply N Rule: yes
Isotope RI (%): 1.00
MSn Logic Mode: AND

Electron Ions: odd
Use MSn Info: yes
Isotope Res: 9000
Max Results: 50

Event#: 1 MS(E+) Ret. Time : 1.947 Scan# : 293

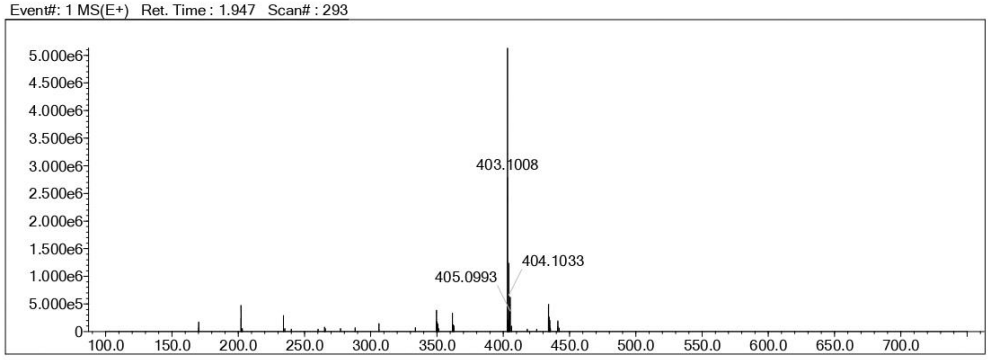

Measured region for 403.1008 m/z

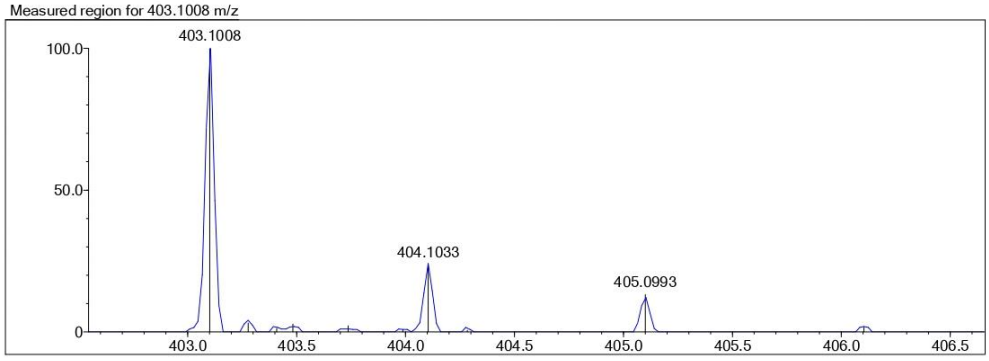

C17 H18 N6 O2 S2 [M+H]+ : Predicted region for 403.1005 m/z

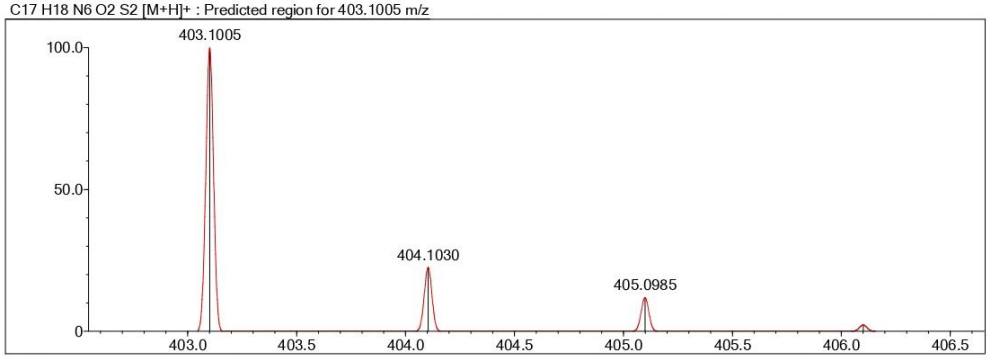

Rank	Score	Formula (M)	Ion	Meas. m/z	Pred. m/z	Df. (mDa)	Df. (ppm)	Iso	DBE
1	91.49	C17 H18 N6 O2 S2	[M+H]+	403.1008	403.1005	0.3	0.74	91.49	12.0

Figure 5.45. *HRMS of compound* ***5h***

5.1.5.9 *N*-[4-(4-Acetamidophenyl)thiazol-2-yl]-2-(benzoxazol-2-ylthio)propanamide (5i)

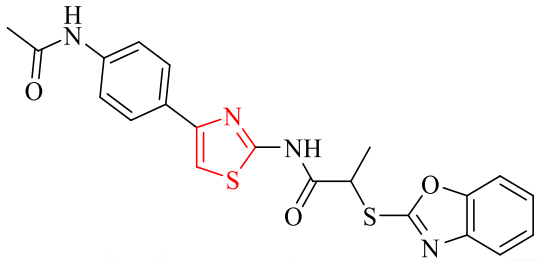

Figure 5.46. *Molecular structure of compound* ***5i***

Physical Characteristics: Material appearance: powder, **Color**: brown, **Yield**: 85%. **M.P.:**159 °C.

IR (ATR) υ_{max} (cm^{-1}): 3244-3180 (N-H stretching), 3107-2931 (C-H stretching), 1678-1660 (C=O stretching, amide), 1598-1406 (C=N stretching, and C=C stretching), 1236-1176 (C-N stretching).

^{1}H-NMR (400 MHz, DMSO-*d*$_6$, ppm) ***δ:*** 1.74 (3H, d, *J*= 7.03 Hz, CH_3), 2.06 (3H, s, $COCH_3$), 4.88 (1H, q, *J*= 6.56 Hz, CH), 7.34 (2H, brs, *J*= 2.16 Hz, benzoxazole -$H_{4,7}$), 7.49 (1H, s, thiazole-H_5), 7.64 (4H, brs, *J*= 7.78 Hz, Ph-$H_{2,6}$, benzoxazole -$H_{5,6}$), 7.82 (2H, d, *J*= 8.40 Hz, Ph-$H_{3,5}$), 10.05 (1H, s, NH),

^{13}C-NMR (100 MHz) (DMSO-*d*$_6$) δ (ppm): 19.48 (CH_3), 24.50 ($CO\underline{C}H_3$), 46.89 (CH), 107.49 (thiazole -C_5), 110.76 (benzoxazole -C_4), 118.91(benzoxazole -C_7), 119.47 (Ph-$C_{3,5}$), 120.64 (benzoxazole -C_5), 122.16 (benzoxazole -C_6), 123.24 (Ph-C_1), 125.02 (Ph-C_4), 125.18 (benzoxazole -C_{7a}), 126.53 (Ph-$C_{2,6}$), 129.73 (thiazole -C_4), 139.39 (benzoxazole -C_{3a}), 141.64(thiazole -C_2), 149.26 (benzoxazole -C_2), 151.65($\underline{C}OCH_3$), 168.79(CO).

HRMS (ESI) (*m/z*): [M + 1] $^{+}$: Calculated for $C_{21}H_{18}N_4O_3S_2$: 439.0893; found 439.0891.

DOPNALAB

	Item	Value
	Acquired Date&Time	22.12.2022 16:19:06
	Acquired by	System Administrator
	Filename	C:\Users\dopnalab\Desktop\MASAÜSTÜ\LEYLA YURTDAŞ\abdurrahman\AB-M\AB-M11.1.is
	Spectrum name	AB-M11.1
	Sample name	AB-M11
	Sample ID	
	Option	
	Comment	
	No. of Scans	15
	Resolution	4 [cm-1]
	Apodization	Happ-Genzel

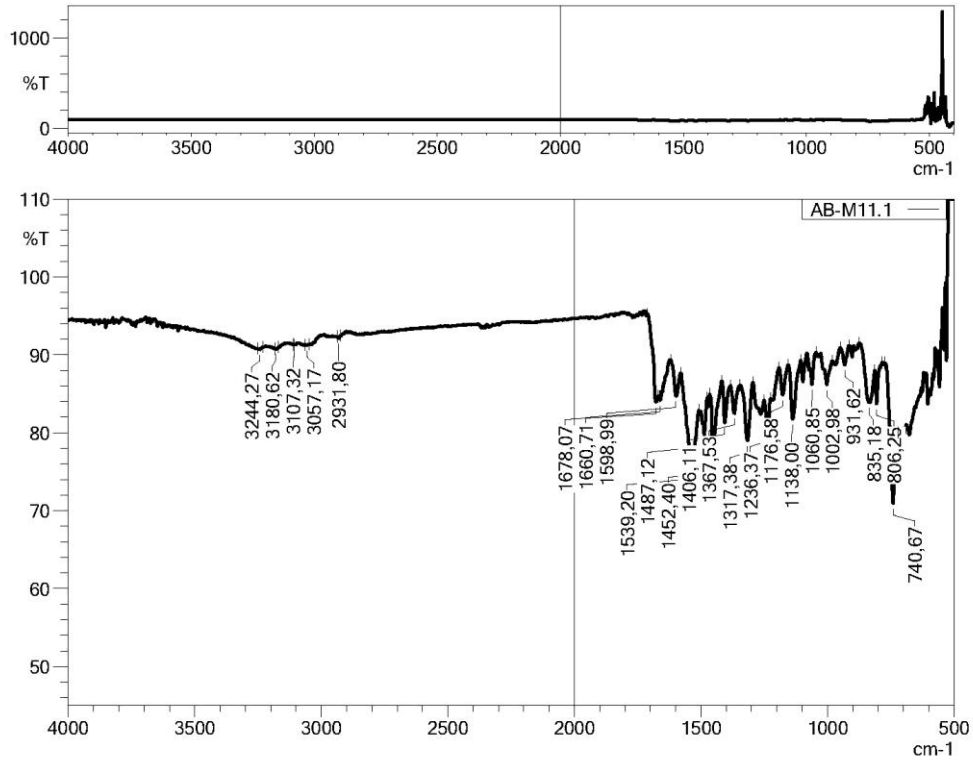

Figure 5.47.*The infrared spectrum of compound **5i***

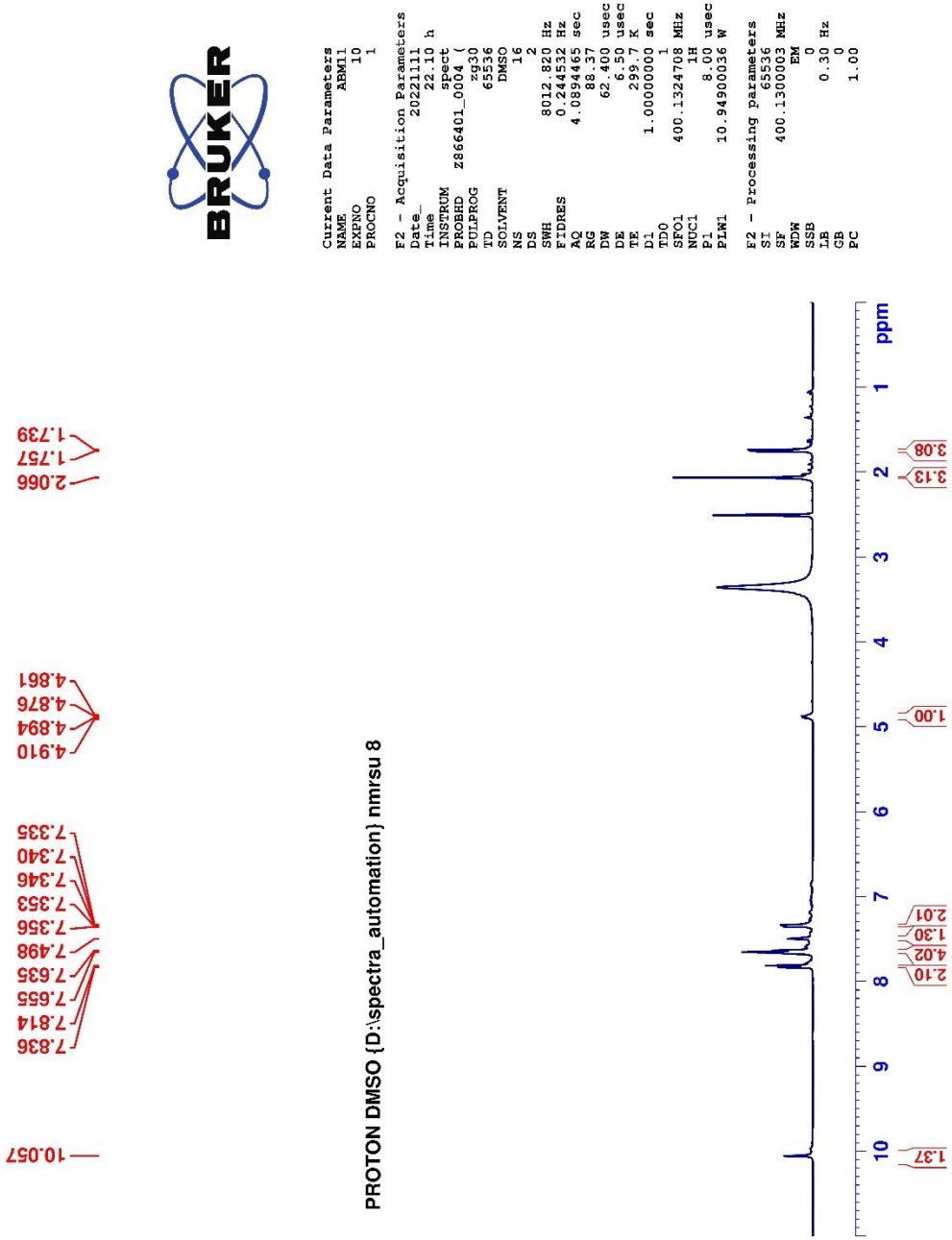

Figure 5.48. *[1]H-NMR spectrum of compound* ***5i***

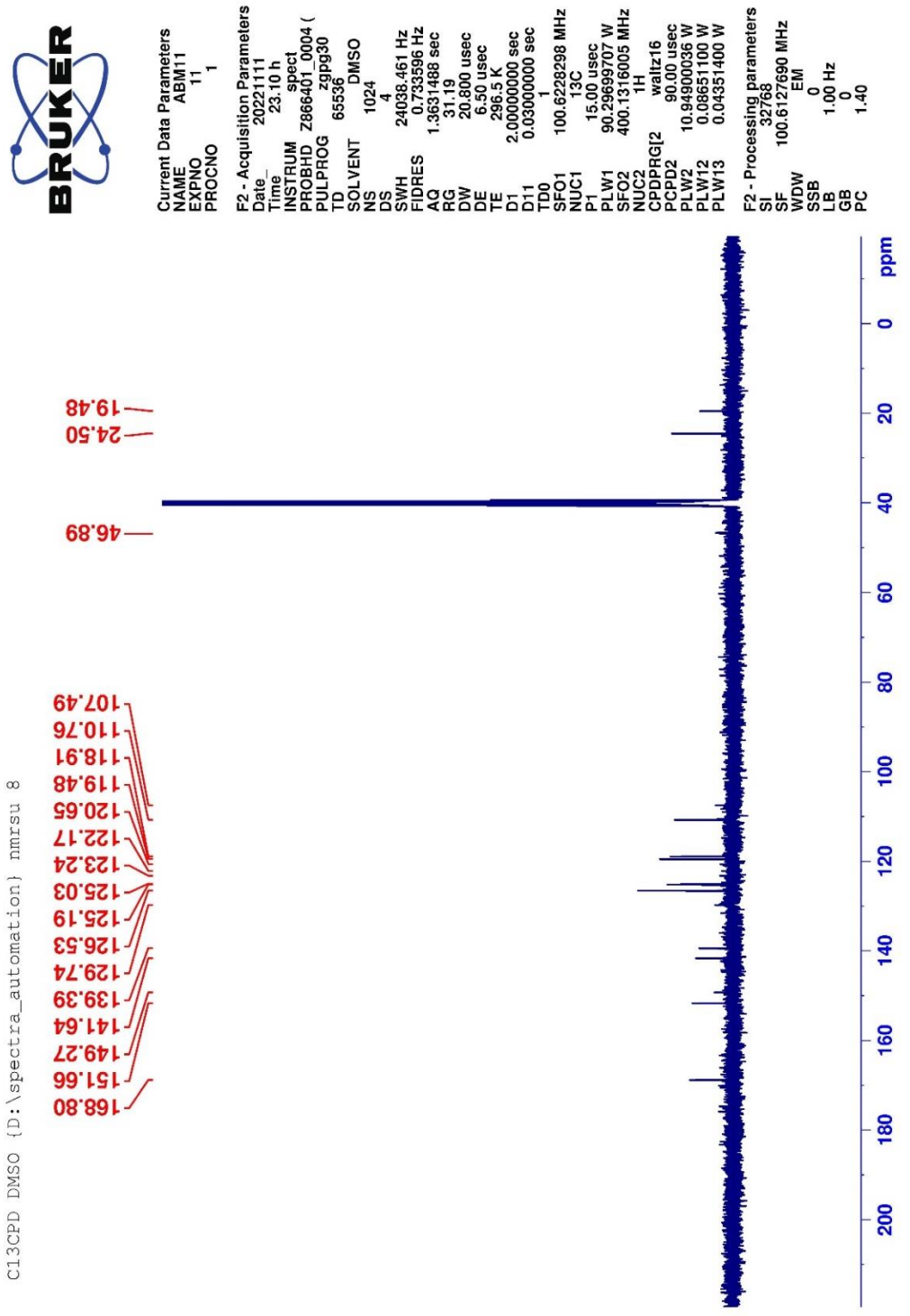

Figure 5.49. *[13]C-NMR spectrum of compound **5i***

Formula Predictor Report - AB-M11_349.lcd

Page 1 of 1

Data File: C:\LabSolutions\Data\Analiz\Asaf\AB-M11_349.lcd

Elmt	Val.	Min	Max	Elmt	Val.	Min	Max	Elmt	Val.	Min	Max	Elmt	Val.	Min	Max	Use Adduct
H	1	0	30	O	2	0	4	S	2	2	2	Ru	2	0	0	H
C	4	0	30	F	1	0	0	Cl	1	0	0	Pd	2	0	0	
N	3	0	6	P	3	0	0	Br	1	0	0	I	3	0	0	

Error Margin (ppm): 5
HC Ratio: unlimited
Max Isotopes: 3
MSn Iso RI (%): 10.00

DBE Range: 5.0 - 25.0
Apply N Rule: yes
Isotope RI (%): 1.00
MSn Logic Mode: AND

Electron Ions: odd
Use MSn Info: yes
Isotope Res: 9000
Max Results: 50

Event#: 1 MS(E+) Ret. Time : 3.053 -> 3.053 Scan# : 459 -> 459

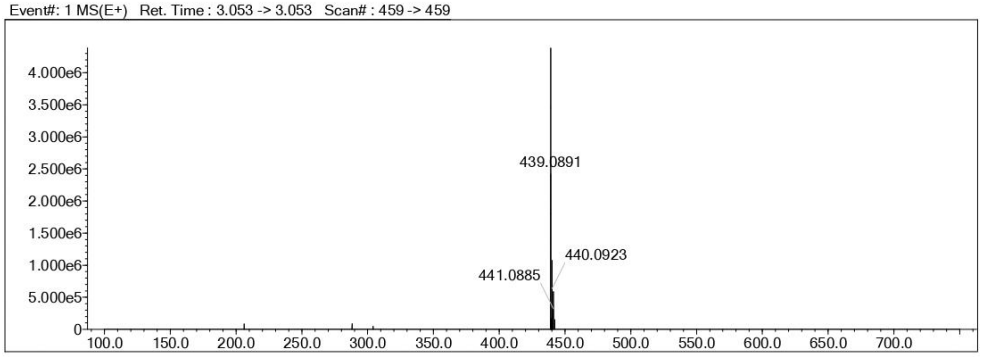

Measured region for 439.0891 m/z

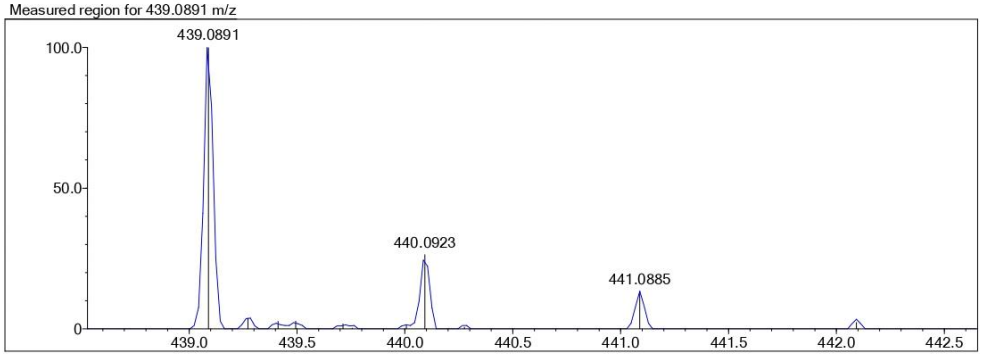

C21 H18 N4 O3 S2 [M+H]+ : Predicted region for 439.0893 m/z

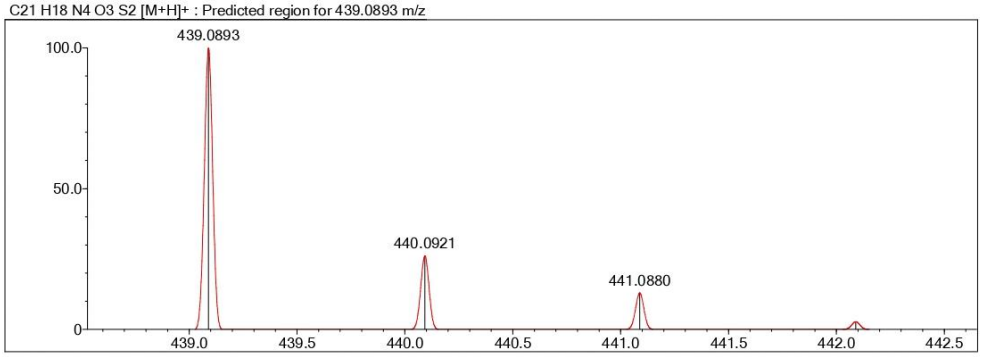

Rank	Score	Formula (M)	Ion	Meas. m/z	Pred. m/z	Df. (mDa)	Df. (ppm)	Iso	DBE
1	88.55	C21 H18 N4 O3 S2	[M+H]+	439.0891	439.0893	-0.2	-0.46	88.55	15.0

Figure 5.50. *HRMS of compound* ***5i***

5.1.5.10 *N*-[4-(4-Acetamidophenyl)thiazol-2-yl]-2-[(5-chlorobenzoxazol-2-yl)thio]propanamide (5j)

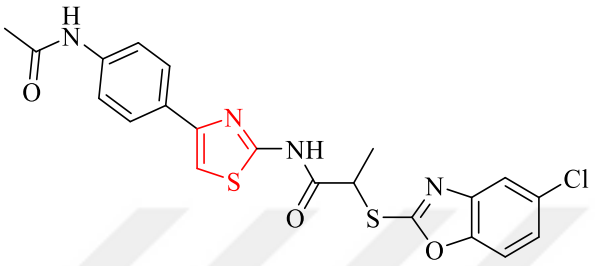

Figure 5.51. *Molecular structure of compound* ***5j***

Physical Characteristics: Material appearance: powder, **Color**: brown, **Yield**: 98%. **M.P.:**165 °C.

IR (ATR) υ_{max} (cm^{-1}): 3180-3115 (N-H stretching), 3066-2933 (C-H stretching), 1688 (C=O stretching, amide), 1597-1446 (C=N stretching, and C=C stretching), 1253-1060(C-N stretching).

^{1}H-NMR (400 MHz, DMSO-d_6, ppm) δ: 1.75 (3H, d, *J*= 6.98 Hz, CH_3), 2.06 (3H, s, $COCH_3$), 4.93 (1H, q, *J*= 7.03 Hz, CH), 7.39 (1H, d, *J*= 8.66 Hz, benzoxazole-H_6), 7.56 (1H, s, thiazole-$H_{5,}$), 7.65 (2H, d, *J*= 8.24 Hz, Ph-$H_{2,6}$), 7.71 (1H, d, *J*= 8.66 Hz, benzoxazole -H_7), 7.82-7.84 (3H, m, *J*= 9.76 Hz, Ph-$H_{3,5}$, benzoxazole -H_4), 10.04 (1H, s, N<u>H</u>$COCH_3$), 12.83 (1H, s, NH).

^{13}C-NMR (100 MHz) (DMSO-d_6) δ (ppm): 19.24 (CH_3), 24.51(CO<u>C</u>H_3), 46.28 (CH), 107.48 (thi-C_5), 112.09 (benzoxazole -C_4), 118.72 (benzoxazole -C_7), 119.48 (Ph-$C_{3,5}$), 125.04 (benzimidazole-C_5), 126.58 (Ph-$C_{3,5}$), 129.43 (Ph-C_1), 129.53 (benzoxazole-C_6), 139.52 (Ph-C_4),142.86 (benzoxazole-C_{7a}), 149.41 (benzoxazole-C_{3a}), 150.49 (thi-C_4) 157,85 (thi-C_2),165.00(benzoxazole-C_2), 168.81 (<u>C</u>OCH_3), 169,42 (CO).

HRMS (ESI) (*m/z*): [M + 1] $^{+}$: Calculated for $C_{21}H_{17}N_4O_3S_2Cl$: 473.0503; found473.0503.

DOPNALAB

	Item	Value
	Acquired Date&Time	22.12.2022 16:23:56
	Acquired by	System Administrator
	Filename	C:\Users\dopnalab\Desktop\MASAÜSTÜ\LEYLA YURTDAŞ\abdurrahman\AB-M\AB-M12.1.is
	Spectrum name	AB-M12.1
	Sample name	AB-M12
	Sample ID	
	Option	
	Comment	
	No. of Scans	15
	Resolution	4 [cm-1]
	Apodization	Happ-Genzel

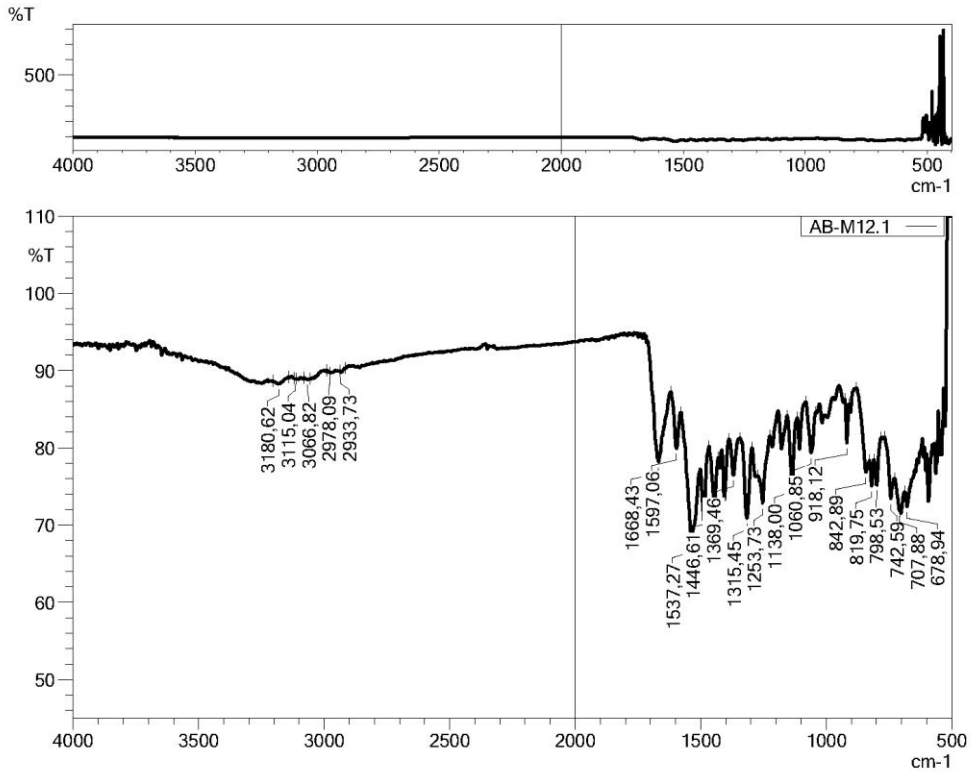

Figure 5.52.*The infrared spectrum of compound* ***5j***

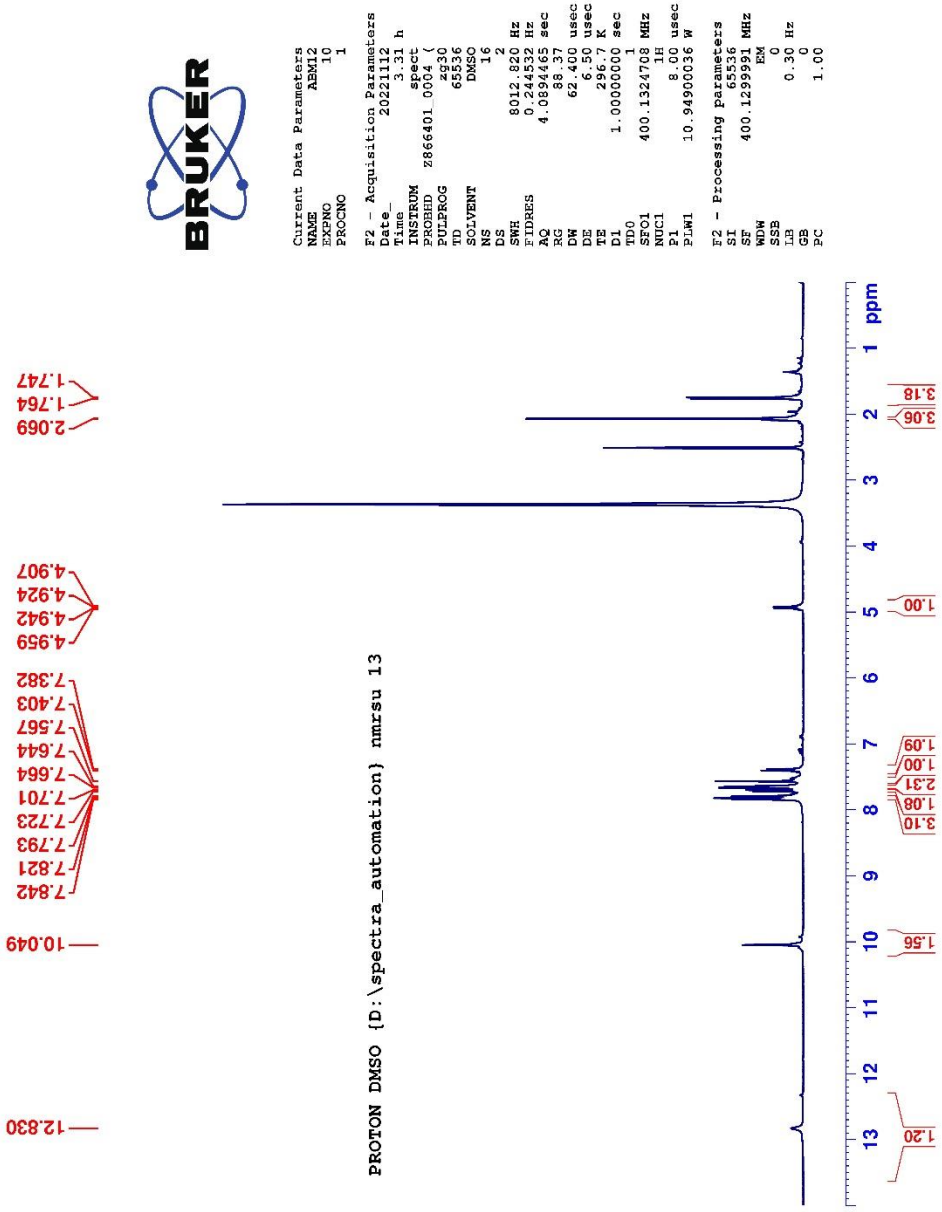

Figure 5.53. *[1]H-NMR spectrum of compound **5j***

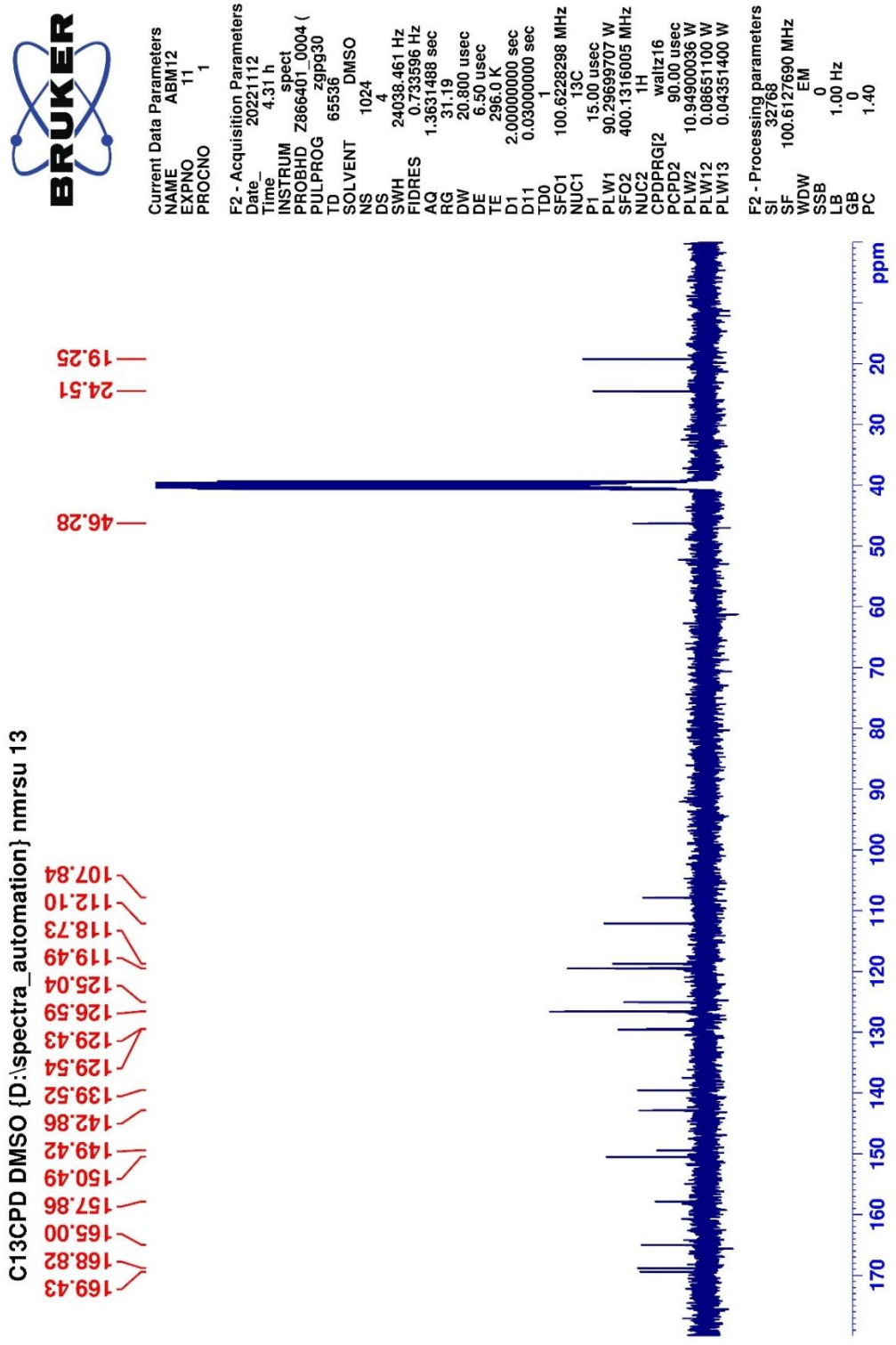

Figure 5.54. *^{13}C-NMR spectrum of compound **5j***

Formula Predictor Report - AB-M12_357.lcd

Page 1 of 1

Data File: C:\LabSolutions\Data\Analiz\Asaf\AB-M12_357.lcd

Elmt	Val.	Min	Max	Elmt	Val.	Min	Max	Elmt	Val.	Min	Max	Elmt	Val.	Min	Max	Use Adduct
H	1	0	30	O	2	0	4	S	2	2	2	Ru	2	0	0	H
C	4	0	30	F	1	0	0	Cl	1	0	1	Pd	2	0	0	
N	3	0	8	P	3	0	0	Br	1	0	0	I	3	0	0	

Error Margin (ppm): 5
HC Ratio: unlimited
Max Isotopes: 3
MSn Iso RI (%): 10.00

DBE Range: 0.0 - 30.0
Apply N Rule: yes
Isotope RI (%): 1.00
MSn Logic Mode: AND

Electron Ions: both
Use MSn Info: yes
Isotope Res: 9000
Max Results: 50

Event#: 1 MS(E+) Ret. Time : 3.987 -> 3.987 Scan# : 599 -> 599

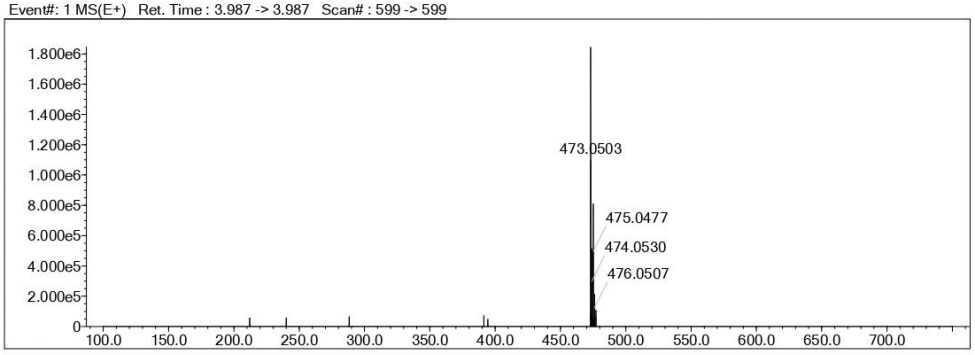

Measured region for 473.0503 m/z

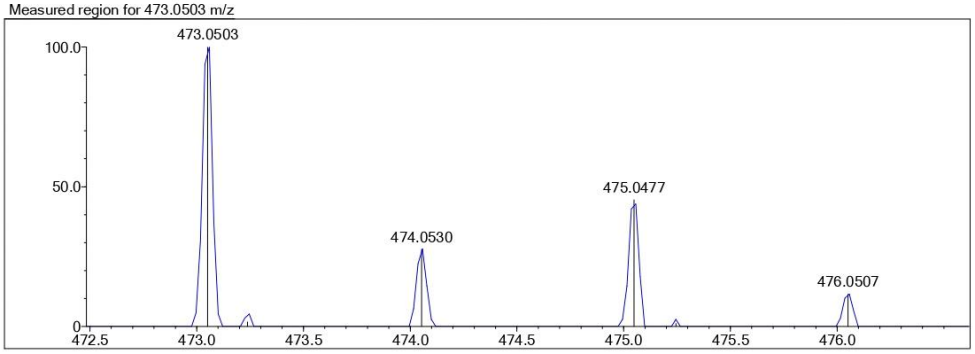

C21 H17 N4 O3 S2 Cl [M+H]+ : Predicted region for 473.0503 m/z

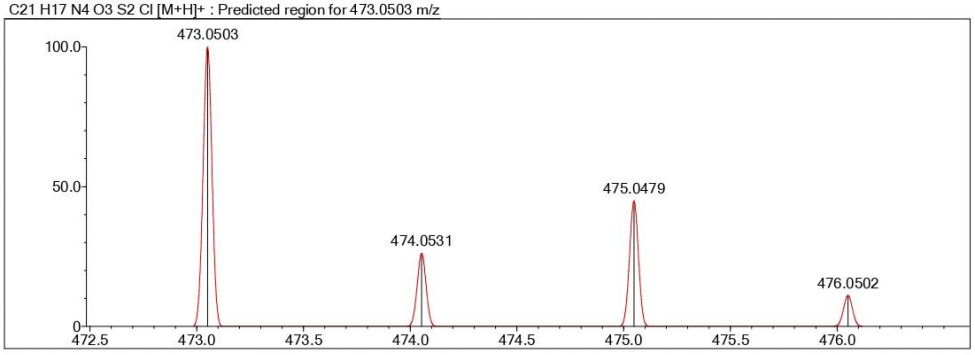

Rank	Score	Formula (M)	Ion	Meas. m/z	Pred. m/z	Df. (mDa)	Df. (ppm)	Iso	DBE
1	100.00	C21 H17 N4 O3 S2 Cl	[M+H]+	473.0503	473.0503	-0.0	0.00	100.00	15.0

Figure 5.55. *HRMS of compound **5j***

5.1.5.11 *N*-[4-(4-Acetamidophenyl)thiazol-2-yl]-2-(pyrimidin-2-ylthio)propanamide (5k)

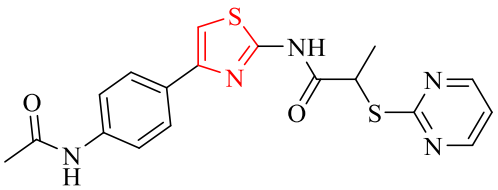

Figure 5.56. *Molecular structure of compound **5k***

Physical Characteristics: Material appearance: powder, **Color**: light yellow, **Yield**: 74%. **M.P.:**153 °C.

IR (ATR) υ_{max} (cm^{-1}): 3255 (N-H stretching), 3115 - 2976 (C-H stretching), 1681-1660 (C=O stretching, amide), 1597-1539 (C=N stretching, and C=C stretching), 1259-1060 (C-N stretching).

^{1}H-NMR (400 MHz, DMSO-d_6, ppm) δ: 1.59 (3H, d, *J*= 7.08 Hz, CH_3), 2.06 (3H, s, $COCH_3$), 4.77 (1H, q, *J*= 7.10 Hz, CH), 7.24 (1H, t, *J*= 4.88 Hz, pyrimidine-H_5), 7.52 (1H, s, thi-H_5), 7.64 (2H, d, *J*= 8.41 Hz, Ph-$H_{2,6}$), 7.82 (2H, d, *J*= 8.48 Hz, Ph-$H_{3,5}$), 8.65 (2H, d, *J*= 4.98 Hz, pyrimidine-$H_{4,6}$), 10.05 (1H, s, N<u>H</u>$COCH_3$), 12.61 (1H, s, NH).

^{13}C-NMR (100 MHz) (DMSO-d_6) δ (ppm): 18.21 (CH_3), 24.51($COCH_3$), 43.70 (CH), 107.47 (thiazole-C_5), 118.11 (pyrimidine-C_5), 119.46 (Ph-$C_{3,5}$), 126.56 (Ph-$C_{2,6}$), 129.54 (Ph-C_1), 139.45 (Ph-C_4), 149.28 (thiazole-C_4), 158.20 (thiazole-C_2), 158.39 (pyrimidine-C_4), 159.03 (pyrimidine-C_6), 168.80 (<u>C</u>OCH_3), 170.35 (CO), 170.84 (pyrimidine-C_5).

HRMS (ESI) (*m/z*): [M + 1]$^{+}$: Calculated for $C_{18}H_{17}N_5O_2S_2$: 400.0896; found 400.0896.

DOPNALAB

	Item	Value
	Acquired Date&Time	22.12.2022 16:29:15
	Acquired by	System Administrator
	Filename	C:\Users\dopnalab\Desktop\MASAÜSTÜ\LEYLA YURTDAŞ\abdurrahman\AB-M\AB-M13.1.is
	Spectrum name	AB-M13.1
	Sample name	AB-M13
	Sample ID	
	Option	
	Comment	
	No. of Scans	15
	Resolution	4 [cm-1]
	Apodization	Happ-Genzel

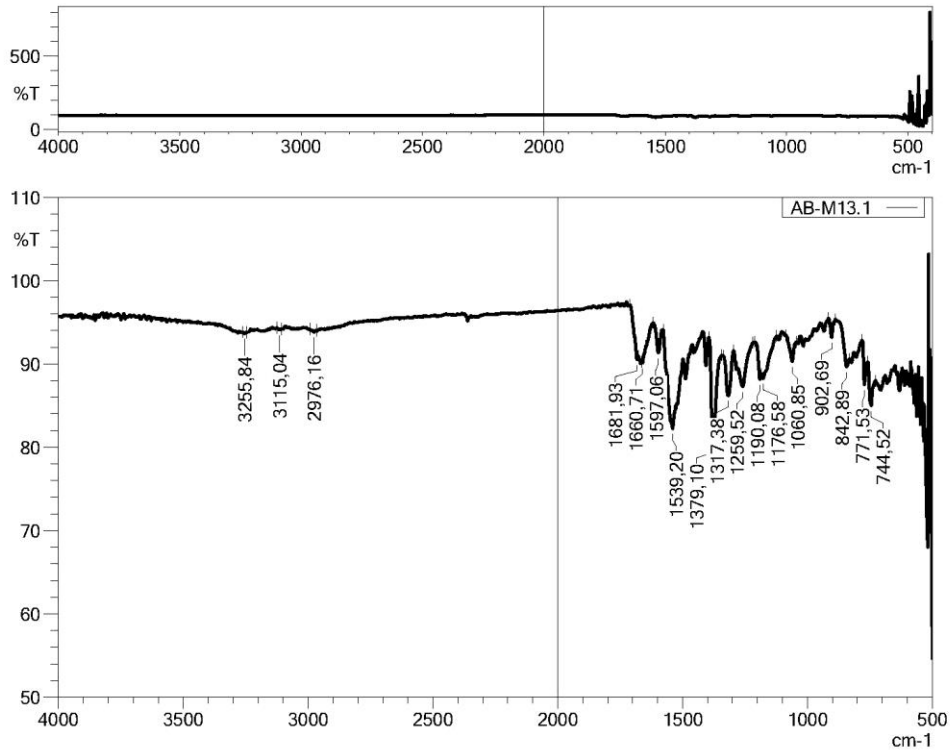

Figure 5.57.*The infrared spectrum of compound* ***5k***

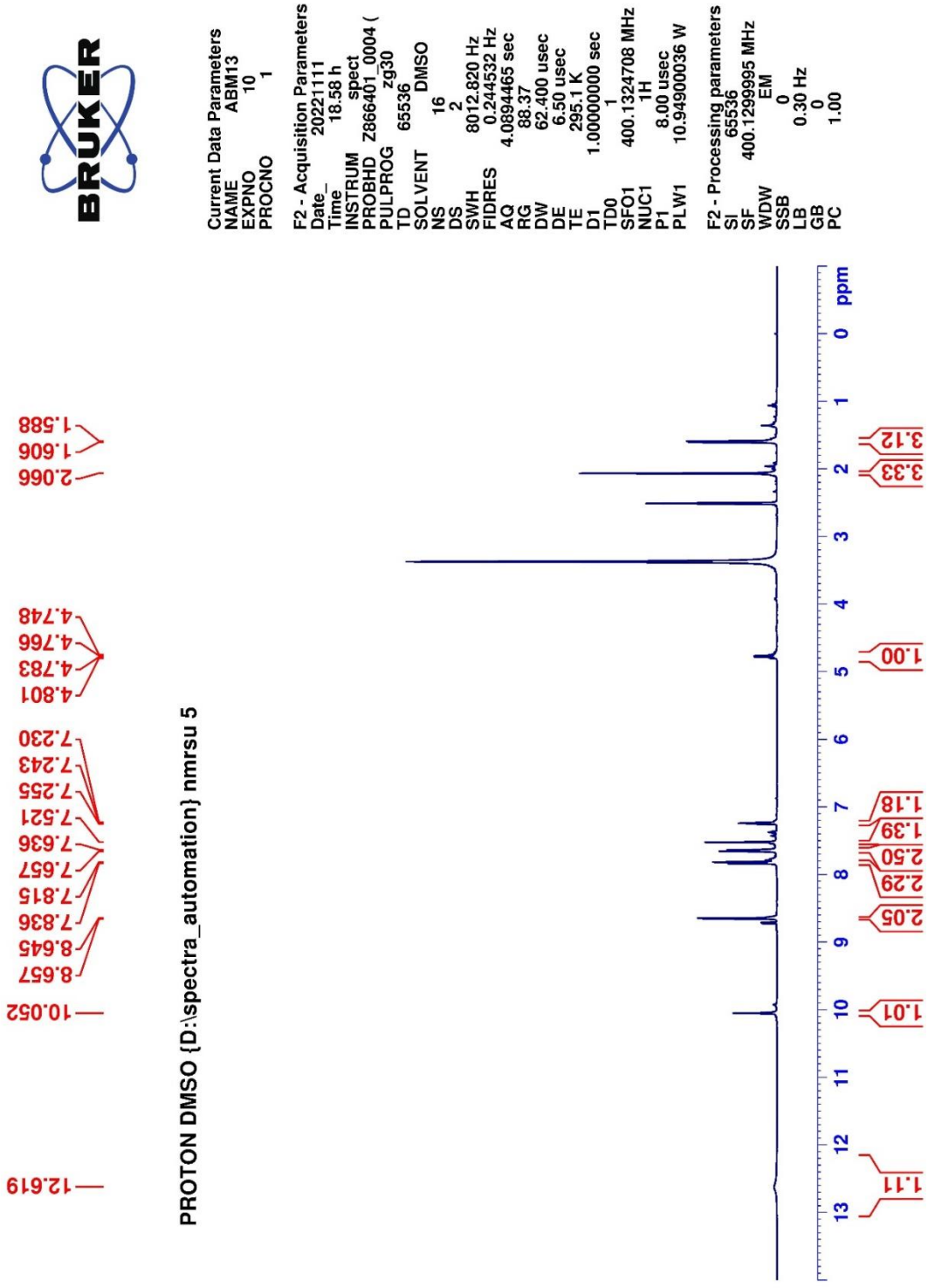

Figure 5.58. *[1]H-NMR spectrum of compound **5k***

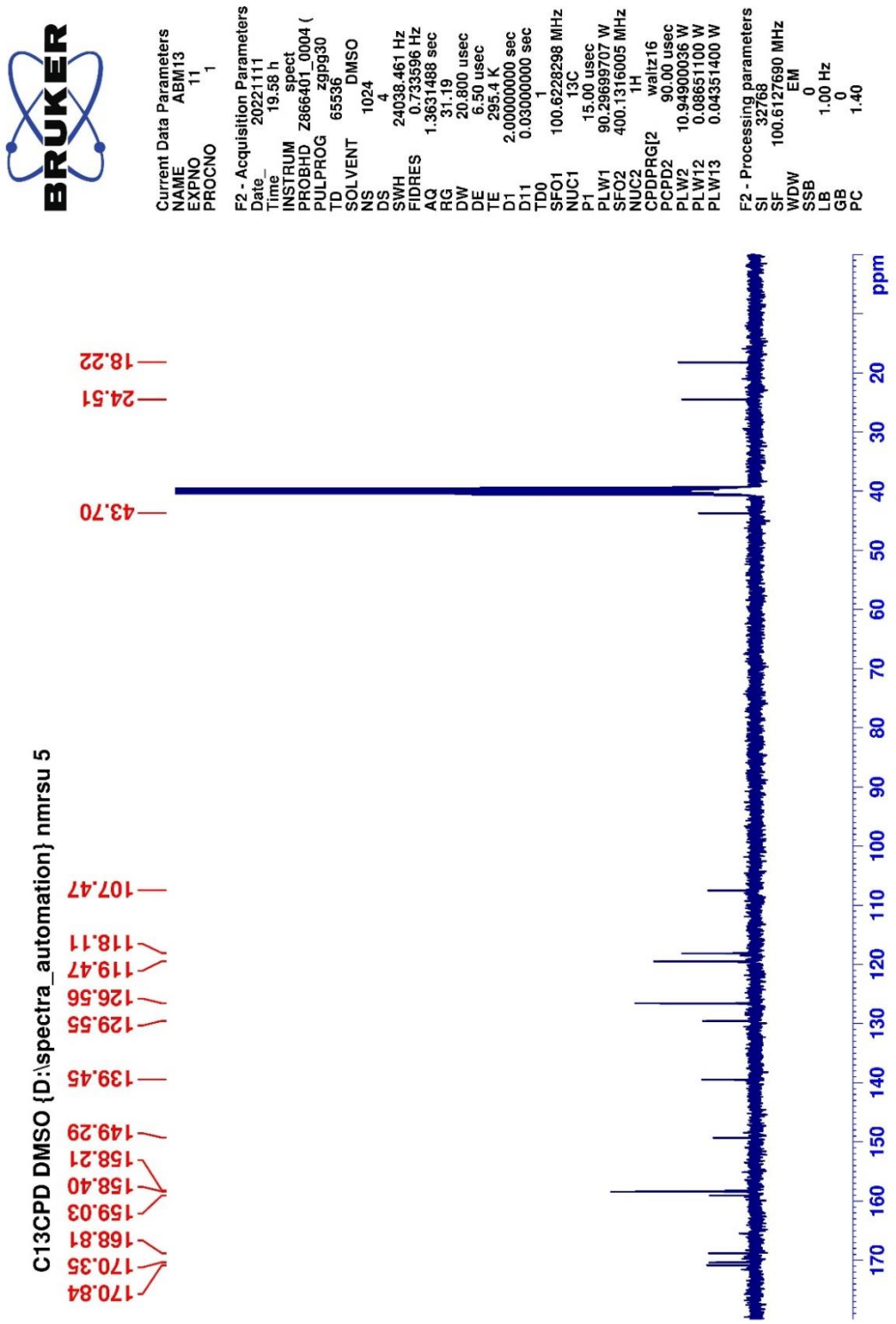

Figure 5.59. *[13]C-NMR spectrum of compound **5k***

Formula Predictor Report - AB-M13_356.lcd

Page 1 of 1

Data File: C:\LabSolutions\Data\Analiz\Asaf\AB-M13_356.lcd

Elmt	Val.	Min	Max	Elmt	Val.	Min	Max	Elmt	Val.	Min	Max	Elmt	Val.	Min	Max	Use Adduct
H	1	0	30	O	2	0	4	S	2	2	2	Ru	2	0	0	H
C	4	0	30	F	1	0	0	Cl	1	0	0	Pd	2	0	0	
N	3	0	6	P	3	0	0	Br	1	0	0	I	3	0	0	

Error Margin (ppm): 5
HC Ratio: unlimited
Max Isotopes: 3
MSn Iso RI (%): 10.00

DBE Range: 5.0 - 25.0
Apply N Rule: yes
Isotope RI (%): 1.00
MSn Logic Mode: AND

Electron Ions: odd
Use MSn Info: yes
Isotope Res: 9000
Max Results: 50

Event#: 1 MS(E+) Ret. Time : 2.307 Scan# : 347

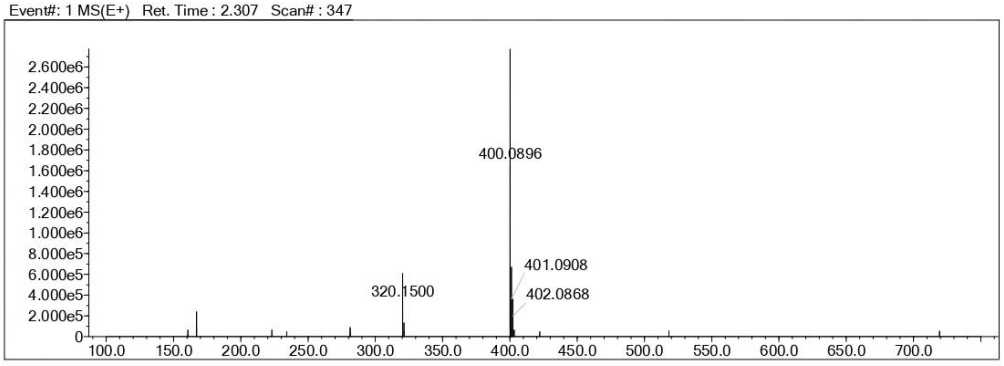

Measured region for 400.0896 m/z

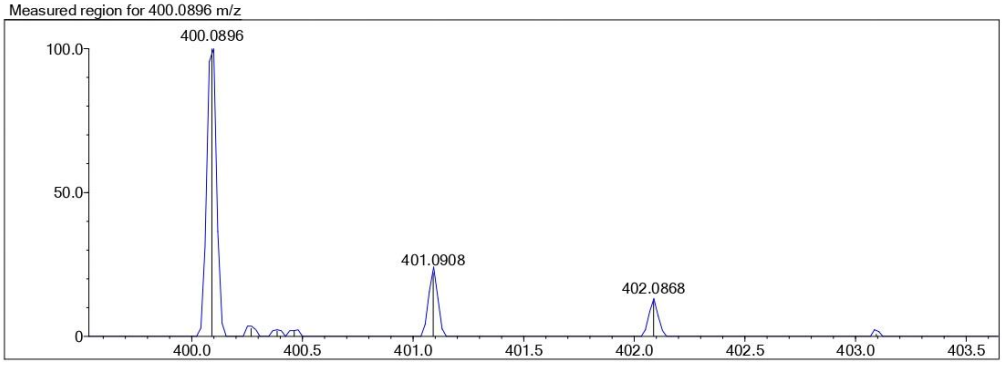

C18 H17 N5 O2 S2 [M+H]+ : Predicted region for 400.0896 m/z

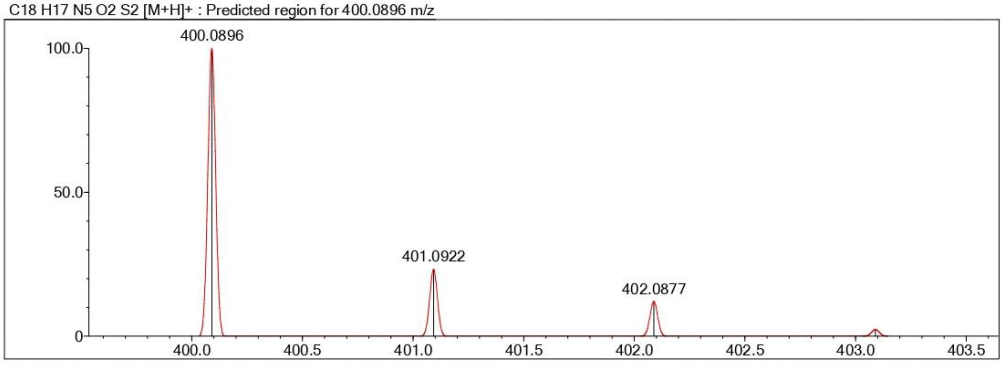

Rank	Score	Formula (M)	Ion	Meas. m/z	Pred. m/z	Df. (mDa)	Df. (ppm)	Iso	DBE
1	98.94	C18 H17 N5 O2 S2	[M+H]+	400.0896	400.0896	-0.0	0.00	98.94	13.0

Figure 5.60. *HRMS of compound* ***5k***

5.1.5.12 *N*-[4-(4-Acetamidophenyl)thiazol-2-yl]-2-[(5-methylbenzoxazol-2-yl)thio]propanamide (5l)

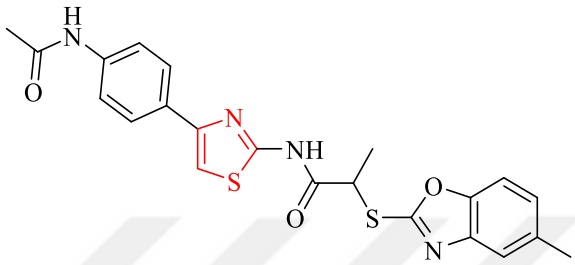

Figure 5.61. *Molecular structure of compound* ***5l***

Physical Characteristics: Material appearance: powder, **Color**: pale yellow, **Yield**: 72%. **M.P.:**140 °C.

IR (ATR) υ_{max} (cm^{-1}): 3292-3184 (N-H stretching), 3111-2978 (C-H stretching), 1688 (C=O stretching, amide), 1539-1408 (C=N stretching, and C=C stretching), 1257-1062 (C-N stretching).

^{1}H-NMR (400 MHz, DMSO-d_6, ppm) δ: 1.73 (3H, d, *J*= 6.95 Hz, C$\underline{H}_3$CHCO), 2.07 (3H, s, $COCH_3$), 2.39 (3H, s, CH_3), 4.90 (1H, q, *J*= 6.91 Hz, CH), 7.14 (1H, d, *J*= 8.26 Hz , benzoxazole -H_6), 7.46 (1H, s, thiazole-H_5), 7.53 (2H, t, *J*= 8.05 Hz, benzoxazole -$H_{4,7}$), 7.65 (2H, d, *J*= 8.26, Ph-$H_{2,6}$), 7.83 (2H, d, *J*= 8.37 Hz, Ph-$H_{3,5}$), 10.05 (1H, s, N$\underline{H}$$COCH_3$), 12.79 (1H, s, NH),

^{13}C-NMR (100 MHz) (DMSO-d_6) δ (ppm): 19.14 ($\underline{C}H_3CHCO$), 21.35(CH_3), 24.51 ($COCH_3$), 45.97 (CH), 107.77 (thiazole-C_5), 110.16 (benzoxazole -C_4), 118.86 (benzoxazole -C_7),119 .49 (Ph-$C_{3,5}$), 125.92 (benzoxazole -C_5), 126.58 (Ph-$C_{2,6}$), 129.46 (Ph-C_1), 134.66 (benzoxazole -C_6), 139.52 (Ph-C_4), 141.78 (benzoxazole -C_{7a}), 149.41 (benzoxazole -C_{3a}), 149.95 (thiazole-C_4), 157.92 (thiazole-C_2), 162.77 (benzoxazole -C_2), 168.81 ($\underline{C}OCH_3$), 169.64 (CO).

HRMS (ESI) (*m/z*): [M + 1] $^{+}$: Calculated for $C_{22}H_{20}N_4O_3S_2$: 453.1050; found 453.1050.

DOPNALAB

	Item	Value
	Acquired Date&Time	22.12.2022 16:33:15
	Acquired by	System Administrator
	Filename	C:\Users\dopnalab\Desktop\MASAÜSTÜ\LEYLA YURTDAŞ\abdurrahman\AB-M\AB-M14.1.is
	Spectrum name	AB-M14.1
	Sample name	AB-M14
	Sample ID	
	Option	
	Comment	
	No. of Scans	15
	Resolution	4 [cm-1]
	Apodization	Happ-Genzel

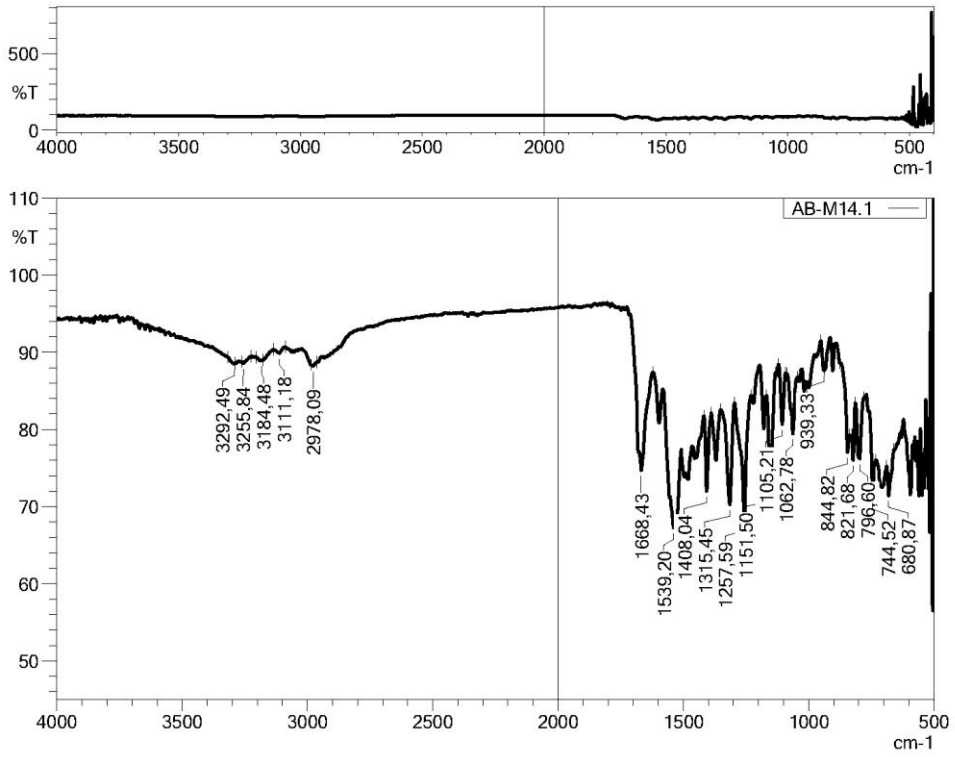

Figure 5.62.*The infrared spectrum of compound* ***5l***

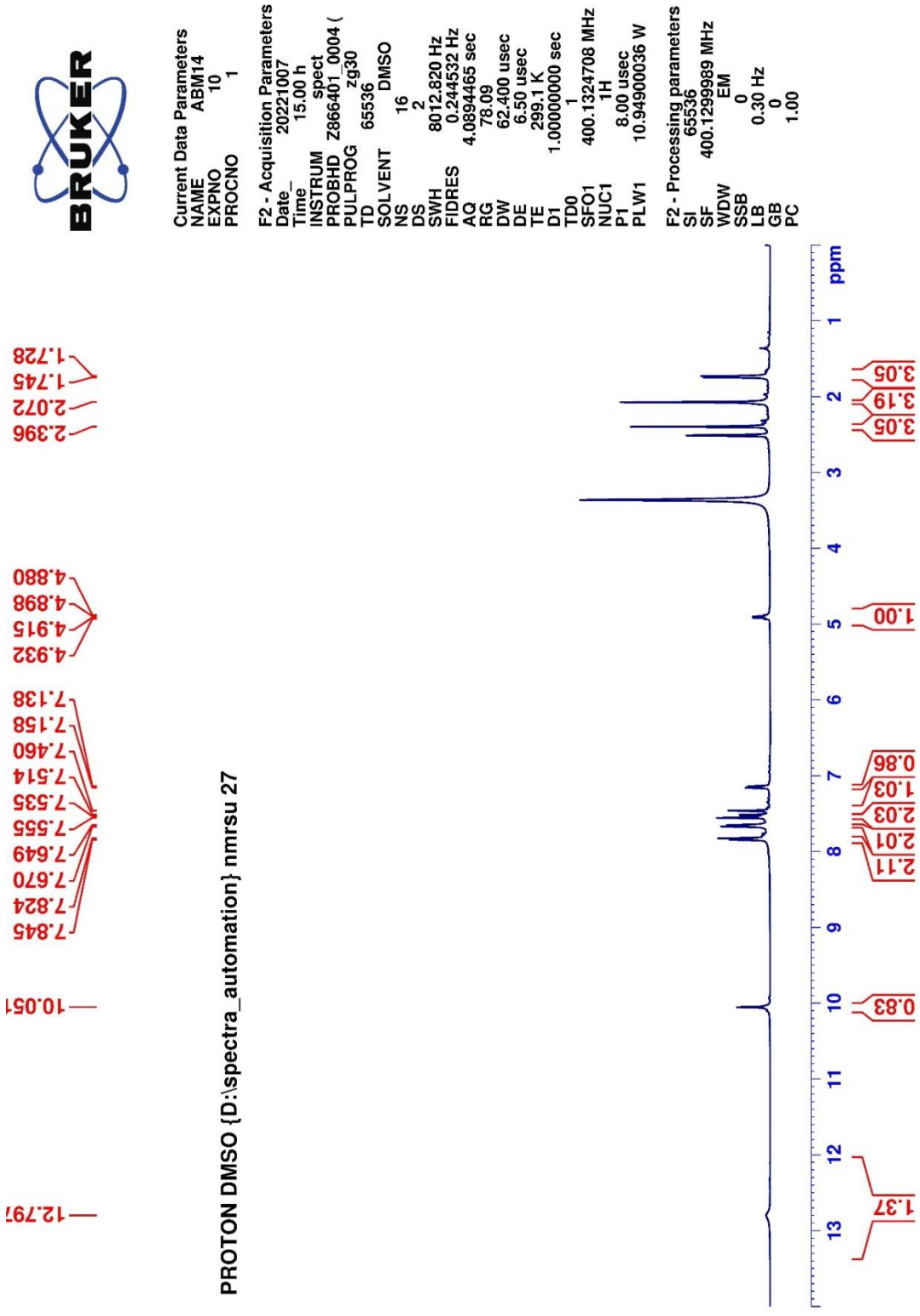

Figure 5.63. *[1]H-NMR spectrum of compound **5l***

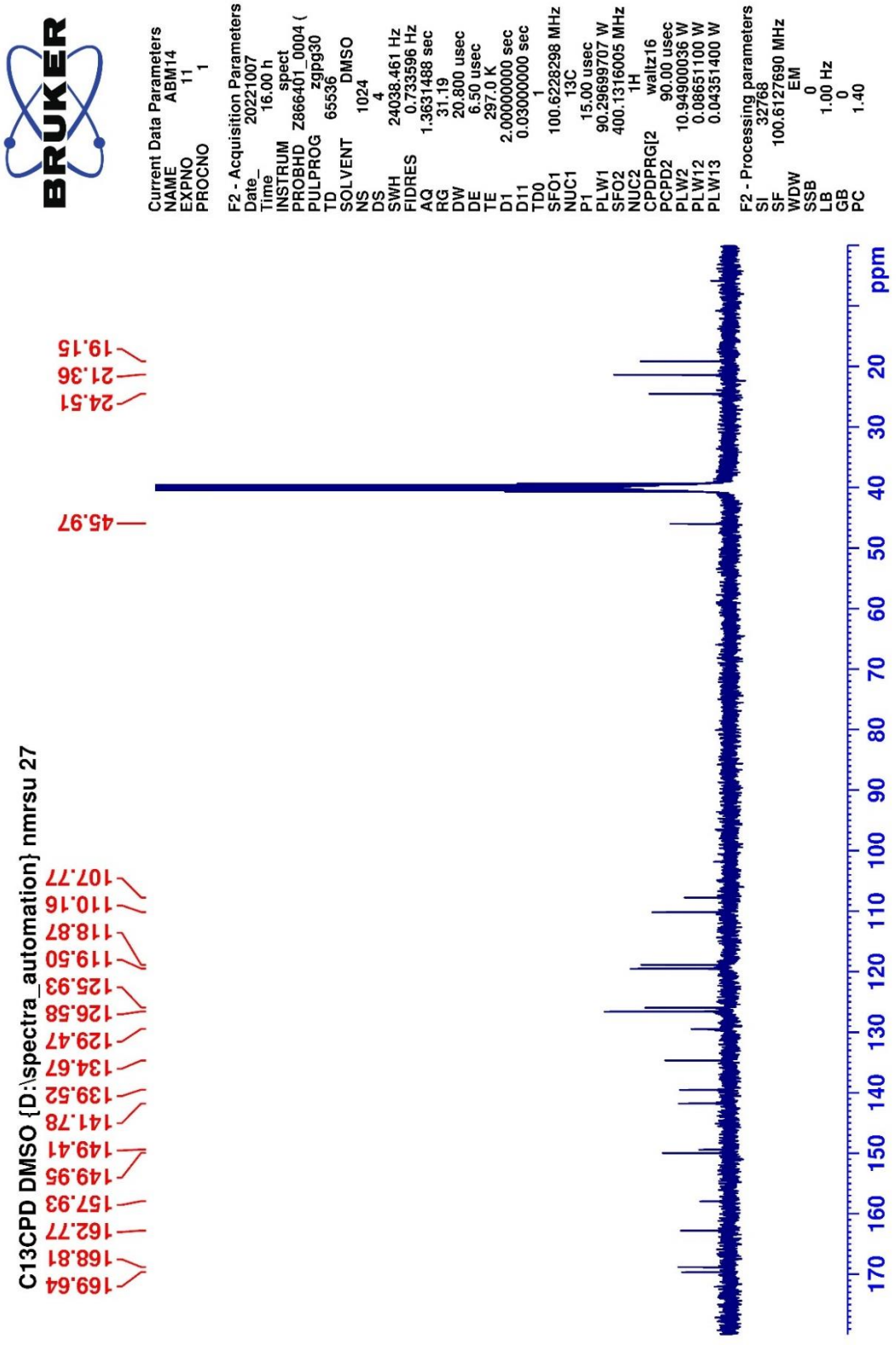

Figure 5.64. *[13]C-NMR spectrum of compound **5l***

Formula Predictor Report - AB-M14_350.lcd

Page 1 of 1

Data File: C:\LabSolutions\Data\Analiz\Asaf\AB-M14_350.lcd

Elmt	Val.	Min	Max	Elmt	Val.	Min	Max	Elmt	Val.	Min	Max	Elmt	Val.	Min	Max	Use Adduct
H	1	0	30	O	2	0	4	S	2	2	2	Ru	2	0	0	H
C	4	0	30	F	1	0	0	Cl	1	0	0	Pd	2	0	0	
N	3	0	6	P	3	0	0	Br	1	0	0	I	3	0	0	

Error Margin (ppm): 5
HC Ratio: unlimited
Max Isotopes: 3
MSn Iso RI (%): 10.00

DBE Range: 5.0 - 25.0
Apply N Rule: yes
Isotope RI (%): 1.00
MSn Logic Mode: AND

Electron Ions: odd
Use MSn Info: yes
Isotope Res: 9000
Max Results: 50

Event#: 1 MS(E+) Ret. Time : 3.627 Scan# : 545

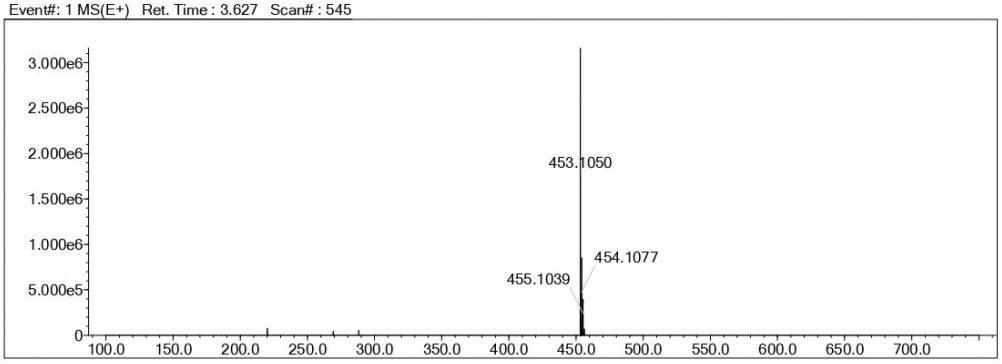

Measured region for 453.1050 m/z

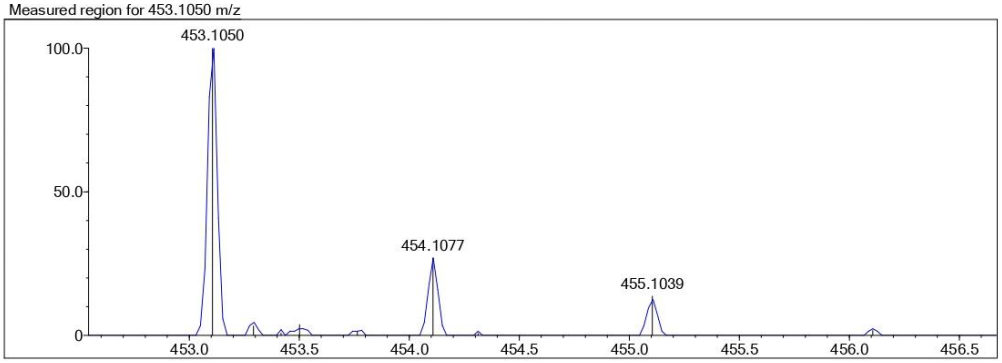

C22 H20 N4 O3 S2 [M+H]+ : Predicted region for 453.1050 m/z

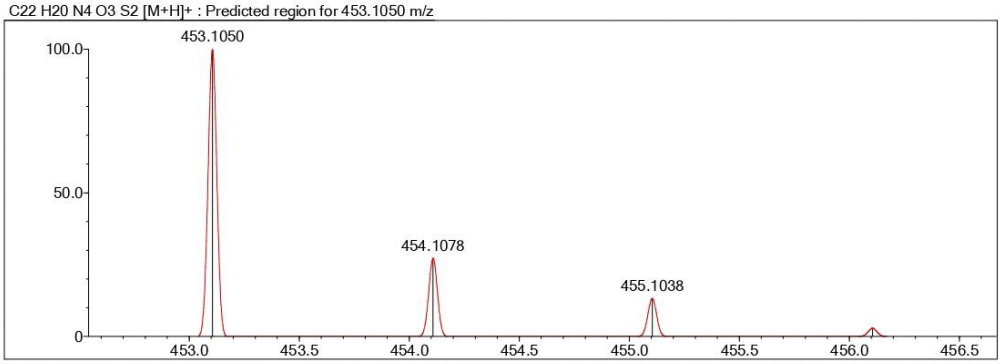

Rank	Score	Formula (M)	Ion	Meas. m/z	Pred. m/z	Df. (mDa)	Df. (ppm)	Iso	DBE
1	93.77	C22 H20 N4 O3 S2	[M+H]+	453.1050	453.1050	0.0	0.00	93.77	15.0

Figure 5.65. *HRMS of compound **5l***

5.2. Chemical Synthesis Evaluation

The compounds were synthesized in the laboratory within five steps. The process started with adding the acetyl group, followed by adding bromine, closing the thiazole ring, adding the acetyl group again, and finally adding the twelve mercaptan compounds in the substitution reaction as shown in the Figure 5.66.

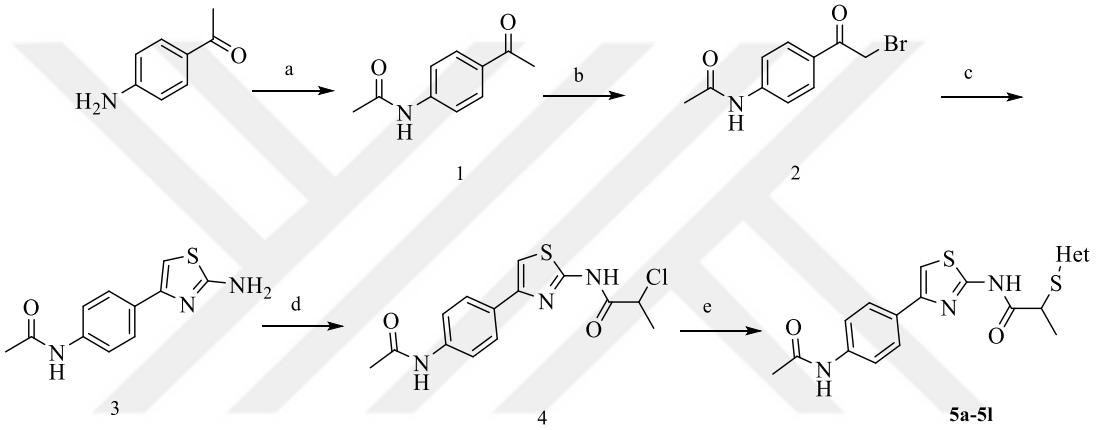

Figure 5.66. *Synthesize route for all molecules*

In the first step, as shown in Figure 5.67 the acetyl group was added to the compound 5-aminoacetophenone by reacting with acetyl chloride in the presence of triethylamine in THF nonpolar aprotic solvent to form *N*-(4-acetylphenyl)acetamide compound via nucleophilic substitution reaction.

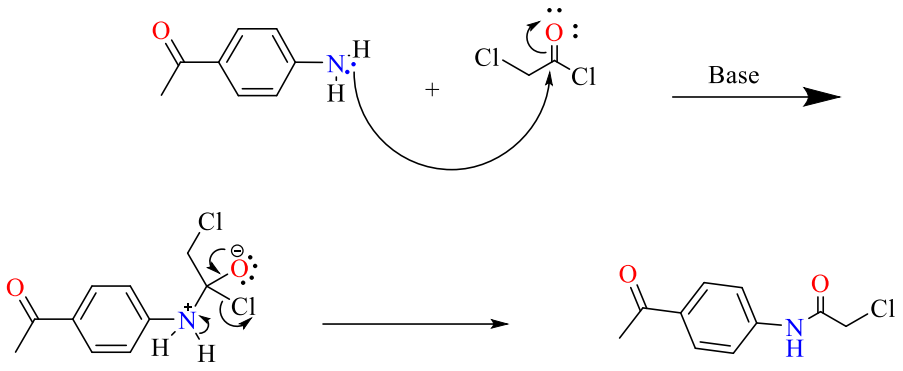

Figure 5.67.*Mechanism of method A*

In the second step, as shown in Figure 5.68 In the protic solvent acetic acid, the *N*-(4-acetylphenyl)acetamide was reacted with bromine in the presence of droplets of hydrobromide acid by an exothermic chemical reaction SN_2 to be *N*-[4-(2-bromoacetyl)phenyl]acetamide.

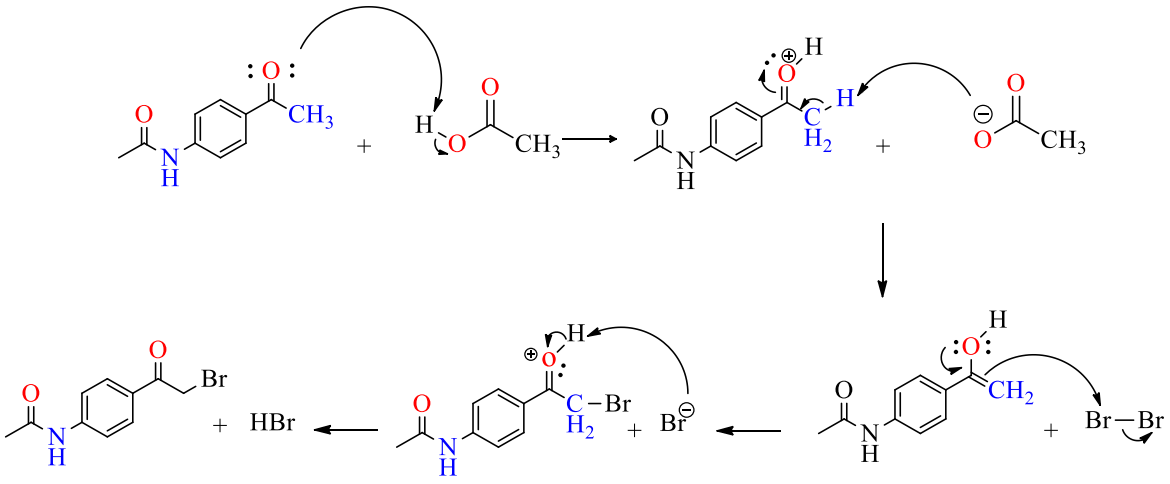

Figure 5.68.*Mechanism of method **B***

In the third step, *N*-[4-(2-bromoacetyl)phenyl]acetamide reacts with thiourea in the ethanol solvent in presence of heat by Hantzsch synthesis reaction to close the thiazole ring and form *N*-[4-(2-aminothiazol-4-yl)phenyl]acetamide as shown in Figure 5.69.

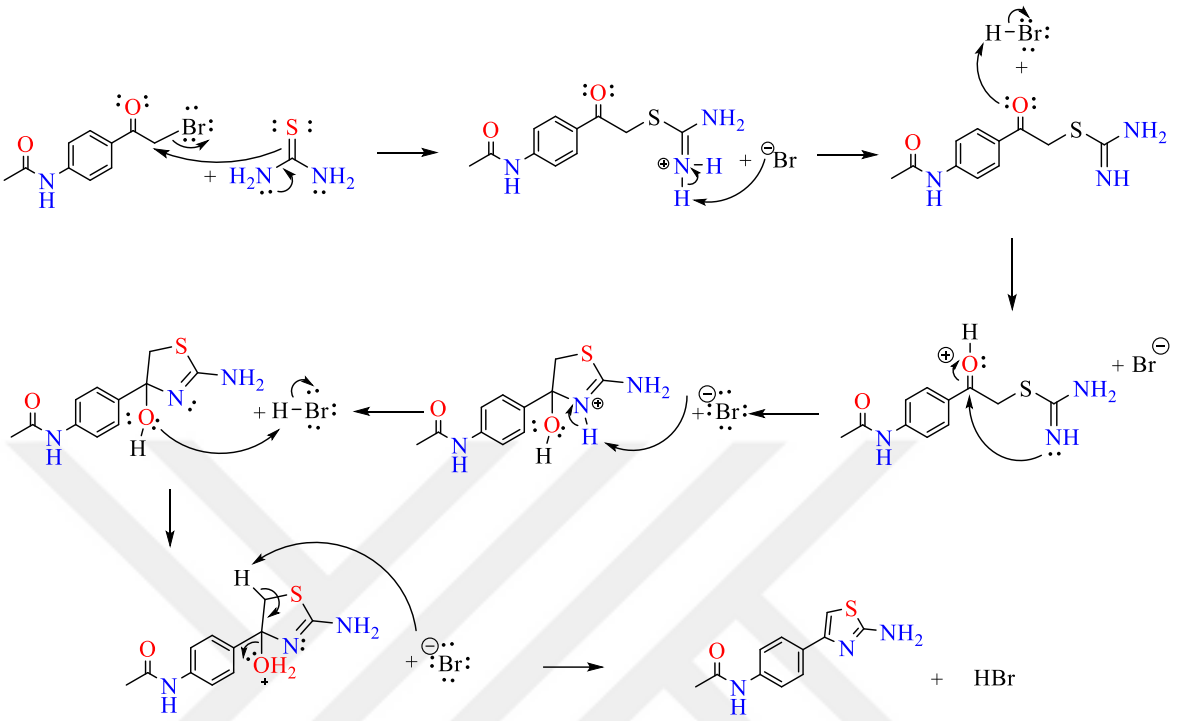

Figure 5.69.*Mechanism of method* ***C***

In the fourth step, a second acetyl group was added using a mechanism similar to that of method A. This was achieved by reacting 2-chloropropionyl chloride with *N*-[4-(2-aminothiazol-4-yl)phenyl]acetamide via nucleophilic substitution reaction in tetrahydrofuran solvent, with triethylamine used as a nucleophile. The resulting product was *N*-[4-(4-acetamidophenyl)thiazol-2-yl]-2-chloropropanamide, as illustrated in Figure 5.70.

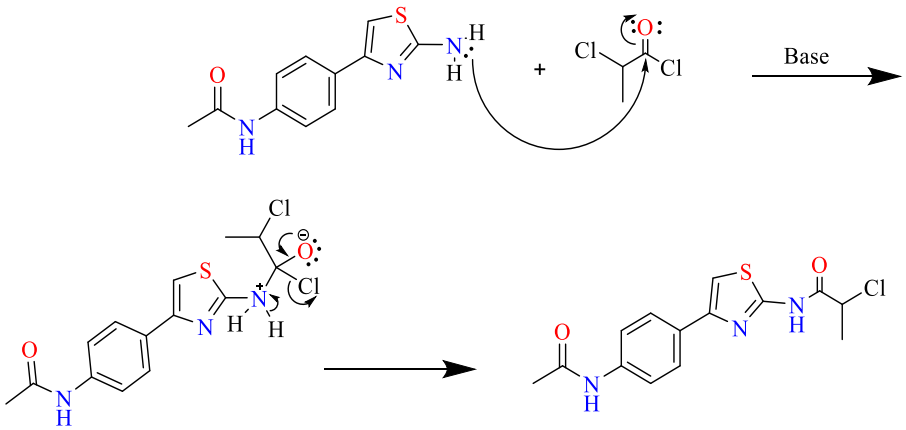

Figure 5.70. *Mechanism of method* ***D***

In the final step, all 12 compounds were synthesized through a reaction between the mercaptan derivatives and *N*-[4-(4-acetamidophenyl) thiazol-2-yl]-2-chloropropanamide in the presence of potassium carbonate as a catalyst, using acetone as a solvent. The reaction was carried out at room temperature for one day as shown in Figure 5.71 .

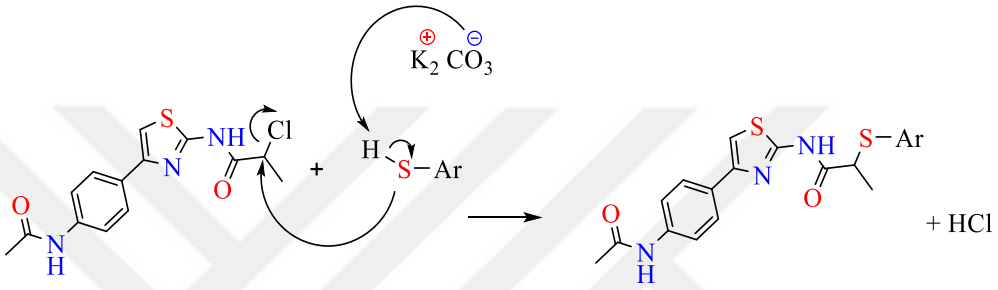

Figure 5.71. *Mechanism of method **E***

All of the synthesized compounds are original derivatives, with yields ranging between 70-98% for the final compounds **5a-5l**. The purity and chemical structure of all targeted compounds were confirmed using chemical spectral analysis techniques such as IR, ^{1}H-NMR, ^{13}CNMR, and HRMS.

5.3. Chemical Analysis Results Evaluation

5.3.1. IR analysis results

The synthesized compounds (**5a-5l**) were subjected to IR analysis to determine their main functional groups. The N-H functional group showed a band above 3000 cm^{-1}, particularly between 3063 and 3292 cm^{-1}. The C-H aromatic of sp^2 hybridized carbons had a value above 3000 cm^{-1}, except for **5g**, which showed a value of 2974 cm^{-1}. The aliphatic C-H of sp^3 hybridized carbons were observed below 3000 cm^{-1}, ranging from 2848-2988 cm^{-1}.

For the (C=O) group, most compounds recorded a band of around 1688 cm^{-1}, with an overall band ranging between 1660 and 1688 cm^{-1}. The aromatic (C=N) functional group showed a general value between 1537-1597 cm^{-1}, except for compound **5g**, which recorded a peak at 1663 cm^{-1}. The (C=C) aromatic group of sp^2 hybridized carbons recorded a band

ranging from 1405-1489 cm^{-1} except for **5k**, which showed a value of 1539 cm^{-1}, while the range of picking in the (C-N) group was observed between 1002-1267 cm^{-1}.

5.3.2. ^{1}H-NMR analysis results

All compounds contain thiazole ring bound with *N*-phenylacetamide on 4th position. The reaction of alkyl chloride moiety with various mercaptan derivatives at the junction no. 2 of propanamide produced a variety of derivatives.

The Bruker UltraShield 400 MHz was utilized for performing NMR analysis. All the samples have been dissolved in DMSO-d_6, which was observed as a quintet at 2.5 ppm in all the spectra. A powerful singlet was observed in the spectra of most compounds at approximately 3.4 ppm, indicating the presence of water protons.

In the aliphatic region there are three carbons containing protons common to all compounds. These protons are doublet (CH_3), singlet ($COCH_3$), quartet (CH), and have found their value within (1.44-1.75), (2.08-2.51) and (4.15-4.96) ppm ranges, respectively. In addition, compounds **5a**, **5b**, **5d, 5h**, and **5l** have singlet aliphatic protons branched from the azo group of the rings. **5a** and **5b** are related to N-CH_3 with a value of 3.59 and 3.97 ppm, respectively, while **5d**, **5h** and **5l** compounds are related to CH_3 with a value of 2.69,3.58, and 2.39 ppm respectively. The reason for the change in values is the deshielding effect of oxygen, nitrogen and sulfur in these compounds.

In the aromatic region the compound **5a**, the C_4 proton in the imidazole ring was found to be single at a value of 7.03 ppm, and the same with C_5 proton, which also appeared single at a value of 7.34 ppm, while both were supposed to appear as doubles, but the reason could be the magnetic force generated by the instrument, which is not strong enough to achieve optimal results.[123, 124] As expected, in compound **5c** the C_4 proton of the benzothiazole group was singlet with 7.92 ppm value, while C_6 and C_7 protons were observed doublet in 7.44 and 8,08 ppm respectively. The **5g** compound also contains a benzothiazole ring and as expected, the protons of C_5, C_4 and C_7 observed peaks triplet, multiplet and doublet at 7.39, 7.85 and 8.04 ppm respectively.

Both **5e** and **5f** contain a benzothiazole ring, where **5e**, as expected, protons of C_5 and C_6 Doublet, while C_4 was single with values of 7.52, 8.08 and 8.33 ppm respectively. But

unexpectedly for the **5f** all the protons of the carbons ring observed singlet peaks with a value of 7.16 ppm for protons C_5 and C_6 and a value of 7.50 ppm for protons C_4 and C_7 respectively.

The compounds **5i**, **5j** and **5l** all contain a benzoxazole ring. Compound **5i** observed two doublet peaks for the benzene ring connected to the oxazole ring as expected, as the values were 7.34ppm for the C_4 and C_7 proteins, while the value was 7.64ppm for the proteins of C_6 and C_5, respectively. As for the **5j** and **5l** compounds, the doublet and triplet peaks were observed as expected, where the values for the protons of C_5 were 7.39 and 7.14 ppm for both compounds respectively, while the C_4 and C_7 peaks were observed 7.71 and 7.81 ppm for the **5g** compound, while the value of 7.53 was given for the **5l** compound.

As for the phenyl ring present in all compounds, it often appears as doublet peaks with values between 7.64 - 7.70 ppm for protons of C_2 and C_6, while it appears at a value between 7.66- 7.85 ppm for protons of C_3 and C_5.

The thiazole ring is the main ring in the all compounds and contains a proton at C_5, which always shows a singlet peaks with a value between 7.46 and 7.56 ppm.

Finally, the proton in the two amide groups that are found in all compounds sometimes appears in the form of a single between 10.03-12.83 ppm and sometimes does not appear, and the reason why the proton does not appear is a link with the nitrogen atom with high negativity that may lose the proton and return gain with the solvent used in the analysis, when absent in the results, it is at the moment of taking the results remained with the solvent used.

5.3.3. ^{13}C NMR analysis results

A Bruker UltraShield instrument operating at a frequency of 100 MHz and using DMSO-d_6 as the solvent was utilized for the ^{13}C-NMR analysis. The solvent peak was detected in the form of a very long peak as a septet, with a chemical shift of approximately 40 ppm. The analysis of each sample necessitated a time investment of 60 minutes.

In the thiazole ring, the peaks of C_2, C_4 and C_5 appear in all compounds between the value of (107.79 - 168.56) ppm, where the C_5 is the least deshilded, while C_2 is the most deshilded, and the reason is because C_2 crosses the most carbon in the thiazole ring, which has a deshilded is that it is located between two atoms with high negativity, which are sulfur and nitrogen.

All aromatic carbons in all compounds from the benzene ring, oxathiazole, thiazole, imidazole, benzothiazole, benzothiazole, tetrazole, triazole and pyrimidine show peaks between about 110-162 ppm.

The carbonyl carbon displayed the greatest degree of deshielding among all compounds. The carbonyl carbon resided within a range of 168.79-170,74 ppm, while in carbonyl attached to CH_3, it was deshielded to a degree of 151.65-168.82 ppm.

5.3.4. Mass spectrometry

The LCMS-IT-TOF was used to analyze the mass spectra of all the synthesized compounds. This technique involved injecting the samples through liquid chromatography before analyzing their mass using a mass spectrometer unit. The obtained results indicated that there were no impurities in the chromatogram, and the [M+1] peaks in the spectra of the mass of all series corresponded to their expected molecular weights. Therefore, the spectra of the all final compounds mass were taken using high-resolution mass-spectrometry device with the ESI method, and the peak of the M+1 ion was detected in all compounds according to their molecular weights [125].

5.4. *In vitro* Anticholinesterase Inhibition Results Evaluation

The synthesized compounds were tested *in vitro* to determine their inhibitory effects on acetylcholine and butyrylcholine esterase. Generally, the compounds showed better efficacy as an acetylcholine esterase inhibitor. To evaluate the percentage of inhibition, Elman's modified method [126] was employed using concentrations of 10^{-3} M and 10^{-4} M for various compounds, with tacrine and donepezil used as reference drugs. Further analysis was conducted on the compounds that exhibited over 50% inhibition activity at both concentrations by testing them at lower concentrations between 10^{-5} and 10^{-9} M to establish their IC_{50} values. **Table 5.1**. lists the results of this research.

All the compounds gave an inhibition efficiency aganist AChE over 50% for a concentration of 10^{-3} M, except for **5b**, **5c**, **5g** and **5h**. While for a concentration of 10^{-4} M only three compounds gave a concentration above 50%, namely **5d**, **5e** and **5j**.

Following the initial evaluation, compounds **5d**, **5e** and **5j** were selected to determine their respective IC_{50} values for acetylcholinesterase inhibition. These compounds were assessed at concentrations ranging from 10^{-5} to 10^{-9} M against AChE, in comparison to the reference medication, donepezil. The IC_{50} value for donepezil is 0.0201 μM, while the IC_{50} values for compounds **5d**, **5e** and **5j** were determined to be 0.223 μM, 0.092 μM, and 0.054 μM, respectively.

N-[4-(4-Acetamidophenyl)thiazol-2-yl]-2-[(5-chlorobenzoxazol-2-yl)thio]propanamide **(5j)** is the best synthesized compound in terms of efficacy against acetylcholine esterase (IC_{50} = 0.054 μM) and this compound contains a benzoxazole group with chlorine at site 5 of the ring bonded with sulfur. Also, the effectiveness was significantly reduced when we replaced the chlorine atom with a methyl group at the same location in the compound **5l** to give IC_{50} >100 at a concentration of 10^{-4}M. Also, the benzoxazole ring is important for effectiveness, but if you replace it with some rings, it may also give effectiveness, but if we replace it with other rings, the effectiveness may decrease, for example, as in the **5d** compound, we replaced the ring with (2-methyl-1,3,4-thiadiazole) and the **5e** compound, we replaced it with (5-nitro-1*H*-benzimidazole), as both compounds gave the effectiveness of IC_{50} 0.223 and IC_{50} 0.092 μM respectively, but when we replaced the ring with some rings like tetrazole, benzothiazole, triazole and pyrimidine, the effectiveness decreased.

On the other hand, unfortunately all compounds gave low efficacy against BChE below 50 % to a concentration of both 10^{-3} or 10^{-4} with notable IC_{50} values.

Table 5.1. *Inhibition rates and IC_{50} (μM) values of the obtained compounds against AChE and BChE enzymes at concentrations of 10^{-3} and 10^{-4} M*

Compound	AChE % Inhibition		AChE IC_{50} (μM)	BChE % Inhibition		BChE IC_{50} (μM)
	10^{-3} M	10^{-4} M		10^{-3} M	10^{-4} M	
5a	**52.323 ±1.122**	42.597 ±1.454	>100	26.462 ±0.834	22.746 ±0.720	>1000
5b	48.154 ±0.936	41.357 ±1.010	>1000	29.375 ±0.920	26.128 ±0.967	>1000
5c	42.759 ±0.806	38.964 ±0.821	>1000	30.613 ±1.258	26.408 ±0.857	>1000
5d	**89.646 ±1.958**	**83.342 ±1.768**	**0.223 ±0.010**	31.045 ±1.041	24.067 ±0.812	>1000
5e	**92.155 ±1.874**	**88.464 ±1.334**	**0.092 ±0.003**	24.246 ±0.865	20.771 ±0.830	>1000
5f	**72.849 ±2.485**	48.328 ±0.889	>100	32.749 ±1.059	26.697 ±0.718	>1000
5g	47.764 ±1.030	31.146 ±1.302	>1000	30.569 ±1.156	20.203 ±0.801	>1000
5h	43.233 ±0.955	29.031 ±0.847	>1000	27.322 ±0.948	22.345 ±0.720	>1000
5i	**57.954 ±1.537**	30.897 ±0.867	>100	28.048 ±0.864	21.470 ±0.869	>1000
5j	**93.576 ±2.846**	**90.655 ±1.920**	**0.054 ±0.002**	26.468 ±0.854	23.876 ±0.778	>1000
5k	**74.290 ±2.110**	47.231 ±0.886	>100	29.567 ±0.975	25.661 ±0.897	>1000
5l	**69.067 ±1.854**	38.468 ±0.736	>100	28.357 ±0.923	22.554 ±0.764	>1000
Donepezil	99.156 ±1.302	97.395 ±1.255	0.0201 ±0.0010	-	-	-
Tacrine	-	-	-	99.827 ±1.378	98.675 ±1.450	0.0064 ±0.0002

5.5. Evaluation of *In vitro* MAO Inhibition Results

The results of the effectiveness of all compounds gave similar results either for MAO-A or for MAO-B, where all % inhibition for MAO-A compounds were between 25.362-38.461 % for a concentration of 10^{-3}, while the compounds gave efficacy values between 20.415 and 31.748 % for a concentration of 10^{-4}, while for MAO-B, the results of inhibition percentage for the compounds are between 30.886 and 45.441 % for a concentration of 10^{-3}, while it gave the values of 23.447 and 32.712 % for a concentration of 10^{-4}. Although the compounds may have given greater efficacy against MAO-B than MAO-A as shown in the Table 5.2, unfortunately all values of MAOs are considered weak compared to Moclobemide and Selegiline.

Table 5.2.*inhibition rates and IC50 (μM) values of the obtained compounds against MAO-A and MAO-B enzymes at concentrations of 10-3 and 10-4 M*

Compound	MAO-A % Inhibition		MAO-A IC_{50} (μM)	MAO-B % Inhibition		MAO-B IC_{50} (μM)
	10^{-3} M	10^{-4} M		10^{-3} M	10^{-4} M	
5a	32.521 ±0.830	26.384 ±0.820	>1000	42.449 ±0.934	32.174 ±0.747	>1000
5b	36.403 ±1.176	29.636 ±0.915	>1000	39.534 ±1.225	31.050 ±1.039	>1000
5c	30.791 ±1.068	20.415 ±0.944	>1000	45.441 ±0.984	28.623 ±1.018	>1000
5d	37.964 ±1.151	21.152 ±0.785	>1000	42.822 ±1.562	32.712 ±0.933	>1000
5e	29.554 ±0.820	22.167 ±0.935	>1000	38.774 ±1.467	31.955 ±1.202	>1000
5f	33.362 ±1.348	28.530 ±0.720	>1000	36.451 ±1.208	29.574 ±1.055	>1000
5g	38.461 ±0.922	29.654 ±0.964	>1000	39.113 ±1.235	29.494 ±0.957	>1000
5h	32.007 ±0.828	30.067 ±0.939	>1000	41.464 ±0.837	31.646 ±1.062	>1000
5i	36.867 ±1.351	31.748 ±1.120	>1000	35.774 ±1.348	30.722 ±1.168	>1000
5j	30.484 ±0.989	24.425 ±0.737	>1000	36.959 ±1.534	32.536 ±0.920	>1000
5k	25.362 ±0.866	21.168 ±1.011	>1000	30.886 ±1.467	23.447 ±0.958	>1000
5l	38.155 ±1.476	33.831 ±1.317	>1000	32.303 ±0.918	24.628 ±0.851	>1000
Moclobemide	94.121 ±2.760	82.143 ±2.691	6.0613 ±0.2625	-	-	-
Selegiline	-	-	-	98.589 ±2.055	94.850 ±1.114	0.0374 ±0.0016

5.6. Physicochemical Properties Evaluation

Table 5.3 displays the anticipated pharmacokinetic characteristics of compounds **5d, 5e, 5j**, as well as the reference drugs Moclobemide and Donepezil.

The SwissADME website have been utilized to expect the pharmacokinetic characteristics of the most effective compounds which are **5d, 5e** and **5j**, where the topological polar surface area (TPSA) value of the compounds was found to be somewhat high as it was 178.65, 199.13 and 150.66 $Å^2$ respectively.

The LogPo/w, which is an indicator of lipophilicity, was computed and found to be within the necessary range of -0.7 to 5, as reported by Daina *et al.* [127].

As for the percentage of Log S (ESOL) which is the percentage of aqueous solubility, all compounds, including Donepezil, are considered medium solubility, except for Molcobemide, which is considered soluble in aqueous. For LogKp (skin permeation) the value of the compounds **5d, 5e** and Moclobemide is all -6 cm/s, while the **5j** and Donepezil are worth the same value -5 cm/s.

Unfortunately, the three compounds with the most effective all give a prediction that the absorption of gastrointestinal will be low.

The number of hydrogen-bond acceptors for Moclobemide is 3 hydrogen-bond and for Donepezil is 4 hydrogen-bond, while **5j** and **5d** shows that 5 hydrogen-bond can be accepted, the highest hydrogen accept compound is **5e**, which can accept 6 hydrogens according to predict of SwissADME website. On the other hand, for the donating of hydrogen bond, the Donepezil drug cannot donate any bond, while the Moclobemide drug can donate one bond, the **5j** and **5d** compounds can donate two bonds, and **5e** can donate 3 bonds.

Table 5.3.*The study focuses on determining how the active compounds **5d, 5e,** and **5j** are processed by the body, including how they are absorbed, distributed, metabolized, and eliminated.*

Compounds	M.W.	TPSA	Log Po/w (XLOGP3)	Log S (ESOL)	(LogKp) cm/s[11]	Lipinski	GI abs	HA	HD
5d	419.54	178.65	3.12	-4.32	-6.64	Yes	low	5	2
5e	482.54	199.13	3.67	-5	-6.64	Yes	low	6	3
5j	472.97	150.66	4.74	-5.71	-5.82	Yes	low	5	2
S1	379.49	38.77	4.28	-4.81	-5.58	Yes	High	4	0
S2	268.74	41.57	1.49	-2.36	-6.88	Yes	High	3	1

Mwt (molecular weight), **TPSA** (the topological polar surface area), **Log P** (partition coefficient), **LogKp:** skin permeation , **Log S**: aqueous solubility (highly soluble > 0 > very soluble > −2 > soluble > −4 > moderately soluble > −6 > poorly soluble > −10 > insoluble), **GI abs** (gastrointestinal absorption), **HA** (Hydrogen bond acceptor), **HD** (Hydrogen bond donor). **S1**: Donepezil; **S2**: Moclobemide

5.7. Molecular Docking Evaluation

5.7.1. Docking with the acetylcholinesterase enzyme's active site.

AChE is a crucial enzyme that is that is fundamental in the regulation of in the regulation of the neurotransmitter acetylcholine. Docking studies have been extensively utlized to predict the binding mode of ligands to the active site of AChE and to identify potential inhibitors of the enzyme.

The AChE active site is a deep and narrow gorge lined with amino acid residues that are include the catalysis and substrate binding. The amino acids involved in the binding site of AChE include tryptophan, tyrosine, histidine, serine, glycine, and glutamate residues. Tryptophan and tyrosine residues form hydrophobic interactions with the ligand, while histidine, serine, and glutamate residues are involved in hydrogen bonding with the ligand. Glycine residues provide flexibility to the active site and allow it to adapt to the ligand [128–131].

The AChE extensively studied using X-ray crystallography, which has provided valuable insights into the architecture of the enzyme and its active site [132, 133]. The binding sites within AChE can be classified into two types: the central catalytic anionic site (CAS) and the peripheral anionic site (PAS). Both sites are involved in the regulation of AChE activity and have been the subject of extensive research [131].

The active site of AChE is mainly composed of two main binding regions: the peripheral anionic site (PAS) and the catalytic active site (CAS). The CAS is a narrow, long, hydrophobic gorge with a length of about 20 Å. It incorporates the acyl binding site that holds Phe295 and Phe297 amino acids, the active center bearing Glu202, Glu450 fragments, the hydrophobic subsite having Trp86, Tyr133, Tyr337, and Phe338 residues, the oxyanion binding site which contains Gly120, Gly121, and Gly123 residues, and a catalytic triad of Ser203-Glu334- His447 amino acids [126, 134].

The catalytic triad of AChE is responsible for the hydrolysis of acetylcholine. The serine residue (Ser203) acts as a nucleophile and attacks the carbonyl carbon of the acetyl group of acetylcholine, leading to the formation of a covalent enzyme-substrate intermediate. The histidine residue (His447) acts as a general base and deprotonates a water molecule, which subsequently attacks the intermediate, leading to the hydrolysis of acetylcholine. The glutamate residue (Glu334) acts as a general acid and protonates the leaving group, which is the choline moiety of acetylcholine [135].

The PAS is mainly constituted of aromatic residues, including Tyr72, Asp74, Tyr124, Trp286, and Tyr341, which provide a binding site for allosteric inhibitors besides their recognition function for acetylcholine at the gorge rim. The PAS plays a crucial role in regulating the activity of AChE by allosterically modulating the enzyme. Ligands that bind to the PAS can affect the activity of AChE by inducing conformational changes in the enzyme, which can alter the accessibility of the substrate to the active site [130].

Docking studies have been used to predict the binding mode of ligands to both the CAS and the PAS of AChE. One study used a combination of molecular docking and molecular dynamics simulations to identify potential inhibitors of AChE that bind to the CAS. The study identified a compound that showed strong binding affinity to the CAS and inhibited the activity of AChE *in vitro* [136].

Another study used molecular docking to predict the binding mode of ligands to the PAS of AChE. The study identified a compound that showed strong binding affinity to the PAS and modulated the activity of AChE allosterically [137].

The following Figure 5.72 shows the most effective compounds that effectively linked to protein in a three-dimensional image.

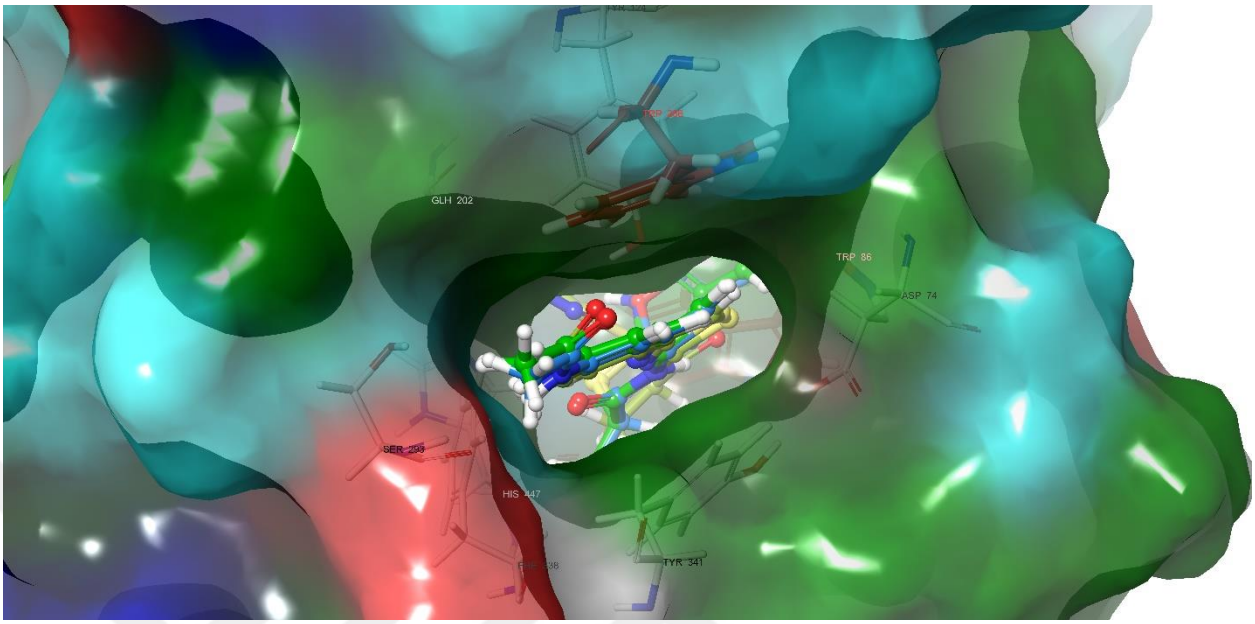

Figure 5.72.*The three most active substances (**5d, 5e**, and **5j**) in the active site of AChE are layered in three dimensions*

5.7.1.1 The molecular docking of compound 5d

The interaction between compound **5d** with the active region in AChE is illustrated in **Figure 5.73** and Figure 5.74. There are five bonds that bind the compound **5d** in AChE, four of them are π-π stacking bonds and a hydrogen bond. Two bonds are located in the CAS region formed between Phe338 and His447 with thiadiazol ring, the other two bonds are located in the PAS region formed between the thiazole ring with Tyr341, and between Trp286 with the benzene ring. The compound formed a fifth bond, a hydrogen bond between the NH-benzene and Ser293.

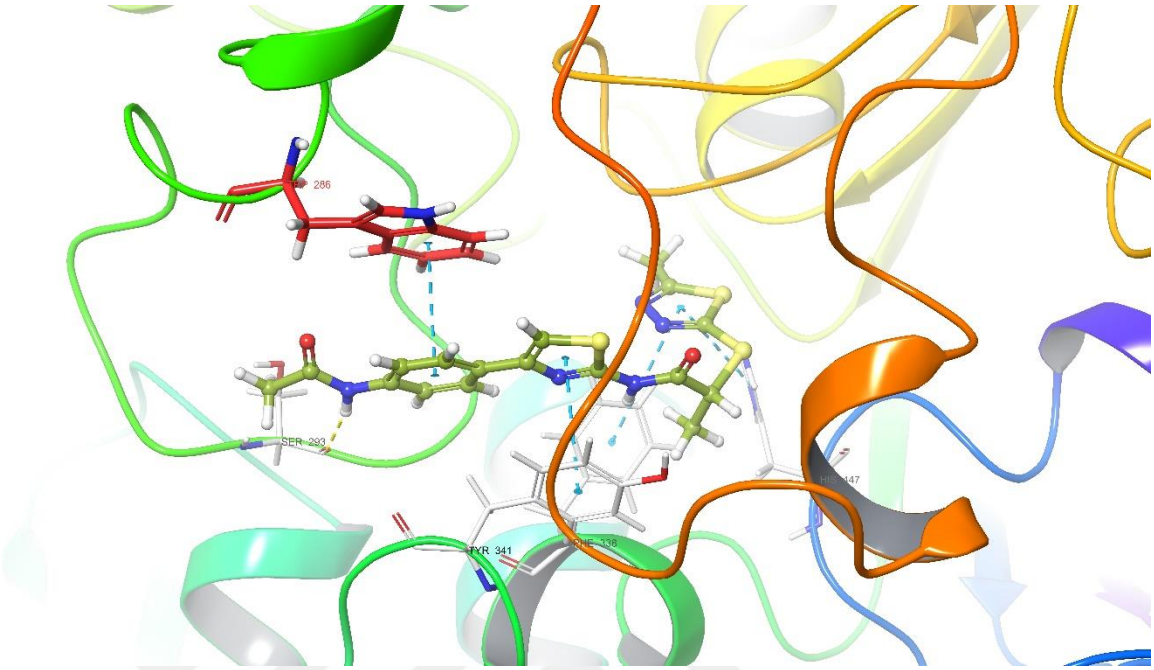

Figure 5.73. *3D interactions of compound **5d** at the (4EY7 / PBDID) binding region of AChE*

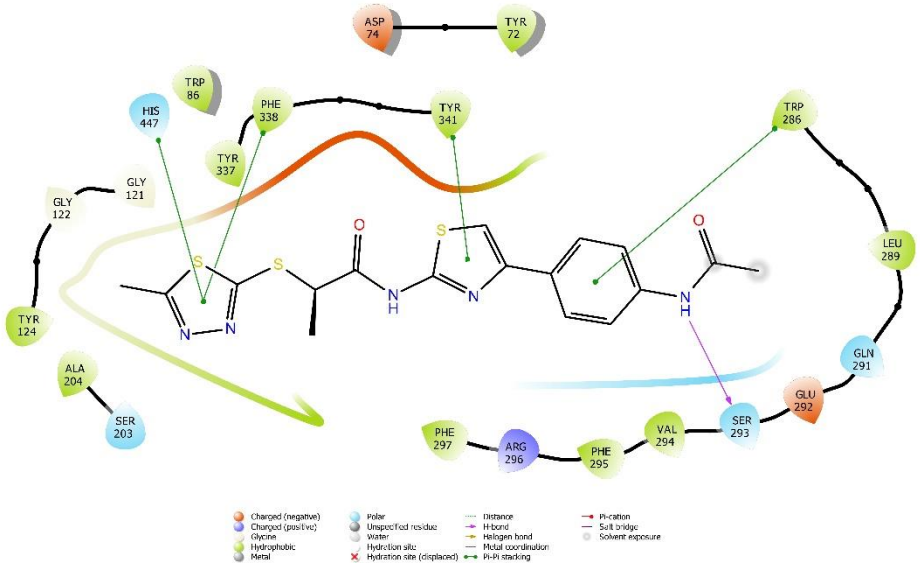

Figure 5.74. *2D interactions of compound **5d** at the (4EY7 / PBDID) binding region of AChE*

5.7.1.2 The molecular docking of compound 5e

The following Figure 5.75 and Figure 5.76 (3D and 2D) illustrate the correlation between AChE and compound **5e** in seven bonds. Three of them between the benzothiazole ring and Trp86 bind by π-π stacking bonds in the CAS region. There are also three bonds Linked by π-π stacking bonds tow between the thiazole ring with Trp124 and Tyr341, and one bond between the benzene ring and the Trp286 in the PAS region. In addition, in the PAS region there is only one hydrogen bond between the NH-benzene and Ser293.

..

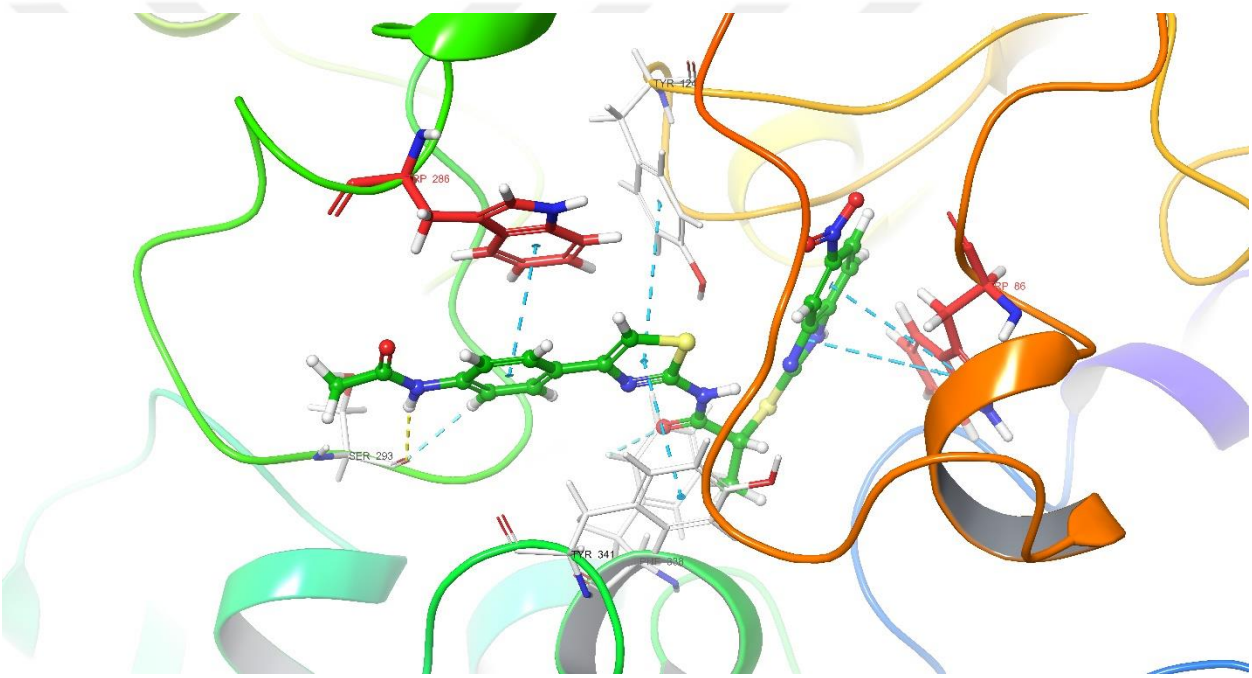

Figure 5.75.*3D interactions of compound* ***5e*** *at the (4EY7 / PBDID) binding region of AChE*

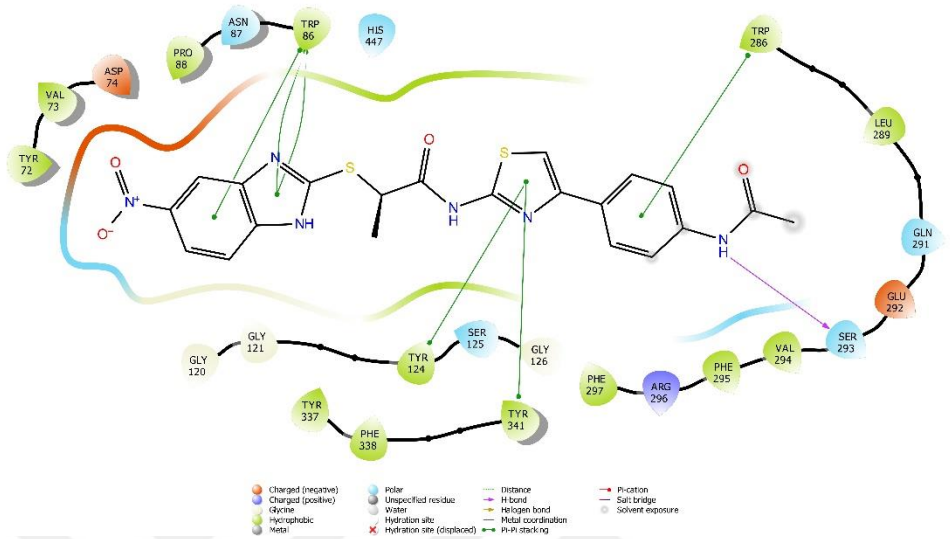

Figure 5.76.*2D interactions of compound* ***5e*** *at the (4EY7 / PBDID) binding region of AChE*

5.7.1.3 The molecular docking of compound 5j

The compound **5j** is the best synthesized compound that has given effectiveness as an anti-acetylcholine esterase. The compound is bonded by many bonds there is a halogenic bond between the chlorine on the oxathiazole ring and Asp74. And four of the bonds formed by the compound are between the oxathiazole ring and Trp86 by the π-π stacking bond in the CAS region. In the PAS region there are also π-π stacking bonds one between the thiazole ring and Tyr341 and two bonds between the benzene ring with Trp286 and Ser 293 as shown in 3D figure. The last bond formed by the compound is a hydrogen bond between the NH-Benzene and Ser293 in the PAS region. The following Figure 5.77 and Figure 5.78 illustrates the interconnection between the **5j** compound and the active site residues.

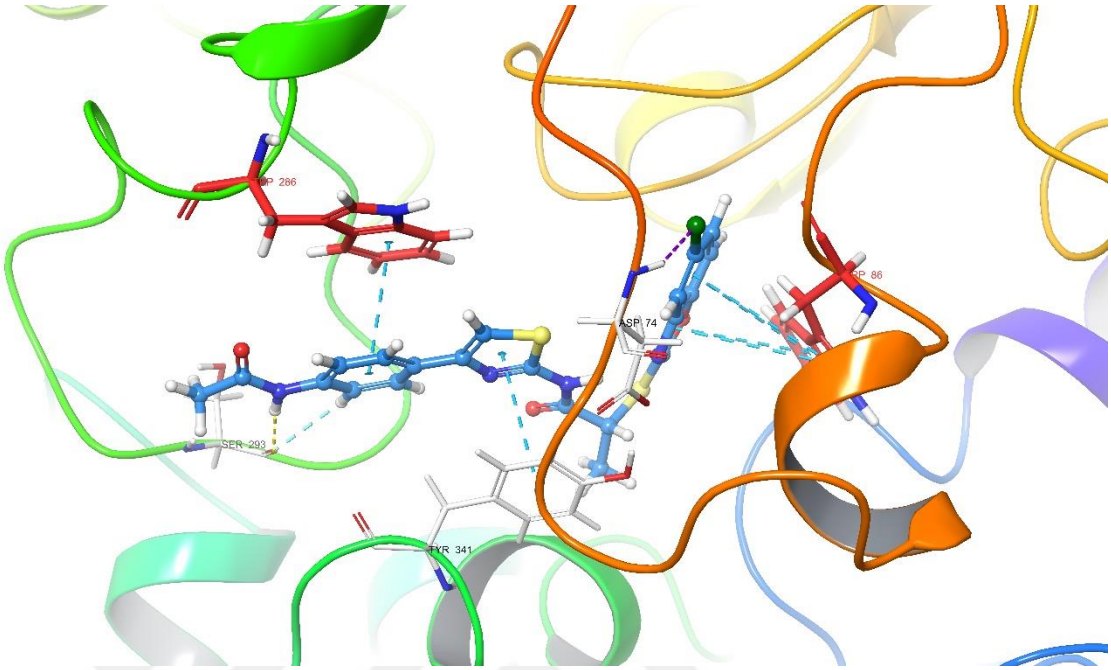

Figure 5.77.*3D interactions of compound **5j** at the (4EY7 / PBDID) binding region of AChE*

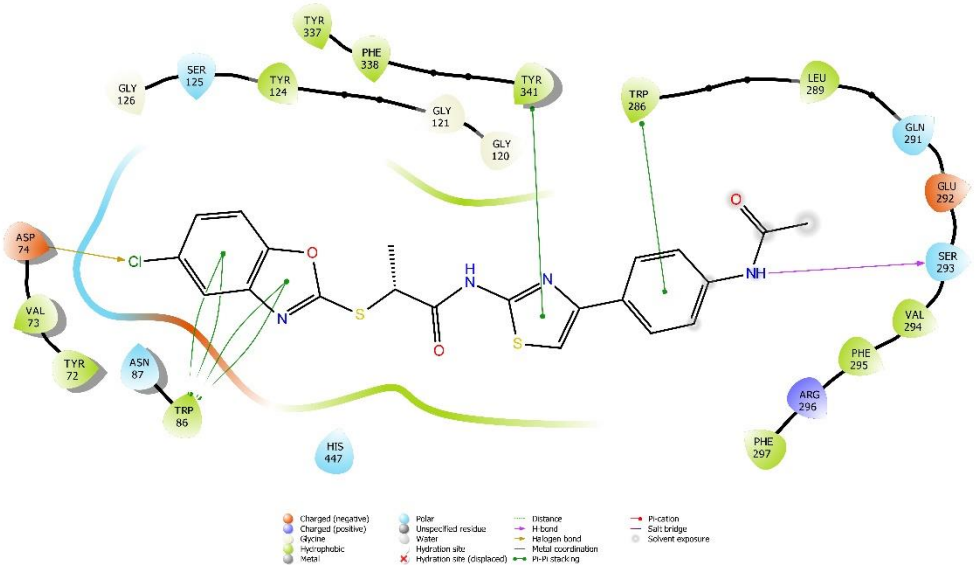

Figure 5.78..*2D interactions of compound **5j** at the (4EY7 / PBDID) binding region of AChE*

5.7.2. Molecular dynamic simulation studies

MDS provide a valuable computational tool for studying the behavior of molecules over time. MDS can provide atomistic-level details on molecular interactions, and they can also offer information on the kinetics and thermodynamics of molecular interactions [138, 139]. Results from MDS can guide drug design and optimization, and help understand the structural and dynamical properties of proteins and other biomolecules [140–142].

MDS were used to assess the binding interactions and time-dependent stability of a ligand-target complex. To conduct the simulations as performed in our previous studies [109, 143–146], the Desmond program was utilized, which employed the standard OPLS3e force field of the Schrödinger Suite with a TIP3P water model, followed by energy minimization of the complex [147, 148]. The system was neutralized using Na+ and Cl- ions. After setting up the system, MDS was performed, and values for radius of gyration (Rg), root mean square deviation (RMSD), and root means square fluctuation (RMSF) were calculated using the Desmond program [149].

5.7.2.1 The MDS of compound 5j

The RMSD plot provides information on the stability and dynamics of the system being simulated. In general, a lower RMSD value indicates that the system is more stable and closer to the starting structure, while a higher RMSD value indicates more structural deviation from the starting structure [150–152]. The plot of RMSD value is 1.8 Å for protein and 1.2 Å, (as shown in Figure 5.79-B), throughout the simulation, the protein-ligand system was found to be stable, as evidenced by the RMSD value of the protein falling within the range of 1-3Å. Also, in radius of gyration (Rg), is a measure of the compactness of a protein-ligand complex. In MDS studies, Rg can be used to evaluate the quality of the predicted complex structure [153]. A lower fluctuation of Rg peaks as shown in (Figure 5.79-A) indicates a more accurate prediction of the binding mode and a more stable complex.

The RMSF values measure the deviation of atomic positions in an MD simulation, providing insights into a molecule's flexibility and dynamics. High RMSF values indicate mobility and potential for interactions, while low RMSF values indicate rigidity. RMSF values can be plotted against residue number to identify flexible and rigid regions, aiding in

the understanding of molecular behavior and interactions. the RMSF value was found to be low for α-helices (red areas) and β-strands (blue areas) in the protein complex, indicating that these regions were relatively rigid and did not experience higher than 1 Å during the simulation same as interacted loop regions. As shown in (Figure 5.79-C) the interaction between the ligand and enzyme observed less than 1 Å at the loop region and This observation provides evidence for a strong interaction between the ligand and protein.

The number of interactions by residue during a simulation is a measure of the frequency and strength of interactions between individual amino acid residues and other molecules. It can provide insights into protein stability and identify key residues involved in specific interactions[137, 154]. Many amino acids have been shown to bind to the **5j** compound as Trp86, Tyr124, His287, Glu292, Phe338 in various concentrations while TYR341 shows highest concentration by 4≤ and continuous line and Trp 286 also shows continuous line with high concentration around 3. which that indicating the stability of ligand inside the protein, as shown in **(**Figure 5.80-D)

As shown in (Figure 5.80-E) different types of interactions contributing to protein stability are color-coded, such as interactions by water-mediated hydrogen bonds were observed in blue between **5j** and Tyr72, Asp72, Thr83,Arg289, Phe295, Gln291, Asn283, Pro290, and regular hydrogen bonds interactions in green with blue water-mediated hydrogen bonds at the same time between the **5j** and Ser125, Ser239, His 287, and Leu289, In addition to an ionic bond association with them and illustrated in pink by the peak of Glu292 amino acid., It also illustrates the hydrophobic interactions with Trp86, Pro88, Trp286, Tyr337, Tyr341 and Phe338 observed purple. The plot helps identify stable and flexible regions of the protein and can be used to design new drugs or better understand protein function.

MDS was studied on the most effective synthetic compound against acetylcholine esterase which is the compound **5j**, as shown in (Figure 5.80-F) The compound was associated with many bonds, including H-bonds, water-mediated H-bonds, π-π Stackings and aromatic H- bonds. The interactions with Trp286, Tyr341 (π-π stackings), Tyr124, His 287 (H-bond), Glu 292 (water-mediated H-bond) were preserved as in 2D (Figure 5.80-F).

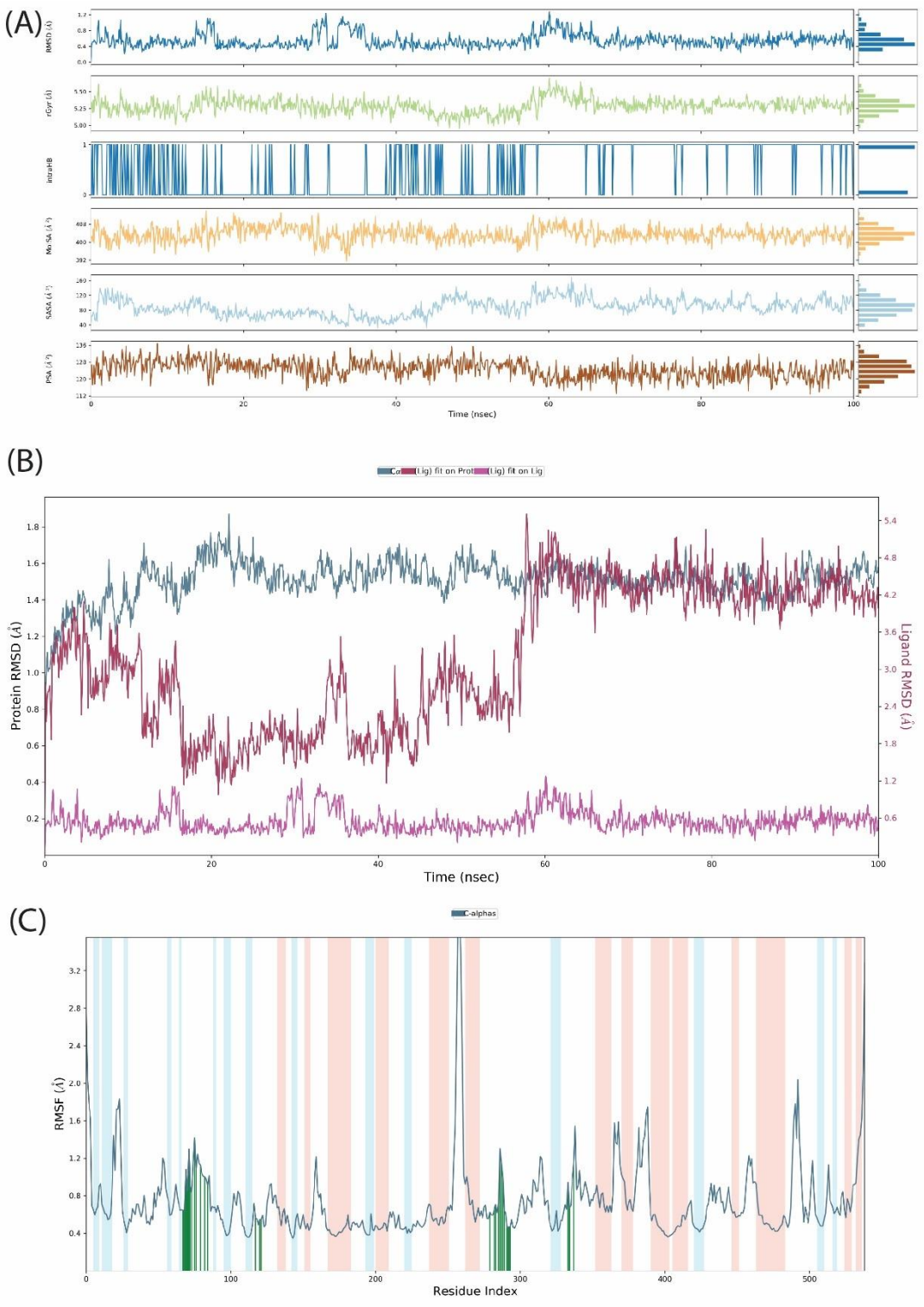

Figure 5.79. *Molecular dynamic simulation (MDS) Results of* ***5j*** *ligand with AChE.* ***(A)*** *Rg, Plot.* ***(B)*** *Plot of root mean square deviation (RMSD) (Å)-time (ns).* ***(C)*** *Plot of root mean square fluctuation (RMSF)-residue index. The areas were represented in light red for the helices, light blue for the strands, and white for the loops*

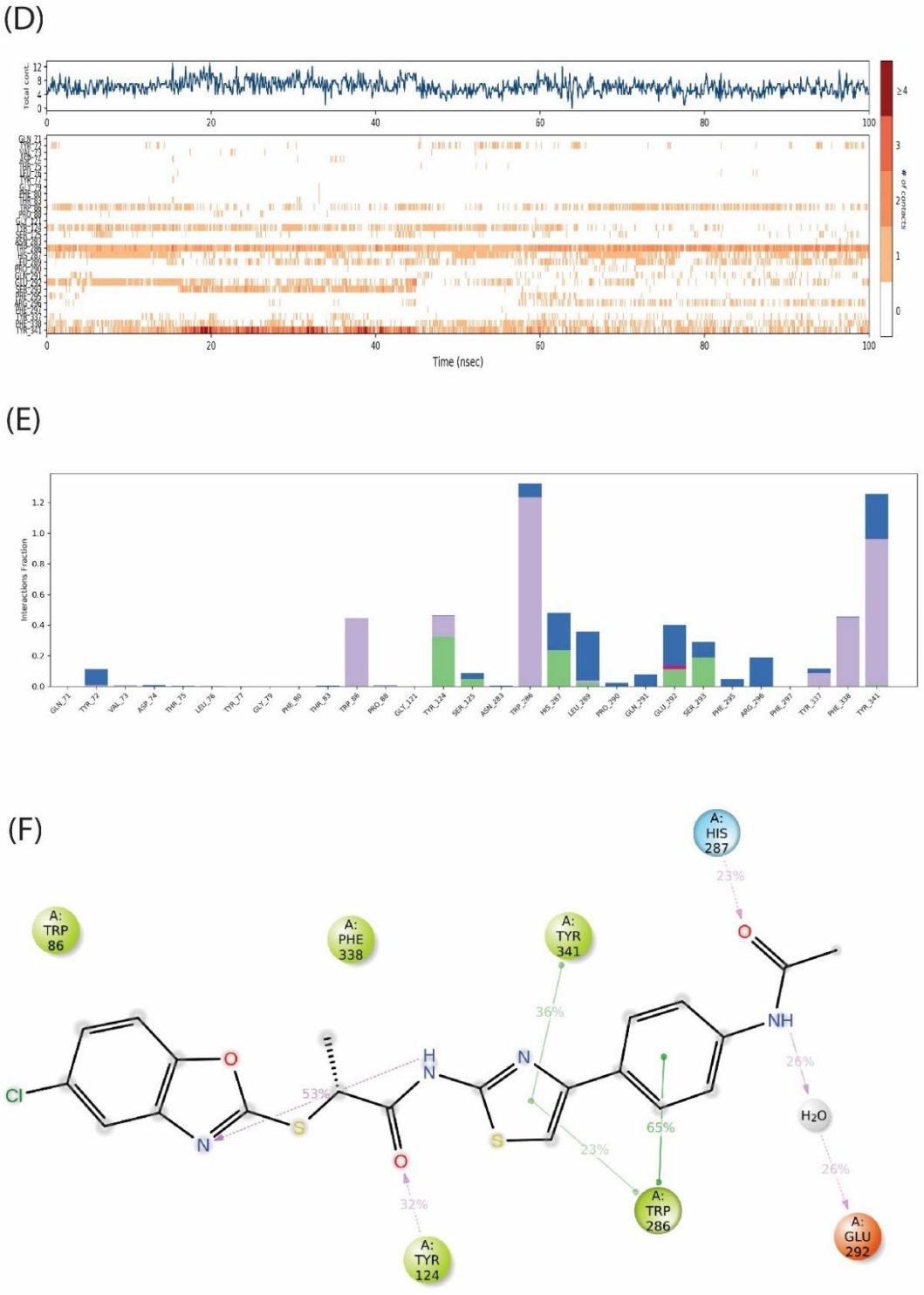

Figure 5.80. *MDS Results of **5j** ligand with AChE **(D)** Number of interactions by residue during the simulation., **(E)** Plot of root mean square fluctuation-residue index (blue: water-mediated H-bond; green: H-bond, pink: ionic interaction, purple: hydrophobic interaction) **(F)** 2D diagram of the interaction strengths (cutoff=20%)*

5.8. Structure-Activity Relationship Evaluation

According to the results of the compounds in the effectiveness and docking on AChE, the SAR of the compounds was observed as follows:

The thiazole ring and benzene ring share many hydrophobic bonds that are formed by π-π stacking overlapping bonds. It contributes to the stability of ligand within the protein, and the thiazole ring has a key role in inhibiting the AChE enzyme.

Also, the two amide groups in the compound showed great importance in the stability of the compound, as the oxygen atom made hydrophilic bonds with amino acids, also the stability of the compound led to good results in terms of effectiveness.

In the R groups we have placed several rings such as benzoxazole, triazole, tetrazole, benzimidazole, thiadiazole, benzothiazole and pyrimidine.

The study found that benzoxazole rings were more effective than benzothiazole and thiadiazole rings, all of them formed π-π stacking bonds with amino acids. As the majority of bonds with benzoxazole that contain four bonds and this indicates its importance in stability and three bonds with benzothiazole and two with thiadiazole . The chlorine atom at the 5th position of the benzoxazole ring was found to be crucial for its effectiveness. Removing this chlorine atom in compound **5i** reduced its effectiveness. Replacing the chlorine atom with a methyl group in compound **5l** resulted in a significant reduction in effectiveness which mean Cl atom meak an important for activity. While the benzoxazole ring was found to be important for effectiveness, replacing it with certain other rings could also result in effectiveness. For example, compounds **5d** and **5e**, which replaced the benzoxazole ring with (2-methyl-1,3,4-thiadiazole) and (5-nitro-1*H*-benzimidazole), respectively. However, replacing the benzoxazole ring with other rings such as tetrazole, benzothiazole, triazole, and pyrimidine led to a decrease in effectiveness.

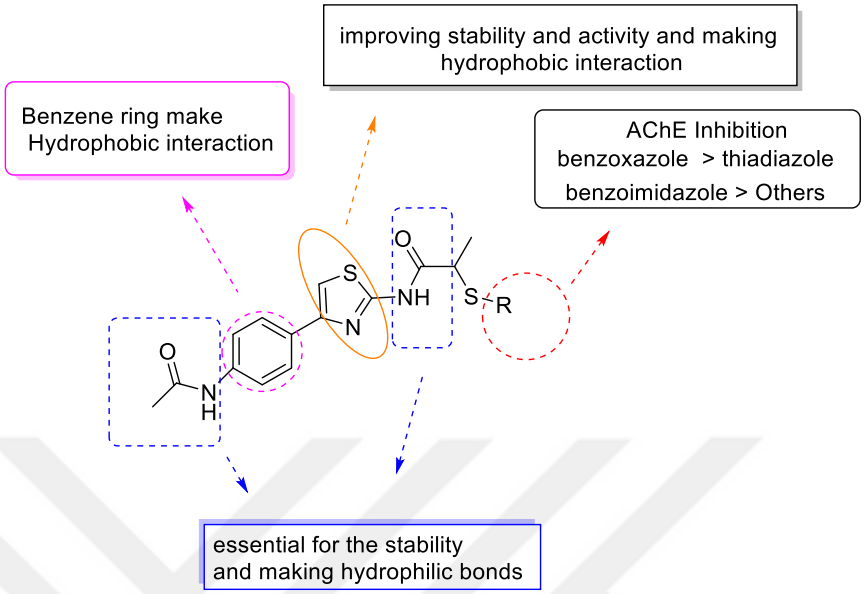

Figure 5.81. *The structure-activity relationship*

6. CONCLUDING REMARKS AND FUTURE RECOMMENDATIONS

The thiazole ring, a potential scaffold for developing drugs to treat neurodegenerative disorders like Alzheimer's and Parkinson's diseases, has been thoroughly investigated. In this study, a thiazole compound containing *N*-[4-(2-bromoacetyl)phenyl]acetamide was synthesized by reacting with thiourea under basic conditions. The compound was then acetylated, and mercaptan groups were added, resulting in a total of 12 compounds (**5a-5l**).

These synthesized compounds demonstrated increased effectiveness as AChE inhibitors. Specifically, compounds **5d**, **5e**, and **5j** showed high inhibition efficiency against AChE with IC_{50} values of 0.223 μM, 0.092 μM, and 0.054 μM, respectively. However, all compounds exhibited low efficacy against BChE below 50% at concentrations of 10^{-3} and 10^{-4}, with significant IC_{50} values. Additionally, the MAO inhibitory activity of all compounds displayed weak inhibition percentages against both MAO-A and MAO-B, ranging from 20.415 to 38.461 % at a concentration of 10^{-4}.

The three most effective compounds were subjected to docking analysis, which revealed strong associations with amino acids through hydrophilic, hydrophobic, hydrogen, and π-π stacking bonds. A detailed MDS study of compound **5j** found a halogen bond between the chlorine on the oxathiazole ring and Asp74, as well as four π-π stacking bonds between the oxathiazole ring and Trp86 in the CAS region. In the PAS region, π-π stacking bonds included one between the thiazole ring and Tyr341, and two between the benzene ring and Trp286 and Ser293.

For future research, it is suggested to introduce atoms such as halogens and nitro groups to the Mercaptan rings. The presence of a chlorine atom and a nitro group in the fifth position of the benzoxazole and benzodiazole rings in compounds **5j** and **5e** showed increased activity compared to compounds **5i** and **5f**, which lack these groups. This indicates that adding atoms and groups to these rings enhances activity and ligand-protein binding, as assessed in the *in vitro* activity and docking study.

REFERENCES

[1] Leoni, A., Frosini, M., Locatelli, A., Micucci, M., Carotenuto, C., Durante, M., Cosconati, S., Budriesi, R. (2019). 4-Imidazo[2,1-b]thiazole-1,4-DHPs and neuroprotection: preliminary study in hits searching. *Eur. J. Med. Chem.*, 16989–102.

[2] Meng, C., Zhang, J.C., Shi, R.L., Zhang, S.H., Yuan, S.Y. (2015). Inhibition of interleukin-6 abolishes the promoting effects of pair housing on post-stroke neurogenesis. *Neuroscience*, 307160–170.

[3] Mc.Conathy, J., Owens, M.J. (2003). Stereochemistry in Drug Action. *Prim. Care Companion J. Clin. Psychiatry*, 05 (02), 70–73.

[4] McKeith, I.G., Boeve, B.F., Dickson, D.W., Halliday, G., Taylor, J.-P., Weintraub, D., Aarsland, D., Galvin, J., Attems, J., Ballard, C.G. (2017). Diagnosis and management of dementia with Lewy bodies: Fourth consensus report of the DLB Consortium. *Neurology*, 89 (1), 88–100.

[5] Kalia, L. V, Lang, A.E. (2015). Parkinson's disease. *Lancet*, 386 (9996), 896–912.

[6] Hardy, J., Selkoe, D.J. (2002). The amyloid hypothesis of Alzheimer's disease: progress and problems on the road to therapeutics. *Science (80-.).*, 297 (5580), 353–356.

[7] Iqbal, K., Liu, F., Gong, C.-X. (2016). Tau and neurodegenerative disease: the story so far. *Nat. Rev. Neurol.*, 12 (1), 15–27.

[8] Prince, M.J., Wimo, A., Guerchet, M.M., Ali, G.C., Wu, Y.-T., Prina, M. (2015). World Alzheimer Report 2015-The Global Impact of Dementia: An analysis of prevalence, incidence, cost and trends.

[9] Hirsch, E.C., Hunot, S. (2009). Neuroinflammation in Parkinson's disease: a target for neuroprotection? *Lancet Neurol.*, 8 (4), 382–397.

[10] Heneka, M.T., Carson, M.J., El Khoury, J., Landreth, G.E., Brosseron, F., Feinstein, D.L., Jacobs, A.H., Wyss-Coray, T., Vitorica, J., Ransohoff, R.M. (2015). Neuroinflammation in Alzheimer's disease. *Lancet Neurol.*, 14 (4), 388–405.

[11] Spires-Jones, T.L., Hyman, B.T. (2014). The intersection of amyloid beta and tau at synapses in Alzheimer's disease. *Neuron*, 82 (4), 756–771.

[12] Cummings, J.L. (2004). Alzheimer's disease. *N. Engl. J. Med.*, 351 (1), 56–67.

[13] Perrin, R.J., Fagan, A.M., Holtzman, D.M. (2009). Multimodal techniques for diagnosis and prognosis of Alzheimer's disease. *Nature*, 461 (7266), 916–922.

[14] Emmerzaal, T.L., Kiliaan, A.J., Gustafson, D.R. (2015). 2003-2013: A decade of body mass index, Alzheimer's disease, and dementia. *J. Alzheimer's Dis.*, 43 (3), 739–755.

[15] IMWtiaz, B., Tolppanen, A.-M., Kivipelto, M., Soininen, H. (2014). Future directions in Alzheimer's disease from risk factors to prevention. *Biochem. Pharmacol.*, 88 (4), 661–670.

[16] Cavalli, A., Bolognesi, M.L., Mìnarini, A., Rosini, M., Tumiatti, V., Recanatini, M., Melchiorre, C. (2008). Multi-target-directed ligands to combat neurodegenerative diseases. *J. Med. Chem.*, 51 (3), 347–372.

[17] Youdim, M.B.H., Edmondson, D., Tipton, K.F. (2006). The therapeutic potential of monoamine oxidase inhibitors. *Nat. Rev. Neurosci.*, 7 (4), 295–309.

[18] Westlund, K.N., Denney, R.M., Kochersperger, L.M., Rose, R.M., Abell, C.W. (1985). Distinct monoamine oxidase A and B populations in primate brain. *Science (80-.).*, 230 (4722), 181–183.

[19] Chaurasiya, N.D., Ganesan, S., Nanayakkara, N.P.D., Dias, L.R.S., Walker, L.A., Tekwani, B.L. (2012). Inhibition of human monoamine oxidase A and B by 5-phenoxy 8-aminoquinoline analogs. *Bioorganic Med. Chem. Lett.*, 22 (4), 1701–1704.

[20] Bach, A.W., Lan, N.C., Johnson, D.L., Abell, C.W., Bembenek, M.E., Kwan, S.W., Seeburg, P.H., Shih, J.C. (1988). cDNA cloning of human liver monoamine oxidase A and B: molecular basis of differences in enzymatic properties. *Proc. Natl. Acad. Sci. U. S. A.*, 85 (13), 4934–4938.

[21] Greenawalt, J.W., Schnaitman, C. (1970). An appraisal of the use of monoamine oxidase as an enzyme marker for the outer membrane of rat liver mitochondria. *J. Cell Biol.*, 46 (1), 173–179.

[22] Grimsby, J., Chen, K., Wang, L.J., Lan, N.C., Shih, J.C. (1991). Human monoamine oxidase A and B genes exhibit identical exon-intron organization. *Proc. Natl. Acad. Sci. U. S. A.*, 88 (9), 3637–3641.

[23] Youdim, M.B.H., Fridkin, M., Zheng, H. (2004). Novel bifunctional drugs targeting monoamine oxidase inhibition and iron chelation as an approach to neuroprotection in Parkinson's disease and other neurodegenerative diseases. *J. Neural Transm.*, 111

(10–11), 1455–1471.

[24] Cesura, A.M., Pletscher, A. (1992). The new generation of monoamine oxidase inhibitors. *Prog. drug Res. Fortschritte der Arzneimittelforschung. Prog. des Rech. Pharm.*, 38171–297.

[25] Guay, D.R.P. (2006). Rasagiline (TVP-1012): a new selective monoamine oxidase inhibitor for Parkinson's disease. *Am. J. Geriatr. Pharmacother.*, 4 (4), 330–346.

[26] Riederer, P., Danielczyk, W., Grünblatt, E. (2004). Monoamine oxidase-B inhibition in Alzheimer's disease. *Neurotoxicology*, 25 (1–2), 271–277.

[27] Saura, J., Luque, J.M., Cesura, A.M., Da Prada, M., Chan-Palay, V., Huber, G., Löffler, J., Richards, J.G. (1994). Increased monoamine oxidase B activity in plaque-associated astrocytes of Alzheimer brains revealed by quantitative enzyme radioautography. *Neuroscience*, 62 (1), 15–30.

[28] Matthew V. Rudorfer, William Z.Potter. (1989). 'Newer' Versus 'Older' Antidepressants. *Drugs*, 37713–738.

[29] Lu, C., Guo, Y., Yan, J., Luo, Z., Luo, H.-B., Yan, M., Huang, L., Li, X. (2013). Design, synthesis, and evaluation of multitarget-directed resveratrol derivatives for the treatment of Alzheimer's disease. *J. Med. Chem.*, 56 (14), 5843–5859.

[30] Kalgutkar, A.S., Dalvie, D.K., Castagnoli, N.J., Taylor, T.J. (2001). Interactions of nitrogen-containing xenobiotics with monoamine oxidase (MAO) isozymes A and B: SAR studies on MAO substrates and inhibitors. *Chem. Res. Toxicol.*, 14 (9), 1139–1162.

[31] Dayan, F.E., Vincent, A.C., Romagni, J.G., Allen, S.N., Duke, S.O., Duke, M. V, Bowling, J.J., Zjawiony, J.K. (2000). Amino- and Urea-Substituted Thiazoles Inhibit Photosynthetic Electron Transfer. *J. Agric. Food Chem.*, 48 (8), 3689–3693.

[32] Huang, W., Yang, G.F. (2006). Microwave-assisted, one-pot syntheses and fungicidal activity of polyfluorinated 2-benzylthiobenzothiazoles. *Bioorganic Med. Chem.*, 14 (24), 8280–8285.

[33] Nour, H.F. (2008). Synthesis and pharmacological activities of some condensed. 5815–27.

[34] Andreani, A., Rambaldi, M., Leoni, A., Locatelli, A., Bossa, R., Chiericozzi, M., Galatulas, I., Salvatore, G. (1996). Synthesis and cardiotonic activity of imidazo[2,1-

b]thiazoles bearing a lactam ring. *Eur. J. Med. Chem.*, 31 (5), 383–387.

[35] Kumar, Y., Green, R., Borysko, K.Z., Wise, D.S., Wotring, L.L., Townsend, L.B. (1993). Synthesis of 2,4-Disubstituted Thiazoles and Selenazoles as Potential Antitumor and Antifilarial Agents: 1. Methyl 4-(Isothiocyanatomethyl)thiazole-2-carbamates, -selenazole-2-carbamates, and Related Derivatives. *J. Med. Chem.*, 36 (24), 3843–3848.

[36] Rahim, F., Ullah, H., Javid, M.T., Wadood, A., Taha, M., Ashraf, M., Shaukat, A., Junaid, M., Hussain, S., Rehman, W., Mehmood, R., Sajid, M., Khan, M.N., Khan, K.M. (2015). Synthesis, in vitro evaluation and molecular docking studies of thiazole derivatives as new inhibitors of α-glucosidase. *Bioorg. Chem.*, 6215–21.

[37] Khan, K.M., Irfan, M., Ashraf, M., Taha, M., Saad, S.M., Perveen, S., Choudhary, M.I. (2015). Synthesis of phenyl thiazole hydrazones and their activity against glycation of proteins. *Med. Chem. Res.*, 24 (7), 3077–3085.

[38] Turan-Zitouni, G., Ozdemir, A., Kaplancikli, Z.A., Altintop, M.D., Temel, H.E., Çiftçi, G.A. (2013). Synthesis and biological evaluation of some thiazole derivatives as new cholinesterase inhibitors. *J. Enzyme Inhib. Med. Chem.*, 28 (3), 509–514.

[39] Siddiqui, N., Arya, S.K., Ahsan, W., Azad, B. (2011). Diverse biological activities of Thiazoles: A Retrospect. *Int. J. Drug Dev. Res.*, 3 (4), 0.

[40] Karched, M., Bhardwaj, R.G., Tiss, A. (2019). Asikainen S. *Proteomic Anal. Virulence Assess. Granulicatella adiacens Secretome*, 9 (104), .

[41] Blau, L., Menegon, R.F., Trossini, G.H.G., Molino, J.V.D., Vital, D.G., Cicarelli, R.M.B., Passerini, G.D., Bosquesi, P.L., Chin, C.M. (2013). Design, synthesis and biological evaluation of new aryl thiosemicarbazone as antichagasic candidates. *Eur. J. Med. Chem.*, 67142–151.

[42] Hansen, A.M., Peng, P., Baldry, M., Perez-Gassol, I., Christensen, S.B., Vinther, J.M.O., Ingmer, H., Franzyk, H. (2018). Lactam hybrid analogues of solonamide B and autoinducing peptides as potent S. aureus AgrC antagonists. *Eur. J. Med. Chem.*, 152370–376.

[43] SÖNMEZ, F., AKGÜN, E., ŞAHİN, Z. Synthesis, DPPH and ABTS Activity of Novel Furfuryl-Chalcone Derivatives. *Sak. Univ. J. Sci.*, 26 (6), 1224–1232.

[44] Khan, E., Khan, S., Gul, Z., Muhammad, M. (2021). Medicinal importance,

coordination chemistry with selected metals (Cu, Ag, Au) and chemosensing of thiourea derivatives. A review. *Crit. Rev. Anal. Chem.*, 51 (8), 812–834.

[45] Salar, U., Khan, K.M., Syed, S., Taha, M., Ali, F., Ismail, N.H., Perveen, S., Wadood, A., Ghufran, M. (2017). Synthesis, in vitro β-glucuronidase inhibitory activity and in silico studies of novel (E)-4-Aryl-2-(2-(pyren-1-ylmethylene) hydrazinyl) thiazoles. *Bioorg. Chem.*, 70199–209.

[46] Bhosle, M.R., Joshi, S.A., Bondle, G.M. (2020). An efficient contemporary multicomponent synthesis for the facile access to coumarin-fused new thiazolyl chromeno [4, 3-b] quinolones in aqueous micellar medium. *J. Heterocycl. Chem.*, 57 (1), 456–468.

[47] Siddiqui, N., Arshad, M.F., Ahsan, W., Alam, M.S. (2009). Thiazoles: a valuable insight into the recent advances and biological activities. *Int. J. Pharm. Sci. Drug Res*, 1 (3), 136–143.

[48] Elzayat, E.M., Ibrahim, M.F., Abdel-Rahman, A.A., Ahmed, S.M., Alanazi, F.K., Habib, W.A. (2017). A validated stability-indicating UPLC method for determination of diclofenac sodium in its pure form and matrix formulations. *Arab. J. Chem.*, 10S3245–S3254.

[49] Mishra, C.B., Kumari, S., Tiwari, M. (2015). Thiazole: A promising heterocycle for the development of potent CNS active agents. *Eur. J. Med. Chem.*, 921–34.

[50] Atamanyuk, D., Zimenkovsky, B., Lesyk, R. (2008). Synthesis and anticancer activity of novel thiopyrano [2, 3-d] thiazole-based compounds containing norbornane moiety. *J. Sulfur Chem.*, 29 (2), 151–162.

[51] Chang, W.-T., Liu, P.-Y., Gao, Z.-H., Lee, S.-W., Lee, W.-K., Wu, S.-N. (2021). Evidence for the Effectiveness of Remdesivir (GS-5734), a Nucleoside-Analog Antiviral Drug in the Inhibition of of I. *Mol. Mech. Voltage-Gating Ion Channels*.

[52] Jayashree, A., Narayana, B., Uppine, G.B., Ghate, V.M., Lewis, S.A., Prakash, B., Kunhanna, S.B., Kumar, M.S. (2019). Zno nanocatalyst mediated convergent synthesis of highly substituted imidazole and imidazole-derived bi-heterocyclic scaffolds as potential antibacterial agents. *J. Heterocycl. Chem.*, 56 (9), 2398–2410.

[53] Nag, S., Krasikova, R., Airaksinen, A.J., Arakawa, R., Petukhovd, M., Gulyas, B. (2019). Synthesis and biological evaluation of [18F] fluorovinpocetine, a potential

PET radioligand for TSPO imaging. *Bioorg. Med. Chem. Lett.*, 29 (16), 2270–2274.

[54] Joule, J.A. (2020). *Heterocyclic chemistry*. CRC Press.

[55] Ullrich, J.W., Mewshaw, R.E. (2007). March's Advanced Organic Chemistry: Reactions, Mechanisms, and Structure. By Michael B. Smith and Jerry March. John Wiley & Sons, Inc., Hoboken, NJ. 2007. xx+ 2354 pp. 16× 24 cm. ISBN 978-0-471-72091-1. $99.95.

[56] Solomons, T.W.G., Fryhle, C.B. (2008). *Organic chemistry*. John Wiley & Sons.

[57] Katritzky, A.R., Ramsden, C.A., Joule, J.A., Zhdankin, V. V. (2010). *Handbook of heterocyclic chemistry*. Elsevier.

[58] Smith, M.B. (2020). *March's advanced organic chemistry: reactions, mechanisms, and structure*. John Wiley & Sons.

[59] Dal, K.M.Y.A.A. (2006). OF SOME BIOLOGICALLY ACTIVE.

[60] Hantzsch, A., Weber, H.J. (1887). Ber Dtsch Chem Ges 20: 3118 [2] Rao RP (1961) J Indian Chem Soc 38: 787 [3] Rao RP. *Singh SR J Indian Chem Soc*, 50 (492), 4.

[61] Arab, K., Rossary, A., Flourie, F., Tourneur, Y., Steghens, J.P., Bakewell, L., Burdge, G.C., Calder, P.C., Barbarich, B.N., D'Willows, N. (2005). Bibliography Current World Literature Vol 18 No. *Diabetologia*, 482365–2375.

[62] Metzger, J. V. (1979). The chemistry of heterocyclic compounds. Thiazole and its Derivatives: A Series of Monographs, Vol. 34.

[63] Eryılmaz, S., Türk Çelikoğlu, E., İdil, Ö., İnkaya, E., Kozak, Z., Mısır, E., Gül, M. (2020). Derivatives of pyridine and thiazole hybrid: Synthesis, DFT, biological evaluation via antimicrobial and DNA cleavage activity. *Bioorg. Chem.*, 95 (November 2019), . Epub ahead of print 2020. DOI: 10.1016/j.bioorg.2019.103476.

[64] Sammes, P.G. (1979). Comprehensive Organic Chemistry. *eds. D. Bart. W. D. Ollis, Pergamon Press. London*, 4398–975.

[65] Dhameliya, D.R., Patel, M.C. (2011). Synthesis, characterization and biological activity of novel pyrrole compounds. *Rasayan J. Chem.*, 4 (3), 580–584.

[66] Zoltewicz, J.A., Deady, L.W. (1978). Quaternization of Heteroaromatic Compounds: Quantitative Aspects. A.R. Katritzky and A.J. Boulton (editors), (p. 71–121). Academic Press.

[67] S. Gabriel. (1910). Synthesis of Oxazoles and Thiazoles II. *EurJIC*, 43 (2), 1283–

1287.

[68] Rajappa, B.S., Nair, M.D., Advani, B.G., Sreenivasan, R., Desai, J.A. 1762 J.C.S. Perkin. (1762), 6–8.

[69] Kabalka, G.W., Mereddy, A.R. (2006). Microwave promoted synthesis of functionalized 2-aminothiazoles. *Tetrahedron Lett.*, 47 (29), 5171–5172.

[70] Das, B., Saidi Reddy, V., Ramu, R. (2006). A rapid and high-yielding synthesis of thiazoles and aminothiazoles using ammonium-12-molybdophosphate. *J. Mol. Catal. A Chem.*, 252 (1–2), 235–237.

[71] Narender, M., Somi Reddy, M., Sridhar, R., Nageswar, Y. V.D., Rama Rao, K. (2005). Aqueous phase synthesis of thiazoles and aminothiazoles in the presence of β-cyclodextrin. *Tetrahedron Lett.*, 46 (35), 5953–5955.

[72] Karade, H., Sathe, M., Kaushik, M.P. (2007). An efficient method for the synthesis of 2-aminothiazoles using silica chloride as a heterogeneous catalyst. *Catal. Commun.*, 8 (4), 741–746.

[73] Garcia-Egido, E., Wong, S.Y.F., Warrington, B.H. (2002). A Hantzsch synthesis of 2-aminothiazoles performed in a heated microreactor system. *Lab Chip*, 2 (1), 31–33.

[74] Willstätter, R., Wirth, T. (1909). Über Thioformamid. *Berichte der Dtsch. Chem. Gesellschaft*, 42 (2), 1908–1922.

[75] Kuznetsov, A. (1939). Thiazoles synthesis and applications.*Azoles: Synthesis, Properties, Applications and Perspectives* (p. 63). London: British Labrary.

[76] Ibrahim, S.A., Rizk, H.F. (2020). Synthesis and biological evaluation of thiazole derivatives.*Azoles-Synthesis, Properties, Applications and Perspectives*. IntechOpen.

[77] Abdelhamid, A.O., Gomha, S.M. (2019). The Chemistry of Acetylpyrazoles and Its Utility in Heterocyclic Synthesis. *J. Heterocycl. Chem.*, 56 (3), 726–758.

[78] Pola, S. (2016). Significance of thiazole-based heterocycles for bioactive systems. *Scope Sel. Heterocycles from Org. Pharm. Perspect.*, 113–62.

[79] By, A. (1948). Studies in the Axole Series. Part X X I I I . 3001 632. Studies in the Axole. (V), 3001–3007.

[80] Tomassetti, M., Lupidi, G., Piermattei, P., Rossi, F. V., Lillini, S., Bianchini, G., Aramini, A., Ciufolini, M.A., Marcantoni, E. (2019). Catalyst-free synthesis of polysubstituted 5-acylamino-1,3-thiazoles via Hantzsch cyclization of α-

chloroglycinates. *Molecules*, 24 (21), . Epub ahead of print 2019. DOI: 10.3390/molecules24213846.

[81] Pz, M., Cook, B.A.H., Ian, S.I.R., Mahadevan, A.P. (1947). Cook, Heilbron, Macdonald, and Mahadeva.Pz : 226. Studies in the Axole Xeries. Part X I I . (1064), 1064–1068.

[82] Material, I., Pressure, A.G.O.F., On, D., Of, C., Through, L., Vertical, T. (1972). O = ~ (1 - - E V) Y | /. 17 (2), 952–956.

[83] Hoggartit, B.E. Hoggnrth : The Rearrangemeflt of 29. The Rearrangement. (114), 114–118.

[84] Vernin, G. (1979). General synthetic methods for thiazole and thiazolium salts. *Chem. Heterocycl. Compd. Thiazole Its Deriv. Part One*, 34165–335.

[85] Kamila, S., Mendoza, K., Biehl, E.R. (2012). Microwave-assisted Hantzsch thiazole synthesis of N-phenyl-4-(6- phenylimidazo[2,1-b]thiazol-5-yl)thiazol-2-amines from the reaction of 2-chloro-1-(6-phenylimidazo[2,1-b]thiazol-5-yl)ethanones and thioureas. *Tetrahedron Lett.*, 53 (37), 4921–4924.

[86] Nayak, S., Gaonkar, S.L. (2018). A Review on Recent Synthetic Strategies and Pharmacological Importance of 1,3-Thiazole Derivatives. *Mini-Reviews Med. Chem.*, 19 (3), 215–238.

[87] Cáceres-Castillo, D., Carballo, R.M., Tzec-Interián, J.A., Mena-Rejón, G.J. (2012). Solvent-free synthesis of 2-amino-4-arylthiazoles under microwave irradiation. *Tetrahedron Lett.*, 53 (30), 3934–3936.

[88] Madhav, B., Narayana Murthy, S., Anil Kumar, B.S.P., Ramesh, K., Nageswar, Y. V.D. (2012). A tandem one-pot aqueous phase synthesis of thiazoles/selenazoles. *Tetrahedron Lett.*, 53 (30), 3835–3838.

[89] Bouherrou, H., Saidoun, A., Abderrahmani, A., Abdellaziz, L., Rachedi, Y., Dumas, F., Demenceau, A. (2017). Synthesis and biological evaluation of new substituted Hantzsch thiazole derivatives from environmentally benign one-pot synthesis using silica supported tungstosilisic acid as reusable catalyst. *Molecules*, 22 (5), . Epub ahead of print 2017. DOI: 10.3390/molecules22050757.

[90] Larraufie, M.-H. (2014). Supporting Information. 79–136.

[91] Dodson, R.M., King, L.C. (1946). The reaction of acetophenone with thiourea and

oxidizing agents. *J. Am. Chem. Soc.*, 68 (5), 871.

[92] Mazzone, G., Pignatello, R., Panico, A., Mazzone, S., Puglisi, G., Pennisi, G., Raciti, G., Mazzone, P., Matera, M. (1992). MAOI activity of some novel series of substituted thiazol-2-yl-hydrazines. *Pharmazie*, 47 (12), 902–910.

[93] Raciti, G., Mazzone, P., Raudino, A., Mazzone, G., Cambria, A. (1995). Inhibition of rat liver mitochondrial monoamine oxidase by hydrazine-thiazole derivatives: structure-activity relationships. *Bioorganic Med. Chem.*, 3 (11), 1485–1491.

[94] Andreani, A., Granaiola, M., Guardigli, M., Leoni, A., Locatelli, A., Morigi, R., Rambaldi, M., Roda, A. (2005). Synthesis and chemiluminescent high throughput screening for inhibition of acetylcholinesterase activity by imidazo[2,1-b]thiazole derivatives. *Eur. J. Med. Chem.*, 40 (12), 1331–1334.

[95] Chimenti, F., Fioravanti, R., Bolasco, A., Manna, F., Chimenti, P., Secci, D., Rossi, F., Turini, P., Ortuso, F., Alcaro, S., Cardia, M.C. (2008). Synthesis, molecular modeling studies and selective inhibitory activity against MAO of N1-propanoyl-3,5-diphenyl-4,5-dihydro-(1H)-pyrazole derivatives. *Eur. J. Med. Chem.*, 43 (10), 2262–2267.

[96] Carradori, S., D'Ascenzio, M., De Monte, C., Secci, D., Yáñez, M. (2013). Synthesis and selective human monoamine oxidase b inhibition of heterocyclic hybrids based on hydrazine and thiazole scaffolds. *Arch. Pharm. (Weinheim).*, 346 (1), 17–22.

[97] Khan, F. Synthesis , Molecular Docking , Acetylcholinesterase and Butyrylcholinesterase Inhibitory Potential of Thiazole An ... *Bioorg. Chem.* DOI: 10.1016/j.bioorg.2015.08.002.

[98] Sun, Z.Q., Tu, L.X., Zhuo, F.J., Liu, S.X. (2016). Design and discovery of Novel Thiazole acetamide derivatives as anticholinesterase agent for possible role in the management of Alzheimer's. *Bioorganic Med. Chem. Lett.*, 26 (3), 747–750.

[99] Abbas, N., Zaib, S., Bakht, S.M., Ibrar, A., Khan, I., Batool, S., Saeed, A., Iqbal, J. (2017). Symmetrical aryl linked bis-iminothiazolidinones as new chemical entities for the inhibition of monoamine oxidases: Synthesis, in vitro biological evaluation and molecular modelling analysis. *Bioorg. Chem.*, 7017–26.

[100] Atli, Ö., Özkay, Y. (2017). Synthesis and MAO inhibitory activity of novel thiazole-hydrazones. *Turkish J. Chem.*, 41 (5), 685–699.

[101] Tripathi, R.K.P., M. Sasi, V., Gupta, S.K., Krishnamurthy, S., Ayyannan, S.R. (2018). Design, synthesis, and pharmacological evaluation of 2-amino-5-nitrothiazole derived semicarbazones as dual inhibitors of monoamine oxidase and cholinesterase: effect of the size of aryl binding site. *J. Enzyme Inhib. Med. Chem.*, 33 (1), 37–57.

[102] Secci, D., Carradori, S., Petzer, A., Guglielmi, P., D'Ascenzio, M., Chimenti, P., Bagetta, D., Alcaro, S., Zengin, G., Petzer, J.P., Ortuso, F. (2019). 4-(3-Nitrophenyl)thiazol-2-ylhydrazone derivatives as antioxidants and selective hMAO-B inhibitors: synthesis, biological activity and computational analysis. *J. Enzyme Inhib. Med. Chem.*, 34 (1), 597–612.

[103] Osmaniye, D., Çevik, U.A., Levent, S. Relationships of Thiazole Analogs as Anticholinesterase Agents for Alzheimer ' s Disease. *MDPI J. List*. DOI: 10.3390/molecules25184312.

[104] Ghotbi, G., Mahdavi, M., Najafi, Z., Moghadam, F.H., Hamzeh-Mivehroud, M., Davaran, S., Dastmalchi, S. (2020). Design, synthesis, biological evaluation, and docking study of novel dual-acting thiazole-pyridiniums inhibiting acetylcholinesterase and β-amyloid aggregation for Alzheimer's disease. *Bioorg. Chem.*, 103 (February), 104186.

[105] Hemaida, A.Y., Hassan, G.S., Maarouf, A.R., Joubert, J., El-Emam, A.A. (2021). Synthesis and Biological Evaluation of Thiazole-Based Derivatives as Potential Acetylcholinesterase Inhibitors. *ACS Omega*, 6 (29), 19202–19211.

[106] Hussain, R., Ullah, H., Rahim, F., Sarfraz, M., Taha, M., Iqbal, R., Rehman, W., Khan, S., Shah, S.A.A., Hyder, S., Alhomrani, M., Alamri, A.S., Abdulaziz, O., Abdelaziz, M.A. (2022). Multipotent Cholinesterase Inhibitors for the Treatment of Alzheimer's Disease: Synthesis, Biological Analysis and Molecular Docking Study of Benzimidazole-Based Thiazole Derivatives. *Molecules*, 27 (18), . Epub ahead of print 2022. DOI: 10.3390/molecules27186087.

[107] Xi, M., Feng, C., Du, K., Lv, W., Du, C., Shen, R., Sun, H. (2022). Design, synthesis, biological evaluation and molecular modeling of N-isobutyl-N-((2-(p-tolyloxymethyl)thiazol-4yl)methyl)benzo[d][1,3] dioxole-5-carboxamides as selective butyrylcholinesterase inhibitors. *Bioorganic Med. Chem. Lett.*, 61 (January), 25–27.

[108] Sağlık, B.N., Kaya Çavuşoğlu, B., Osmaniye, D., Levent, S., Acar Çevik, U., Ilgın, S., Özkay, Y., Kaplancıklı, Z.A., Öztürk, Y. (2019). In vitro and in silico evaluation of new thiazole compounds as monoamine oxidase inhibitors. *Bioorg. Chem.*, 85 (October 2018), 97–108.

[109] Osmaniye, D., Evren, A.E., Sağlık, B.N., Levent, S., Özkay, Y., Kaplancıklı, Z.A. (2022). Design, synthesis, biological activity, molecular docking, and molecular dynamics of novel benzimidazole derivatives as potential AChE/MAO-B dual inhibitors. *Arch. Pharm. (Weinheim).*, 355 (3), 2100450.

[110] Evren, A.E., Nuha, D., Dawbaa, S., Sağlık, B.N., Yurttaş, L. (2022). Synthesis of novel thiazolyl hydrazone derivatives as potent dual monoamine oxidase-aromatase inhibitors. *Eur. J. Med. Chem.*, 229114097.

[111] DeLano, W.L. (2002). Pymol: An open-source molecular graphics tool. *CCP4 Newsl. Protein Crystallogr*, 40 (1), 82–92.

[112] Avdeef, A. (2001). Physicochemical profiling (solubility, permeability and charge state). *Curr. Top. Med. Chem.*, 1 (4), 277–351.

[113] Lipinski, C. op, & methods, t.(2000). *Drug-like Prop. causes poor solubility poor permeability*, 44 (1), 235–249.

[114] Hou, T., Wang, J., Zhang, W., Xu, X. (2007). ADME evaluation in drug discovery. 7. Prediction of oral absorption by correlation and classification. *J. Chem. Inf. Model.*, 47 (1), 208–218.

[115] (PDB). The Protein Data Bank. https://www.rcsb.org/.

[116] Morris, G.M., Huey, R., Lindstrom, W., Sanner, M.F., Belew, R.K., Goodsell, D.S., Olson, A.J. (2009). AutoDock4 and AutoDockTools4: Automated docking with selective receptor flexibility. *J. Comput. Chem.*, 30 (16), 2785–2791.

[117] Friesner, R.A., Banks, J.L., Murphy, R.B., Halgren, T.A., Klicic, J.J., Mainz, D.T., Repasky, M.P., Knoll, E.H., Shelley, M., Perry, J.K. (2004). Glide: a new approach for rapid, accurate docking and scoring. 1. Method and assessment of docking accuracy. *J. Med. Chem.*, 47 (7), 1739–1749.

[118] Sureshkumar, B., Mary, Y.S., Resmi, K.S., Suma, S., Armaković, S., Armaković, S.J., Van Alsenoy, C., Narayana, B., Sobhana, D. (2018). Spectroscopic characterization of hydroxyquinoline derivatives with bromine and iodine atoms and theoretical

investigation by DFT calculations, MD simulations and molecular docking studies. *J. Mol. Struct.*, 116795–106.

[119] Impact, S. LLC, New York, NY, 2016; Prime, Schrödinger, LLC, New York, NY, 2020. *Google Sch. There is no Corresp. Rec. this Ref.*

[120] Liu, X., Shi, D., Zhou, S., Liu, H., Liu, H., Yao, X. (2018). Molecular dynamics simulations and novel drug discovery. *Expert Opin. Drug Discov.*, 13 (1), 23–37.

[121] Yurttaş, L., Özkay, Y., Akalın-Çiftçi, G., Ulusoylar-Yıldırım, Ş. (2014). Synthesis and anticancer activity evaluation of N-[4-(2-methylthiazol-4-yl)phenyl]acetamide derivatives containing (benz)azole moiety. *J. Enzyme Inhib. Med. Chem.*, 29 (2), 175–184.

[122] Dickey, J.B., Towne, E.B., Bloom, M.S., Moore, W.H., Hill, H.M., Heynemann, H., Hedberg, D.G., Sievers, D.G., Otis, M. V. (1959). Azo Dyes from Substituted 2-Aminothiazoles. *J. Org. Chem.*, 24 (2), 187–196.

[123] Kadi, A.A., Al-Abdullah, E.S., Shehata, I.A., Habib, E.E., Ibrahim, T.M., El-Emam, A.A. (2010). Synthesis, antimicrobial and anti-inflammatory activities of novel 5-(1-adamantyl)-1, 3, 4-thiadiazole derivatives. *Eur. J. Med. Chem.*, 45 (11), 5006–5011.

[124] El-Emam, A.A., Lehmann, J. (1994). Adamantane derivatives IV: Unexpected debenzylation on ring closure of 1-(1-adamantylcarbonyl)-4-benzylthiosemicarbazide with sulphuric acid. *Monatshefte für Chemie/Chemical Mon.*, 125 (5), 587–591.

[125] Glish, G.L., Vachet, R.W. (2003). The basics of mass spectrometry in the twenty-first century. *Nat. Rev. drug Discov.*, 2 (2), 140–150.

[126] Bourne, Y. (1995). Acetylcholinesterase Inhibition by Fasciculin : Crystal Structure of the Complex. 83 (1993), 503–512.

[127] Daina, A., Michielin, O., Zoete, V. (2017). SwissADME: a free web tool to evaluate pharmacokinetics, drug-likeness and medicinal chemistry friendliness of small molecules. *Sci. Rep.*, 7 (1), 42717.

[128] Kenyon, K., Contente, S., Trackman, P.C., Tang, J., Kagan, H.M., Friedman, R.M. (1991). Lysyl oxidase and rrg messenger RNA. *Science (80-.).*, 253 (5021), 802.

[129] Millard, C.B., Kryger, G., Ordentlich, A., Greenblatt, H.M., Harel, M., Raves, M.L., Segall, Y., Barak, D., Shafferman, A., Silman, I. (1999). Crystal structures of aged phosphonylated acetylcholinesterase: nerve agent reaction products at the atomic

level. *Biochemistry*, 38 (22), 7032–7039.

[130] Harel, M., Schalkt, I., Bouett, F., Goeldnert, M., Hirtht, C., Axelsen, P.H., Silmanii, I., Sussman, J.L. (1993). Quaternary ligand binding to aromatic residues in the active-site gorge of acetylcholinesterase. 90 (October), 9031–9035.

[131] Shintani, Y. (2006). Takashima S, Asano Y, Kato H, Liao Y, Yamazaki S, Tsukamoto O, Seguchi O, Yamamoto H, Fukushima T, Sugahara K, Kitakaze M, Hori M. *Glycosaminoglycan Modif. neuropilin-1 Modul. VEGFR2 signaling. EMBO J*, 253045–3055.

[132] Harel, M., Kryger, G., Rosenberry, T.L., Mallender, W.D., Lewis, T., Fletcher, R.J., Guss, J.M., Silman, I., Sussman, J.L. (2000). Three-dimensional structures of Drosophila melanogaster acetylcholinesterase and of its complexes with two potent inhibitors. *Protein Sci.*, 9 (6), 1063–1072.

[133] de Gouveia Dal Pino, E.M., Kowal, G. (2015). Particle acceleration by magnetic reconnection. *Magn. Fields Diffus. Media*, 373–398.

[134] Martorana, A., Giacalone, V., Bonsignore, R., Pace, A., Gentile, C., Pibiri, I., Buscemi, S., Lauria, A., Palumbo Piccionello, A. (2016). Heterocyclic scaffolds for the treatment of Alzheimer's disease. *Curr. Pharm. Des.*, 22 (26), 3971–3995.

[135] Greenblatt, H.M., Kryger, G., Lewis, T., Silman, I., Sussman, J.L.Y. (1999). Structure of acetylcholinesterase complexed with (3) -galanthamine at î resolution 2 . 3 A. 463321–326.

[136] Choudhary, S., Silakari, O. (2018). Chapter 7 - Thiazine: A Versatile Heterocyclic Scaffold for Multifactorial Diseases. O. Silakari (editor), *Key Heterocycle Cores for Designing Multitargeting Molecules* (p. 247–284). Elsevier.

[137] Reddy, R.H., Kim, H., Cha, S., Lee, B., Kim, Y.J. (2017). Structure-based virtual screening of protein tyrosine phosphatase inhibitors: Significance, challenges, and solutions. *J. Microbiol. Biotechnol.*, 27 (5), 878–895.

[138] Shaw, D.E., Deneroff, M.M., Dror, R.O., Kuskin, J.S., Larson, R.H., Salmon, J.K., Young, C., Batson, B., Bowers, K.J., Chao, J.C. (2008). Anton, a special-purpose machine for molecular dynamics simulation. *Commun. ACM*, 51 (7), 91–97.

[139] Piana, S., Lindorff-Larsen, K., Shaw, D.E. (2012). Protein folding kinetics and thermodynamics from atomistic simulation. *Proc. Natl. Acad. Sci.*, 109 (44), 17845–

17850.

[140] Durrant, J.D., McCammon, J.A. (2011). Molecular dynamics simulations and drug discovery. *BMC Biol.*, 9 (1), 1–9.

[141] Lemmon, G., Meiler, J. (2012). Rosetta Ligand docking with flexible XML protocols. *Comput. Drug Discov. Des.*, 143–155.

[142] Karplus, M., McCammon, J.A. (2002). Molecular dynamics simulations of biomolecules. *Nat. Struct. Biol.*, 9 (9), 646–652.

[143] Yücel, N.T., Evren, A.E., Kandemir, Ü. (2022). Antidepressant-like effect of tofisopam in mice : A behavioural , molecular docking and MD simulation study. Epub ahead of print 2022. DOI: 10.1177/02698811221095528.

[144] Tay, N.F., Yurtta, L. (2022). Synthesis , anticholinesterase activity , molecular docking , and molecular dynamic simulation studies of 1 , 3 , 4 - oxadiazole derivatives. (June), . Epub ahead of print 2022. DOI: 10.1002/ardp.202200294.

[145] Çevik, U.A., Işık, A., Evren, A.E., Kapusız, Ö., Gül, Ü.D., Özkay, Y., Kaplancıklı, Z.A. (2022). Synthesis of new benzimidazole derivatives containing 1,3,4-thiadiazole: their in vitro antimicrobial, in silico molecular docking and molecular dynamic simulations studies. *SAR QSAR Environ. Res.*, 33 (11), 899–914.

[146] Osmaniye, D., Evren, A.E., Karaca, Ş., Özkay, Y., Kaplancıklı, Z.A. (2023). Novel thiadiazol derivatives; design, synthesis, biological activity, molecular docking and molecular dynamics. *J. Mol. Struct.*, 1272134171.

[147] Zhao, G., Tong, Y., Luan, F., Zhu, W., Zhan, C., Qin, T., An, W., Zeng, N. (2022). Alpinetin: a review of its pharmacology and pharmacokinetics. *Front. Pharmacol.*, 13814370.

[148] Luo, A.-L., Zhao, Y.-H., Zhao, G., Deng, L.-C., Liu, X.-W., Jing, Y.-P., Wang, G., Zhang, H.-T., Shi, J.-R., Cui, X.-Q. (2015). The first data release (DR1) of the LAMOST regular survey. *Res. Astron. Astrophys.*, 15 (8), 1095.

[149] Wang, Q., Zhao, Y., Chen, X., Hong, A. (2022). Virtual screening of approved clinic drugs with main protease (3CLpro) reveals potential inhibitory effects on SARS-CoV-2. *J. Biomol. Struct. Dyn.*, 40 (2), 685–695.

[150] Case, D.A., Cheatham III, T.E., Darden, T., Gohlke, H., Luo, R., Merz Jr, K.M., Onufriev, A., Simmerling, C., Wang, B., Woods, R.J. (2005). The Amber

biomolecular simulation programs. *J. Comput. Chem.*, 26 (16), 1668–1688.

[151] Schweitzer-Stenner, R. (2014). Cytochrome c: a multifunctional protein combining conformational rigidity with flexibility. *New J. Sci.*, 2014.

[152] Lindorff-Larsen, K., Piana, S., Palmo, K., Maragakis, P., Klepeis, J.L., Dror, R.O., Shaw, D.E. (2010). Improved side-chain torsion potentials for the Amber ff99SB protein force field. *Proteins Struct. Funct. Bioinforma.*, 78 (8), 1950–1958.

[153] Durrant, J.D., Amaro, R.E., Xie, L., Urbaniak, M.D., Ferguson, M.A.J., Haapalainen, A., Chen, Z., Di Guilmi, A.M., Wunder, F., Bourne, P.E. (2010). A multidimensional strategy to detect polypharmacological targets in the absence of structural and sequence homology. *PLoS Comput. Biol.*, 6 (1), e1000648.

[154] Huang, J., Rauscher, S., Nawrocki, G., Ran, T., Feig, M., De Groot, B.L., Grubmüller, H., MacKerell Jr, A.D. (2017). CHARMM36m: an improved force field for folded and intrinsically disordered proteins. *Nat. Methods*, 14 (1), 71–73.

CURRICULUM VITAE

Name and Surname: Abd Al Rahman ASFOUR

Languages: Arabic (Native), English, Turkish.

Education:

- Bachelor's Degree: Sana'a University Faculty of Pharmacy 2011-2016 -Yemen.
- High School: Hayel Saeed Anam 2010-2011 – Sana'a Yemen.

Experience:

- Worked in Al-Farhan Pharmaceutical Company as a Medical Representative for five Months (YEMEN -SANA`A) - 2019
- Worked in Al-Jabal Pharmaceutical Company as a Medical Representative for one year (YEMEN -SANA`A)-2018/2019.
- Worked in Abu-Hazim Pharmacy for two years (YEMEN -SANA`A) 2016/2017.